UNIVERSITÉ DE FRANCHE-COMTÉ, BESANÇON FRANCE
"POLITEHNICA" UNIVERSITY OF TIMISOARA ROMANIA
AUTOMATICS and COMPUTER SCIENCE
Department : Automatique et Systèmes Micro-Mécatroniques

Parkinson's Disease Prognosis using Diffusion Tensor Imaging Features Fusion

Pronostic de la Maladie de Parkinson, basé sur la fusion des caractéristiques d'Images par Résonance Magnétique de Diffusion

P H D T H E S I S

to obtain the title of

PhD of Automatics

of the University of Franche-Comté
Ecole Doctorale Sciences Physiques pour l'Ingénieur et Microtechniques

---

Defended by: Roxana Oana TEODORESCU

Thesis Advisors:
A/Prof. HDR. Daniel RACOCEANU CNRS Singapore
Prof. Dr. Vladimir Ioan CRETU PUT Romania

prepared at Franche-Comté University France and "Politehnica" University of Timisoara Romania
defended on April 11, 2011

Jury :

Reviewers :	Touradj EBRAHIMI	-	EPFL Switzerland
	Pierre JANNIN	-	Univ. Rennes France
President :	Henning MÜLLER	-	UniGe Switzerland
Advisors:	Daniel RACOCEANU	-	CNRS Singapore
	Vladimir-Ioan CRETU	-	PUT Romania
	Noureddine ZERHOUNI	-	UFC/ENSMM France

Abstract: Nowadays, in most of the major hospitals, Parkinson's Disease (PD) is mainly diagnosed using cognitive testing. These tests place the patients according to their scores on one of the scales determining the severity of the disease: Unified Parkinson's Disease Rating Scale (UPDRS) or Hoehn&Yahr (H&Y) rating scale. As a consequence of both of these procedures, the diagnosis is only possible after the installation of PD, which occurs years from its onset, determining irreversible changes in the physiology of the patient. Early diagnosis and even prognosis would definitely offer the specialists the possibility to study the disease at the pathology onset and maybe reverse or significantly slow its effects.

In this context, the primary purpose of our research concerns the use of medical imaging as PD's early biomarker. The present study focuses on several aspects: the context of the biomarkers for PD and the place of medical imaging in this context, the advantages of the use of medical imaging as biomarker and the procedure to employ them without damaging the information and maximizing its exploitation.

After determining the specific anatomical regions affected by PD, able to be detected and quantified in MRI images, a feasibility study establishes if the medical imaging information is correlated with the disease and if extraction can affect it. Starting from the validation of these fundamental aspects, we design a fully automatic system, handling the medical image information. This automatic system receives the medical images as input, in the format adopted by clinicians, being able to supply the severity of PD on one of the scales used by the neurologist to determine PD. Studying the PD pathology, medical clinicians determined that the dopamine, one of the main neurotransmitters, is the main factor in PD pathology. It is produced in the midbrain area by the anatomical structure called Substantia Nigra. As this structure is not well delineated, we are studying the midbrain area. During the feasibility study, we determine if this area, extracted from the medical image, can be correlated with PD on the anisotropy level. The anisotropy is one of the measures used to determine the dopamine quantity. In this case, the medical image is the supplier of information and the source used for PD detection. This represents the difference from all the other biomarkers which use the medical information only as a supplier, not as a source. Exploiting it in this way we aim at bridging the gap between the pathophysiology represented by the medical image information and the clinical level represented by the PD severity.

A total of 143 subjects, among whom, 68 patients diagnosed clinically with PD and 75 control cases, underwent DTI imaging. These MRI images are specific for PD studies as they reveal the anisotropy level. Among the DTI images, the EPIs have lower resolution but provide essential anisotropy information related to the neural fibers affected by the dopamine. As the neuromotor tract affected by PD pathology represents one of the specific symptoms that determine the diagnosis, we are trying to detect and study the dopamine level on this tract. For this purpose, a tractography process is required. Based on the fact that the tract starts from the midbrain area and that another volume of interest could refine the detected tract, we determine the second anatomical region used as target for the fibers. With two volumes of interest (VOI), the accuracy of the neuromotor tract detection is increased using a global tractography. The two volumes in our study are represented by the midbrain and the Putamen. The Putamen is chosen due to previous studies, indicating physiology changes on this structure and due to its relative positioning to the midbrain area, representing an endpoint for the trajectory of the neuromotor tract.

For using the fibers as a measurable element during PD diagnosis, we introduce new metrics: fiber density (FD) and fiber volume (FV). Furthermore, comparing patients based on the extracted fibers and evaluating them according to Hoehn&Yahr (H&Y) scale can be done using these measures. The determined fibers, evaluated with our own metrics, represent the source of information during the decisional stage. Thus, during this stage, we require the extracted features on which we perform PD diagnosis and prognosis.

Keywords: Medical Image Processing, Medical Image Analysis, Automatic VOI detection, Parkinson's Disease, Parkinson's Disease Detection, Diagnosis, Prognosis, Information fusion, Neuro-fuzzy systems

Résumé :À l'heure actuelle, dans la majeure partie des services hospitaliers spécialisés, la maladie de Parkinson (PD) est déterminée en utilisant des tests cognitifs. Ces tests classifient les patients sur unes des échelles utilisées pour détecter la sévérité de la maladie : UPDRS (Unified Parkinson's Disease Rating Scale - l'échelle unifiée de la sévérité de la maladie de Parkinson) ou Hoehn & Yahr (H&Y). La diagnostic est possible seulement après l'installation de la maladie, des années après son apparition. À ce moment là, le processus est irréversible. Le diagnostic précoce pourrait ainsi offrir la possibilité d'étudier la pathologie de la maladie avec une chance réelle d'inverser les symptômes ou de freiner considérablement l'évolution de la maladie.

La contribution principale de nos recherches est représentée par la possibilité d'utiliser l'imagerie médicale comme biomarqueur pour déterminer la maladie de Parkinson. L'étude présente plusieurs aspects, liés au contexte d'utilisation des biomarqueurs pour la maladie de Parkinson et la place de l'imagerie dans cet environnement.

Notre étude détermine quelles sont les formations cérébrales affectées par la maladie, formations détectables à partir de l'Imagerie par Résonance Magnétique (IRM). Une étude de faisabilité a été menée pour déterminer si l'information contenue au niveau de l'imagerie est corrélée avec la maladie, et si l'extraction peut affecter cette information. Une fois ces aspects validés, nous étudions un système pour l'extraction, la fusion et l'aide au pronostic à partir de l'image médicale de type IRM. Ce système doit être capable de recevoir l'image médicale dans le format utilisé par les cliniciens et générer comme résultat la valeur de sévérité de la maladie de Parkinson par rapport à une des échelles utilisées cliniquement pour le diagnostic.

Dans l'étude de la maladie de Parkinson, les cliniciens ont établi que la dopamine, un des neurotransmetteurs du cerveau, est le facteur principal dans la pathologie de Parkinson. Ce neurotransmetteur est produit par-delà région du Substantia Nigra (SN) dans le mésencéphale. Cette région n'étant pas très bien délimitée, on étudie habituellement le mésencéphale. Pendant l'étude de faisabilité, on étudie la corrélation entre cette région - extraite de l'image - et la maladie, en utilisant le niveau de l'anisotropie. Cette mesure détermine le niveau de la dopamine dans les réseaux neuronaux. Dans ce cas, l'image médicale est la source de l'information primordiale, mais elle représente aussi les données utilisées pour la détection. Ceci représente une caractéristique fondamentale du bio-marqueur que représente l'image médicale.

Notre étude utilise une base de données formée par 143 patients : 68 patients détectés avec la maladie et 75 cas de contrôle. Entre les IRM, les images du tenseur de diffusion (DTI - diffusion tensor images) sont utilisées dans la maladie de Parkinson grâce à leur capacité de déterminer le niveau de l'anisotropie. Entre les images DTI, les images écho planaires (EPI), même si caractérisées par une résolution médiocre, sont capables de déterminer les faisceaux neuronaux. Le nerf neuromoteur représente un des faisceaux affectés par le manque de dopamine, caractéristique à cette maladie. Pour le déterminer le niveau de présence de la dopamine, on utilise la tractographie. Ce processus a une finesse supérieure si on lui fournit la source et la fin des faisceaux (tractographie globale). La source est le mésencéphale et une des destinations est le Putamen. Cette région anatomique est située dans le trajet de la dopamine et elle est traversée par le nerf neuromoteur.

Pour pouvoir utiliser les fibres comme mesure dans la détection de la maladie, nous introduisons des métriques spécifiques : la densité et le volume des fibres. En se basant sur ces mesures, on peut comparer les patients sur l'échelle de H&Y. Pour arriver à ce point, après avoir détecté les fibres et les avoir évalué avec les métriques évoquées, on les analyse en utilisant une procédure de décision neuro-floue. Cette procédure utilise les faisceaux moteurs pour générer un diagnostic et le pronostic associé, en corrélation avec l'échelle H&Y.

Mots clès : Traitement d'Images Médicales, Analyse d'Images Médicales, Détection automatique des VOI, Diagnostic, Pronostic, Maladie de Parkinson

Acknowledgments

All the hard work and the determination, all the results and the algorithms would have not been possible without knowing that God is on our side.

The work presented in the thesis has been the result of a collaboration with **Dr. MD Ling-Ling Chan** and her team from **Singapore General Hospital (SGH)**. We would like to express our gratitude for all the brain anatomy and diagnostic radiology lessons and the images, as well as for her work for gathering the database and make it available for us.

At the beginning, we have collaborated with **Dr. MD Karl Olof Lövblad** from the **Universities Hospitals of Geneva** and we thank him for his time and his patience.

The research stages made in Singapore from 2007 until 2009 have been useful in the research and by the help of **IPAL**[1], **NUS**[2] and **UPT**[3] all this work was possible. This stages have been supported by **CNRS** [4] and the **CNCSIS** [5] scholarship TD[6] 46/2008 from the Romanian government.

[1] Image and Pervasive Access Lab - http://ipal.i2r.a-star.edu.sg/
[2] National University of Singapore - http://www.nus.edu.sg/
[3] "Politehnica" University of Timisoara -http://www.cs.upt.ro
[4] French National Research Center - http://www.cnrs.fr
[5] http://www.cncsis.ro/
[6] TD - Young PhD students Scholarship

Content

List of Figures

List of Tables

List of Abbreviations

T_1 weighted MRI sequence that uses gradient echo (GRE) sequence with short echo time (T_E) and short repetition time (T_R)

T_2 MRI sequence use a spin echo (SE) sequence with long T_E and long T_R

T_E echo time

T_R repetition time

Anisotropic - state of an optical medium in which the optical properties are not the same in all directions, due to the fact that the refractive index is not the same for all directions. An incident ray will be divided, within a uniaxial anisotropic medium, into two refracted rays; an ordinary ray which obeys Snell's law and an extraordinary ray which follows a different law. Most crystals are anisotropic.

AUC area under the ROC curve

Biomarkers (biological markers): A characteristic that is objectively measured and evaluated as an indicator of normal biological processes, pathogenical processes or pharmacological responses to a therapeutic intervention. [from the Biomarkers Definitions Working Group]

BPNN Back propagation neural network

Computer Aided Diagnosis (CAD) Computer based system that uses software programs in diagnosis

Classifier Independent Feature Analysis (CIFA) measure of importance of features when classifying an object

Clinical end-point: A characteristic or variable that reflects how a patient feels, functions or survives. [from the Biomarkers Definitions Working Group]

Cerebrospinal fluid (CSF) a clear bodily fluid that occupies the subarachnoid space and the ventricular system around and inside the brain and spinal cord

Digital Imaging and Communications in Medicine (DICOM) medical standard used for medical image storage and management encapsulating the clinical information, acquisition protocol and the image itself.

Diffusion Tensor Imaging (DTI) A refinement of magnetic resonance imaging that allows the doctor to measure the flow of water and track the pathways of white matter in the brain. DTI is able to detect abnormalities in the brain that do not show up on standard MRI scans.

Echo-Planar Imaging (EPI) a technique for obtaining a magnetic resonance image in less than 50 msec

Fractional Anisotropy Imaging (FA) : imaging diffusion image representing the anisotropy values on the neural fibers where the pixels represent values obtained computing the anisotropy.

Fractional Anisotropy(FA) a scalar value between zero and one that describes the degree of anisotropy of a diffusion process.

FC Fuzzy Control a fuzzy set, which represents a type II typology (type I is a monotonic typology and type III is a linear function of state)

Fluid attenuated inversion recovery (FLAIR) a pulse sequence used in magnetic resonance imaging inversion-recovery pulse sequence that has null signal from fluids

Fluid attenuated inversion recovery (FLAIR) inversion-recovery pulse sequence that has null signal from fluids

Functional MRI (fMRI) is able to measure signal changes that represent neural activity in the brain

Grey Matter (GM) a major component of the central nervous system, consisting of neuronal cell bodies

H&Y Hoehn & Yahr scale - representing the Parkinson's disease severity degree

IAPE our prognosis method called Independent Adaptive Polynomial Evaluation

KMeans clustering method that classifies

K Nearest Neighbor (KNN) method used for classification when the number of classes is known (k)

MedINRIA Medical project by INRIA laboratory at Sophia Antipolis with modules dedicated to medical image processing, Diffusion Tensor Imaging and fiber tracking http://www-sop.inria.fr/asclepios/software/MedINRIA/ - last accessed on May 2010

Magnetic Resonance Imaging (MRI) a method of visualizing soft tissues of the body by applying an external magnetic field that makes it possible to distinguish between hydrogen atoms in different environments.

PD-APE our prognosis method called PD Adaptive polynomial evaluation method

Parkinson's Disease (PD) Neurodegenerative disease affecting elderly people, manifesting with tremor and loss of cognitive impairment.

Proton Emission Tomography (PET) Functional imaging used for highlighting the cerebral activity.

Putamen - the large dark lateral part of the basal ganglion which comprises the external portion of the corpus striatum and which has connections to the caudate nucleus. [from Merriam Webster Dictionary]

RBF Radial Basis Function Network

Relative Feature Importance (RFI): used as metric to make a ranking among features

Receiver Operating Characteristic (ROC) statistic evaluation curve plotted with true positive fraction

Region of interest (ROI) 2D area represented as region aimed by the segmentation algorithm, in our case, a specific tissue type

Substntia Nigra (SN) Cerebral anatomical structure inside the midbrain that produces the dopamine, one of the main neurotransmitters

Slice Of Interest (SOI) Slice, inside the volume stack, that contains the region needed to be detected

Single-Photon Emission Computed Tomography (SPECT) Functional imaging used for highlighting the neural activity

Statistical Parameter Mapping (SPM) a MATLAB software package implementing Statistical Parametric Mapping for neuroimaging data

Surrogate marker: A biomarker that is intended to substitute for a clinical end-point. A surrogate end-point predicts clinical benefit - A subset of biomarkers.[from the Biomarkers Definitions Working Group]

T-Test a statistical test involving confidence limits for the random variable t of a t distribution and used especially in testing hypotheses about means of normal distributions when the standard deviations are unknown [from http://www.merriam-webster.com/dictionary/t-test]

TSK the Takagi-Surgeno-Kang inference method

Unified Parkinson's Disease Rating Scale (UPDRS) Unified Parkinson's Disease Rating Scale - used for rating PD severity

Voxel Based Morphometry a neuroimaging analysis technique that allows investigation of focal differences in brain anatomy, using the statistical approach of so-called statistical parametric mapping

Volume Of Interest (VOI) 3D volume aimed by the segmentation algorithms, representing an anatomical structure

volumetric pixel -voxel- represents the value on a regular grid http://www.webopedia.com/TERM/V/voxel.html-lastaccessedon02June2010

Weighted Absolute Weight Size (WAWS): uses eigenvectors and eigenvalues for discriminant analysis

White Matter (WM) one of the two components of the central nervous system and consists mostly of myelinated axons

Chapter 1

Introduction

Contents

Using the medical DTI as biomarker in Parkinson's disease detection and prediction represents a major challenge for early clinical diagnosis and prognosis. The work presented in this thesis concerns a systematic algorithm of the use of medical imaging as a biomarker for this important neurodegenerative disease. We present the feasibility study and the technical demarche all the way in producing a prototype that puts in practice our theoretical premises in a translational approach.

Biomarkers offer information about the disease progression and its characteristics, elements that are not available at the clinical level, valuable as well for drug development. For Parkinson's Disease (PD) the need for biomarkers is acute as it can provide an illustration of the disease on the pre-motor period, before it becomes irreversible. PD can be diagnosed only after the trembling affects the patients, after the motor tract is affected. The pre-motor period is not diagnosable yet. The tremor representing the motor manifestation of the disease is due to the lack of dopamine, one of the main neurotransmitters produced by the midbrain structure called Substantia Nigra (SN). Its loss affects the motor tract causing one of the first clinical diagnosable symptoms for PD. Due to the fact that the neurotransmitter does not deliver the signal trough the motor fibers, it affects them and the result of this is the tremor. In these conditions, the relevant markers for PD are linked to the pathology determining the dopamine production.

The loss of dopaminergic production is often estimated by visualizing the motor functionality or neuromotor activity once the symptoms appear. The heterogeneity of the motor fibers physiology, as well as the slow pathological progression of PD require markers capable to detect clinical and pathobiological symptoms for PD detection and progression. Pathology studies have showed that by the time these symptoms are installed, at the pre-motor stage, about 50-60% of dopamine is lost [Marck 2008] and about 80% once this stage is reached. This dopamine lost is acknowledged when the symptomatic stage develops onto the clinical phase of the disease and the diagnosis can be given [Today 2009] only at this level. The need for a biomarker that reaches from the clinical stage into the pre-motor phase is given by these percentages. The fact that by the time the specific symptoms appear- there are approximately 5-8 years from the disease installation- represents another justification for early diagnosis efforts.

Developing a biomarker at the pre-motor stage is entirely dependent by the pathology information, but the clinical aspect is not validated yet. In this case, the reverse engineering, based on the clinical information and using the pathobiological and physiological information of PD. The clinical stage can be shifted in time by transfer of information to an earlier point on the disease development mechanism.

The main challenge in PD diagnosis is represented by the analysis phase of the symptoms and markers as several symptoms are common to a few diseases. Due to this fact, finding appropriate and reliable biomarkers represents a complex and difficult process.

The current markers are incomplete due to the lack of correlation between the clinical features and the pathobiological ones. The imaging is linked to the physiology of each patient and can provide information at the pathological level. While the clinical aspect represents a visible manifestation of the disease, the imaging represents a physiological measure for dopamine loss, constituting the link with the pathology and offering a visual of the PD source. The need for a measurable feature at the physiological level and breaking the gap between the clinical and pathophysiological level could both be solved by breaking the semantic gap at the technical level. The imaging information for PD is not currently considered as a reliable biomarker, due to this gap and the lack of correlation with the clinical level.

The clinical stage, reached after the motor symptoms installation, is currently diagnosed based exclusively on cognitive testing. According to their cognitive testing scores, the patients are placed on a predefined scale: Unified Parkinson's Disease Rating Scale or Hoehn&Yahr (H&Y). This manner of diagnosis does not take into account the information provided by the images. Performing image analysis and finding an association between the effect, represented by image specific indicators, and PD severity, estimated independently from the image, determines an inclusion of the medical image in the diagnose decision as well. Following this new procedure presents the advantage of compounding the cognitive aspects with the anatomy-physiological ones.

The medical images needed for this study should have high anatomical detail, as well as specific pathology for the disease so that the physiology and the clinical phenotype can be detected. Magnetic Resonance Imaging (MRI) together with the Computer Tomography (CT) imaging are currently used in PD. Specific CT imaging like positron-emission tomography (PET) and Single Proton Emission Computed Tomography (SPECT) are used as biomarkers providing dopaminergic information at the SN level. From the MRI imaging there are studies on the functional imaging like Diffusion Weighted Imaging (DWI) as these functional images are usually used to determine correlations between the physical changes in the brain and the mental functionalities. Functional MRI (fMRI), due to the dopaminergic dysfunction, highlighted as dopamine transporter binding these images [Dorsey 2006] show relevant changes on the posterior area of the Putamen.

The specific anatomical structure affected by the PD pathology and their physiology is changed and this aspect is revealed by the medical images. Taking the medical images and proposing their use as a biomarker encapsulates several levels of study. The need for a new marker among the existing ones, defines the gap that needs to be filled and the additional information that this new approach brings in relation with the existing diagnosis.

1.1 The need for new markers for Parkinson's Disease

Parkinson's Disease affects the population that has, on average, 61 years, even if it begins around 40 years [Disease 2009]. From this point of view, the continuous aging of the population, combined with the actual late detection and the impossibility to reverse or stabilize the PD evolution justifies strong concerns for a prediction system. By the time the disease is detected, the patient has already lost 80-90% of the dopamine cells [Today 2009]. The treatments are less effective after the disease develops. Thus, a prognosis of this disease could diminish the effect of the PD or even reverse it.

The fact that PD is detected only after reaching stage 2 on H&Y scale, rarely stage 1.5,

the early detection, before the disease is installed or signs correlated with the disease are hard to determine and prove. In these conditions, detection in early stage for diagnosis and prognosis is very challenging using just the symptoms. By using early detection, there is a chance to study the disease and deploy an early treatment for stopping or slowing down its progression.

The need for these markers is represented by early detection and prediction factors that are determined by analyzing the markers. The early detection offers the possibility to study the disease development and provide time for the therapeutic treatments. The fact that the PD severity is expressed as numerical values on different scales adds a value on the disease. Numerical values representing the disease severity at the image level provide values from the pathology. The affected physiological landscape affects the values extracted at the image level. As these values are affected by pathology and physiology, they are complementary to the values on the PD scale, obtained by cognitive testing. Values correlated with the disease severity on the same scale as the clinical diagnosis provide a global and more complete view of the disease.

The difference between susceptible individuals and normal cases - control cases - provides the sensitivity measure for markers, while the true idiopathic PD cases form the similar diseases provide specificity. Parkinson's Disease is a neurodegenerative affective disorder that can be confounded with other disease like the essential tremor, Multiple System Atrophy (MSA) and Progressive Supranuclear Palsy (PSP) [Mitchell 2004].

The biomarker makes the difference between the Lewy body formation, neural degeneration or dopamine depletion and/or Parkinson's Disease. The main problem in PD is the clinicopathological correlation, not relining on the pathology to describe the clinical development of the disease. The confusion with other diseases is encountered at this point where the behavior of many diseases is similar, thus the diagnosis based on this pathological elements is just symptomatic, not affecting the disease if it is not the correct one.

1.2 Thesis structure

Following the idea of using the medical imaging as biomarker, the thesis represents a complete study surrounding this goal. There are several points of view involved in this study: *the scientific perspective, including the technicalities and methods involved in achieving the main purpose, and the clinical one, with the medical relevance.*

The thesis is structured in three parts concerning *the context of PD biomarkers, the possibility that medical imaging offers as a biomarker and the contributions.* Medical imaging contains not only anatomical information, but also the pathophysiology of the disease at the tissue level and this aspect is the one that our approach aims on exploiting and bringing it to the clinical level for early diagnosis and prognosis.

For this purpose there are several aspects that we are studying, not just the context of PD biomarkers, but the medical images as well. As they provide the information that needs analysis to be used further, the context of the medical images is represented by their characteristics and their ability to provide the pathophysiology needed. A feasibility study is needed to determine if the medical imaging contains all the information that should provide and that this information can be used to reflect the PD severity.

The technical approach together with our proposed methods is created in close relation with the feasibility study and its conclusions. The medical premises that link the pathophysiology with the clinical condition contribute to our approach. Taking each chapter in consideration we are presenting the main ideas that are considered next.

The main elements concerning the context of PD biomarkers, different types of biomark-

ers and the criterion for defining new ones are presented and defined in **chapter 2**. After defining the meaning of the terms and the existing PD biomarkers we develop the standpoint for the current place of biomarkers on the PD pathology relative to the clinical detection. Following the pathology development, we define the main landmarks for physiology in correlation with the PD stages.
As we are proposing the medical imaging as specific PD biomarker, we define the current context of head medical imaging with emphasis on the specific properties highlighted by the PD physiological changes. The way medical images are used in PD detection reveals the important anatomical area, those that are affected by the disease pathology. The specific images currently used in PD study are presented as well.

In **chapter 3** we present our feasibility study in the context of the PD pathology and the disease development. The premises for this study, the theoretical hypothesis determining it and the main aspects of the feasibility are presented, together with the test approach and parameters. This study determines parameters for image handling and challenges for patient management. Facing the variability and defining algorithms from digital image processing and analysis domain for the pre-processing level of our study defines the transition from the feasibility study to data processing.

For the processing level we define the main elements in **chapter 4**. The context provided by the image on to the feasibility study and the pre-processing level prepare the means for information extraction. The proposed methods from the image processing and analysis perspectives are presented in relation with the current technical landscape, highlighting our contribution. Evaluating the quality of the extracted information provides the relevance for the disease.

For the analysis of the extracted information and its exploitation, the approach is presented in **chapter 5**. As the clinical level is the final aspect where the biomarker is mapped, the system is defining a Computer Aided Diagnosis (CAD) system that determines if the information provided by the image can define the situation of the patient. The context for the analysis part is provided by the modalities from the computer vision domain linked to fuzzy networks on the technical level and the currently used scale for the disease on the clinical level.

The results of the study are presented in **chapter 6**. The presented methods with regard to existing ones are evaluated, but the results for the entire study are those regarding the diagnosis and prognosis. These results determine the validity of the medical image as a biomarker. The test conditions and machine requirements are contained in the same chapter.

The final **chapter 7** deals with the scientific and technical conclusions. Using medical imaging as biomarkers brings into the bioinformatic area significant contributions for the PD. The clinical relevance of the study determines its relevance on the medical field as well and it is presented in the same chapter. Future research areas and possibilities to follow this study are presented with the scientific perspectives at the end.

Chapter 2

Current landscape for Parkinson's Disease Biomarkers

Contents

As we are proposing the use of structural medical images- the DTI (Diffusion Tensor Imaging)- as biomarkers, we are first making an analysis of these type of information, defining them and highlighting elements that are specific for PD. This disease represents a neurological disorder, a chronic neurodegenerative disorder [Mitchell 2004] with pathology and evolution in time difficult to study and master.

The Biomarkers Definition Working Group refer to the biological markers (biomarkers) as characteristics that are objectively measured and used to determine not only the normal biological process, but also pathogenic processes or pharmacological response to treatment [Marck 2008].

The markers represent measures of manifestation of different stages of the disease that trough analysis are converted in values representing stages of disease. *An ideal biomarker should show changes at the pathological or clinical level and measures must be reproducible, as well as cheap, non-invasive and quick.* These markers include not just detecting the disease vulnerability, but also the pre-motor symptoms like *olfactory* and *autonomic disfunction*, *depression*, *sleep disorder* or *neurophysiological impairment* [Berg 2008]. Changes in *Substantia Nigra (SN)*, anatomical region situated in the midbrain area, that presents hyperechogentricity, can be included among the pre-motor symptoms. This aspect is currently studied using the Computer Tomography (CT) images. This anatomical region is the producer of dopamine and the changes in its physiology are due to the fact that the neurotransmitter is no longer produced. Symptoms like olfactory dysfunctions or *cerebrospinal fluid* can be correlated with Alzheimer's disease as well. These two neurodegenerative diseases have common markers, but PD clinical diagnosis is made only after the motor symptoms are installed.

The distinction between biomarkers in general and the surrogate markers resides at the granularity level. Surrogate markers are a subset of biomarkers, just like the clinical endpoints are. **Surrogate markers** are tested in several interventions, can be used as clinical meaningful validation or as clinical end-point and represent a subset of biomarkers. The

clinical end-points represent indicators of the way the patient is feeling and they are used in the diagnosis process. The biomarkers provide values for the symptomatic and pre-symptomatic manifestations of the disease, providing surrogate markers and demonstrating the clinical efficiency.

The current markers target the risk for the disease or its progression and can be used for determining the disease stage or the effect of the medication. The pre-motor stage can be illustrated by using the **risk evaluation markers** and after the onset of the symptoms the **diagnosis markers** can be further used. The risk markers are the predictive factors and the diagnosis ones can be used as response to therapy markers. **Clinical diagnostic biomarkers** can be risk markers that are used to evaluate subjects with clinical manifestation of the disease, but they do not relay on clinical features based on the clinical manifestation of the disease [Marck 2008]. Other biomarkers like *blood*, *serum* and *plasma*, *cerebro-spinal fluid (CSF)* and *urine* have been studied to determine systemic metabolic dysregulation [Graeber 2009].

2.1 Existing biomarkers for PD

The ability to predict the pathology - diagnose - from clinical phenotype is difficult due to the lack of correlation. The biomarker linked to the pathology does not include the clinical information as well. The idea is to have both pathology and clinical information evaluated by a biomarker. Starting from the primary purpose of the biomarker, the complementary information is acquired by correlation and/or analysis. There are biomarkers that investigate the progression of PD during the pre-motor period and those that are used after the clinical phenotype is established, after specific symptoms are detected and the diagnosis is set.

For PD there are several markers, clinical markers and biomarkers [Marck 2008]:

- Clinical Markers
  - Cognition
  - Affective: depression, apathy, anxiety
  - Autonomic: constipation, bladder, sexual, cardiac
  - Olfaction
  - Sleep: Rapid eye movement Behavioral Disorder (RBD)
  - Skin
  - Motor analysis
  - Speech
- Biomarkers
  - Imaging Phenotomics
    - SPECT/PET: dopamine, dopamine transporter (DAT), F-dopa, vesicular transporter(VMAT)
    - SPECT/PET: nondopamine, fluorodeoxyglucose (FDG), metaiodobenzyguanidine (MIBG), targets for norepinephrine(NE), 5-hydroxytryptamine (5-HT) A2a, nicotine
    - MRI: spectroscopy
    - Functional MRI

Biomarker	Imaging Technique	Investigators
Cerebral blood flow (CBF)	MRI / Arterial spin labeling	Hoge R
Directed molecular probes	PET Optical	Weissleder R
Dopamine transporter (DAT) density	SPECT (using I-123 altropane)	Fischman A Halpern E Sahani D
Dopamine binding potential	SPECT (using I-123 altropane)	Fischman A Halpern E Sahani D
Dopaminergic neurotransmitter activity	fMRI PET	Fishman A Livni E Rosen B
N-acetylaspartate (NAA) levels over time	MRS	Gonzales RG Jenkins BG

Table 2.1: Parkinson's Disease imaging biomarkers from Massachusetts General Hospital/ HST - Center for Biomarkers in Imaging [Center For Biomarkers in Imaging 2007]

    - Nigral ultrasound
- Genetics
    - Synuclein, LRRK2
    - Parkin DJ-1, Pink 1
- Cerebrospinal fluid (CSF), blood (Proteomics, Transcriptomics, Metablomics)

Analyzing the existing clinical markers and biomarkers, their area of influence and the information defining them, we perceive the need for well-defined quantitative biomarkers. In clinical and preclinical stages great efforts have been made into Translational Science (TS)[1] so that the passage of compounds into clinical development can be done [Jensen 2010]. The biomarkers are subtler and represent the pathological dimension of the disease that determines physiological changes detected as symptoms and manifested as clinical markers. Diminishing the path to the clinical acknowledgement for PD represents the main purpose in using biomarkers.

When talking about new possibilities for biomarkers, Mitchell and al. [Mitchell 2004] considers three categories: imaging as biomarker, clinical testing procedures and biochemical together with genetic tests. We will discuss just the first case, as we do not intend in using the other two categories. The medical imaging currently used as biomarkers for PD, according to the Center for Biomarkers in Imaging (CBI),[2] are presented in Table 2.1.

Imaging biomarkers are generally used as surrogate endpoints as they are able to determine the disease on the pre-motor state, offering an alternative to the current trial endpoints. Surrogate endpoints represent measurements that can be used in clinical trials for evaluating either the therapy, or the disease level. In table 2.1 there are two separate columns for Biomarker and the Imaging technique which puts the imaging on the position of supplier of information where the actual marker, the one correlated with the disease, is the one followed at the image level. As presented in figure 2.1, there are two separate levels where the biomarker and the medical image are placed: the information and the source

[1] Biomarker Commons http://biomarkercommons.org/news/imaging-biomarkers

[2] Center for Biomarkers in Imaging: http://www.biomarkers.org/NewFiles/biomarkers/diseases.html accessed in November 2010

layer. Using the medical image as both the source and the evaluated information makes it a biomarker. The fact that medical image is used as extracted information directly in the clinical process eliminates one level of analysis. In this case the marker is not based on the clinical manifestation of the disease. This aspect integrates medical imaging among the clinical diagnosis markers and/or clinical end-points.

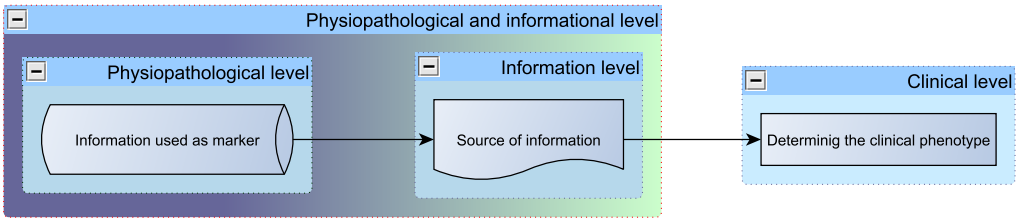

Figure 2.1: Informational layer and the biomarker relative to the clinical diagnoses process

Starting from the representation of the pathology progression in time by Michel et al. in [Mitchell 2004], we present in figure 2.2 the physiology changes due to PD development and manifestation. As the diagnosis detection can be done only after the dopamine loss reaches an irreversible level, there is a small time gap, when the diagnostic can be moved towards the pre-motor area, space filled by the clinical diagnosis markers. Studying the specific elements that determine the specific symptoms there is the possibility of improving even more the diagnosis onto the non-specific symptomatic area by pushing the analysis of specific symptoms to an earlier point and changing the area of the clinical end-points as well. There is a need to determine a reliable biomarker without relying on symptoms. In this case, the physiological changes should be the ones determining the measure of the marker in the pathological progression of the disease.

The need for biomarkers detecting the early stage of the disease is not related to the pathology of PD, but to the motor symptoms as currently the diagnosis is set after cognitive testing on the post-motor area. The prediction factor is linked with the non-specific symptoms and should make the difference between PD patients and other diseases by taking into account a specific marker. In this case the marker can detect pre-symptomatic manifestation of the disease and is regarded as risk evaluation markers.

The time-line from figure 2.2 presents 5 years until the symptoms arise, after the pathology onset, and additional 2-3 years until the diagnosis is set. These time gaps represent the target places for new biomarkers and diminishing them or reversing the disease in one of these time spaces by treatment in early stage represents the final aim of biomarkers. Representing the PD path after the onset of the disease emphasizes the clinical and pathological stages. The progression of PD in time starting with the onset of the pathology (figure 2.3) expresses a direct physiological progress that is detected by the existing biomarkers. The diagnosis set after the motor symptoms are detected, based on the cognitive testing, denotes a late attempt to control the manifestation of the disease.

2.1.1 Current usage of Medical imaging

In vivo imaging is currently used for PD as it is non-invasive and follows the displacement of dopamine transporter (DAT). This medical imaging is used later on when following the effects of drug development, to determine the effects. It can follow the disease progression, but it has potential, as it can be combined with symptomatic dopaminergic treatment and can offer an advantage to simple markers. The two main in vivo imaging modalities used

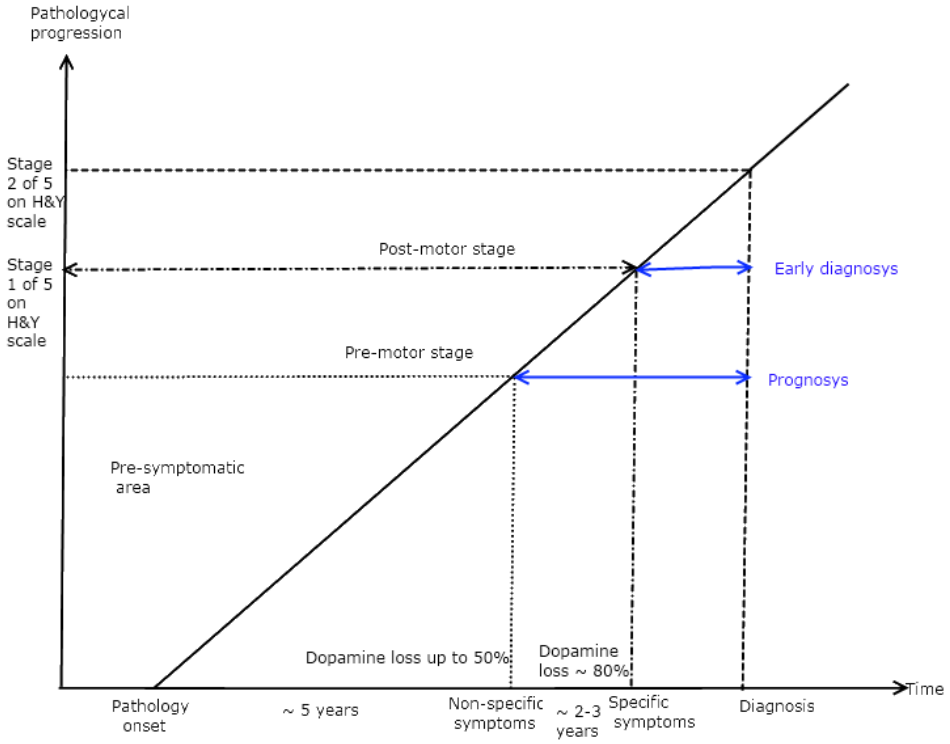

Figure 2.2: PD pathological progression in time with the physiological changes

for PD with biomarkers are the Computer Tomography (CT) and the Magnetic Resonance Imaging (MRI).

Computer Tomography (CT) images are obtained using a tomograph, which produces an X-ray beam that parses the 3D volume of the body in a process known as windowing. From these type of imaging the Proton Emission Tomography (PET) and Single Positron Emission Computed Tomography (SPECT) are the ones that presently show potential as biomarkers.

Currently just the functional imaging are used in PD diagnosis and treatment, because they posses the attributes to be used as such. PET and SPECT encapsulate the cerebral blood flow, one of the biomarkers with the highest potential in PD. This type of medical imaging can highlight the decline in neurotransmitter functionality. While PET provides better resolution, SPECT is more accessible but harder to validate, it is specific to certain conditions and it is not reliable. The pre-symptomatic PD detection using these images is not possible yet, but it is currently studied [Mitchell 2004]. These image modalities have great variation among subjects, but the PET provides up to 70% agreeing among the imaging and the clinical diagnosis for differentiating the PD patients form those with other diseases and similar manifestation. The Caudate and the Putamen signals on these images are used for differentiating the clinical diagnosed strationigral degeneration for PD patients. Limitations for the functional imaging are present among the normal cases and the disease affected ones where the image cannot differentiate them.

Magnetic Resonance Images (MRI) are used in radiology for their detailed visualization of the internal structure of the human body. As one of the versatile medical imaging modality, MRI has the property to provide both the metabolic and functional aspects of

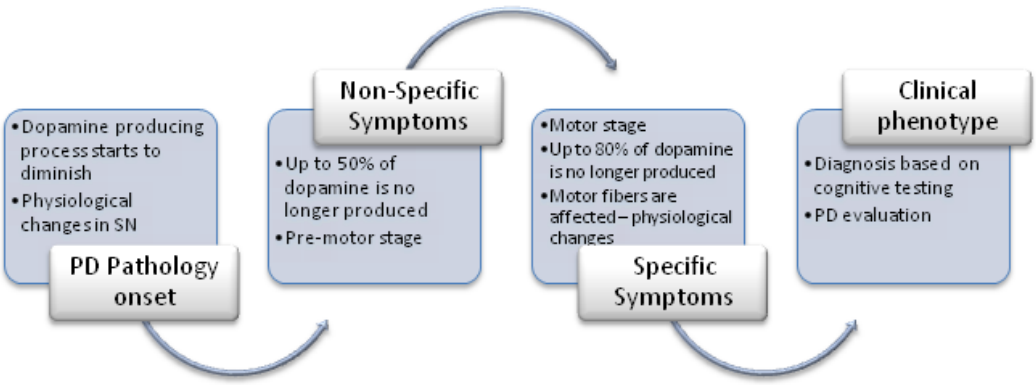

Figure 2.3: The Pathological development of PD

human body tissue, offering biophysical parameters that can be used as biomarkers. The contrast offered by these types of images is able to make the difference between the soft tissues inside the body, especially in neurology, providing the physiology of different neural tissue types. Having the physiological information that supports the specific pathology, combined with the high resolution of the images provide necessary elements for using MRI as biomarkers. There are several types of MRI scans that differ depending on the protocol parameters and techniques used for acquisition.

T_1 **weighted** use a gradient echo (GRE) sequence with short echo time (T_E) and short repetition time (T_R)

T_2 **weighted** use a spin echo (SE) sequence with long T_E and long T_R

Specialized MRI scans are based on more complex techniques for acquisition of images, depending on the application area:

- Diffusion MRI represents the diffusion of water molecules at the tissue level - is able to acquire several types of imaging types: diffusion weighted imaging (DWI), echo planar imaging (EPI)
- Fluid attenuated inversion recovery (FLAIR) is based on the inversion-recovery pulse sequence that has null signal from fluids
- Functional MRI (fMRI) is able to measure signal changes that represent neural activity in the brain

There are other types of MRI sequences, as well as other specialized MRI scans that combine techniques in order to obtain better images. Currently each of the MRI sequence responds to a certain need from the medical domain, being predefined for a certain type of application, or a certain body part and/or disease specific. For PD usually the functional MRI is used, due to the information provided for the motor tract, or the diffusion MRI, as it contains the anisotropy information.

The motor tract is one of the indicators of PD that can reveal the pre-symptomatic physiology as well as the pathology progress. Another medical imaging used for study of the pre-symptomatic phase is the *transcranial ultrasound*. In these medical images the analysis of SN physiology and the Putamen one from the PET image are the methods currently used to complete the research. In [Marck 2008] the hyperechogentricity of SN is studied by using another medical imaging, the nigral ultrasound. The scintigraphy, more

precise the cardiac metaidobenzylguanidine (MIBG), provides 89.7% sensitivity and 94.6% specificity among the PD and multiple system atrophy (MSA) patients based as well on the same anatomical area.

Lateral Substantia Nigra (SN) pars compacta abnormalities can be detected in high field strength MRI even in early PD [Graeber 2009] cases, corresponding to known anatomical distribution for the dopamine produced.

There are also several *dopaminergic tracers* like F-dopa, DAT ligands and the vesicular transporter (VMAT2) that determine the PD affected patients. These studies depend on the accuracy of the DAT imaging or Datscan, used as a diagnostic marker in Europe [Marck 2008]. Another imaging modality form the DAT nomenclature is currently studied. Even if the results reveal that the distinction between different PD types and similar diseases cannot be made yet, the Fluorodeoxyglucose imaging is viewed as a technique with high possibilities in this area.

2.2 New possibilities for biomarkers

For introducing *new biomarkers* and validating them we need to analyze their *potential* and their correlation with the disease, in order to test their reliability and reveal their new contribution in both pathological and clinical context. For a new marker to be valid there are several aspects that must be fulfilled [Marck 2008]:

- Meaningfulness/Relevancy of the marker to the disease
- The performance characteristics of the marker
- The degree of generalization of the marker

The first criteria is linked to the disease in pathology and clinical relevance. A correlation on the disease severity and the marker values expresses a relevant estimation of the pathology of a subject. When taking the performance of a marker into account, the accuracy accomplishments are analyzed. Any marker should be able to perform on all patients and in any conditions, providing the generalization needed. This aspect is affected by the effect of disease, age, sex, medications and race or environment. The influence of any of these aspects on the biomarker should be minimal.

The CT image is used for PD due to the high detail provided for SN tissue and the MRI, due to the functionality information, because only the functionality is able to capture the physiopathology manifested by trembling. This functionality is able to bridge *the gap between the clinical aspect represented by the tremor and the pathology* at the motor tract level. The pathology, even if it is not measurable, determines measurable changes at the functional level, expressed by the anisotropy values on the MRI images.

The usage of medical imaging as biomarker delineates a complex process with several informational levels. An important aspect of this process is the validation phase. In concordance with the three requirements for a biomarker presented earlier, our approach has three main tasks:

- Clinical marker(s) that provide the biomarker with meaningfulness
- Pathology highlighted at the image level, representing the physiological change
- Correlation function with the PD severity - performance and generalization

Using these steps we might be able to bridge *the gap between the clinical markers and the pathophysiology* by using the medical image at the neural tissue level. Some of the widely accepted markers at this level include MRI images for their capacity to distinguish abnormalities. The DTIs are used for the olfactory tract studies, in addition to the volumetric ones. The CT images like the SPECT and PET imaging are used for visualizing perfusion abnormalities and amyloidal burden [Berg 2008].

2.3 Head Medical Imaging used for PD

From all the clinical symptoms used as markers in neurodegenerative diseases, the trembling is one of the specific symptoms, making the distinction between other neurodegenerative diseases and Parkinson's Disease. The symptoms are produced by pathology changes visible at the image level as physiological abnormalities. The neuromotor tract is the one affected by the pathology in this case as the tremor is generated by abnormal changes at this level. The PD research in this case is concentrated on the head neuroimaging.

The head imaging contains the clinical markers as part of the pathology, determining changes in the physiology of several anatomical structures involved on PD development. The detected abnormalities on the physiology of these structures, the possibility to extract concluding information is to be tested and in the case of a detected correlation, a validation is mandatory. The extracted features could be affected by the exactitude of the process, the image resolution and/or the visual environment. Under these conditions the pathological values together with the disease correlation could be biased.

From the head medical imaging, the structural computerized tomography (CT), as well as the magnetic resonance imaging (MRI) are both used to supervise PD. According to [Seibyl 2005] there are three ways of using imaging for PD: neuroimaging for disease detection (diagnosis), monitoring the progression of the disease and evaluation of treatment. The CT and MRI imaging, together with other medical imaging are usually stored in Digital Imaging and Communications in Medicine (DICOM) format.

By processing the medical image we acquire supplementary specific information on each image, but medical standards, like DICOM, include more information in a file than just the usual general standard image. There are several medical imaging standards, providing, together with the digital image, some basic information about the patient and the protocol used to acquire the image.

Digital Imaging and Communications in Medicine (DICOM) is a standard used for managing medical imaging. This standard has its own file format definition and a network communications protocol [1752 2008].

From the technical point of view, the relevance of the imaging format resides in the automatic detection of the volumes of interest and the management of the medical images for the fiber growth algorithm. For the medical image processing part working with the DICOM format implies knowing the specifications of this standard. This medical image format consists of a header file and the image information encapsulated in the same DICOM file. The header file contains information about the patient and the technique used for acquiring the image, as well as some characteristics.

Another file format used for medical imaging is called Analyze, but in this case for each instance of a medical file two files are created: one containing the header information (*.hdr file) and the other containing the image data (*.img) file. The DICOM file format has the advantage of compressing the files in order to reduce the image size [University 2008] [1752 2008]. The header file for this protocol does not contain as much information as the DICOM one: it does not have any information regarding the acquisition method and

protocol parameters (e.g. angulations for the acquisition plane, the series type for the image, the slice number, the diffusion direction).

The DICOM header is contained in the first 794 bits of the digital image. This header contains the image characteristics, as well as image information about the parameters of the scan. In this file we have the elements 0002:0010 encapsulating the information about the structure of the image data described by the 'Transfer Syntax Unique Identification'. The image characteristics are stored for some color images (e.g. RGB) on 3-samples per pixel (one each for red, green and blue) and the monochrome images store on only one sample per image. For each image there are 8-bits (256 levels) stored or 16-bits per sample (65,536 levels), even if some scanners save data in 12-bit or 32-bit resolution. A RGB image that stores 3 samples per pixel at 8-bits per can potentially describe 16 million colors (256 cubed) [1752 2008].

These characteristics determine the format of the DICOM header, providing the physical characteristics of the images and the contextual information regarding the patients, used for statistical purpose.

2.3.1 The current usage of medical imaging in PD

PD indicators regarding the specific pathology of the disease involve clinical markers and biomarkers. In vivo imaging, especially on the nigrostriatal dopaminergic system, is able to reveal progressive dopaminergic neuron loss in PD. The study presented in [Marek 2009] uses $[^{123}I]\beta - CIT$ or $[^{18}F]$Dopa imaging to determine the PD progression. Positron emission tomography (PET)/$[^{18}F]$Dopa and single proton emission computerized tomography (SPECT)/$[^{123}I]\beta - CIT$ are widely used to determine clinical trials and to measure striatal dopamine activity. According to this study, dopamine lost can be detected using imaging even before the detection of the symptoms. Dopamine transporter imaging using PET and SPECT has been used to determine progression of PD at the dopaminergic neurons level, correlated with clinical values on UPDRS. These longitudinal studies using medical imaging showed only minimal correlation, due either to medications or the fact that PD was in an early stage. In this case it is susceptible to affect the UPDRS measurement because the disease does not progress linearly. Another study, using the same imaging, shows that normal striatal from the imaging can be used to make the distinction between the PD patients and those with similar symptoms [Piccini 2004]. Positron emission tomography (PET) and single proton emission computerized tomography (SPECT) are mainly used to highlight dopamine transporters and dopa-decarboxylase in the Putamen area [Mizuno 2010].

Using clinical markers the cognitive aspects are usually tested with the current PD diagnosis system. On the olfactory tract, the studies reveal a correlation with the disease [Scherfler 2006]. In this study the diffusion weighted imaging (DWI) and the trace diffusion tensor (Trace D) are used because of the diffusivity aspect that offers capability to determine the structural integrity of the nervous tissues without prior study of the same patients. The voxel clusters that represent the olfactory tract are correlated with the PD severity, as the diffusivity for the affected cases is higher compared to the controls. Using fMRI to investigate brain activity related to the olfactory process is presented in [Westermann 2008]. This study revealed that PD patients even in early stage of the disease can be detected by using this imaging technique.

The midbrain is another clinical marker that is the subject of several approaches, as it contains the SN, perceptible at image level as well. The SN area, producer of dopamine, is one of the most studied PD biomarkers. The midbrain pathology detects dopaminergic neurons lost from SN area. The homogeneity on this area studied using fMRI technique combined with the dopaminergig responses from the PET imaging [Duzel 2009]. Another

imaging method, the Diffusion Tensor Imaging (DTI) has been considered in studies on mice concerning the same area, the SN, only to determine that indeed a correlation with the disease exists, even for early cases of PD [Vaillancourt 2009]. These studies acknowledged as well that fractional anisotropy represents another important marker of the SN transformation due to PD evolution, discovered with post-hoc analysis.

The imaging represents a non invasive method backed up by the post-hoc study. Corticostriatial connections have been studied in primates with applicability in humans to prove that the DTI images are able to track the neural fibers and reveal connections on humans as well [Lehericyr 2004].

2.3.2 Functional imaging vs. Structural imaging

Functional imaging is used because of its ability to disclose the neurotransmitter function, the metabolic process and the immune responses so that PD pathology can be determined. PET, SPECT, magnetic resonance spectroscopy (MRS) and functional magnetic resonance imaging (fMRI) are the functional imaging used currently for PD study. The neurochemical alterations and chemical connectivity are detectable on functional imaging. The nigraostrial integrity in particular is studied using these type of PD imaging providing meaningful insights of the pathology of the disease regarding both motor and non-motor dysfunction from the striatial dopaminergic transmission [Nandhagopal 2007].

The structural imaging on PD is linked to the brain anatomy associated with the disease progression, volumetric and molecular composition of brain tissue [Parkinson's Disease 2010]. From this type of imaging the ones used for PD are the MRI, ultrasound and optical coherence tomography (OCT). As structural changes are not currently detectable on PD patients, these types of imaging are not used as biomarkers.

One of the MRI imaging technique that is able to provide structural information, together with anisotropy and diffusivity is the Diffusion Tensor Imaging (DTI). The DTI is used in the study of the brain as it offers the possibility to examine areas of the brain at the axon level. The water molecules in the biological tissues have special comportment. The DTI image technique is a medical image type where the diffusion of the water molecules is used to follow the neural impulse through the brain tissues. Following the water molecules in several directions provides an image of the impulse propagation in those directions. The more directions followed, more complex the image of the neural fibers conducting the neural impulse is.

Taking into account these functional aspects that follow the physiology regarding the neural impulses, the DTI provide the information necessary to follow the dopamine flow for the motor tract. In this manner, we can study the pre-motor manifestation as well for the mild cases, as the dopamine is lost up to 50% until the specific symptoms are detectable. This lost is discernible at the neural level.

2.3.3 Diffusion Tensor Imaging (DTI) specificity

Naturally the water molecules do not have a regular movement, but at the tissue level, the diffusion of these molecules can be anisotropic. Due to the fact that the axon of a neuron does not usually cross a myelin membrane, the water molecule will be diffused along the neural fiber. Using this propriety and by analyzing the diffusion in different directions, the main neural fibers can be detected by tractography. There are different types of DTI scans, depending on the diffusion parameters following different acquisition protocols.

2.3.3.1 DTI sequences characteristics

Even though all the DTI images are based on diffusion, they each have specific characteristics. The fact that each DTI scan has a different purpose, supplying us with different characteristics that can be combined and can complement each other provides a more accurate analysis contributing on PD marking.

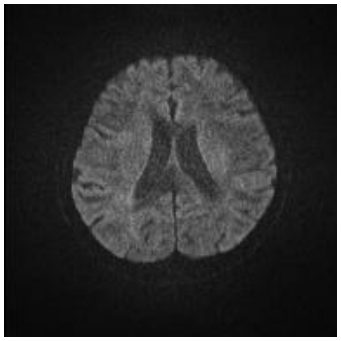

Figure 2.4: Echo planar axial 2D image example

The Echo Planar (EPI) sequence provides a volume image for each diffusion direction. These DTI images have been generated using a value for B0=800 and several diffusion directions compose for each direction a volume image. The *B value* is used for changing the level of sensibility for diffusion - diffusion weighting value (e.g. standard value for adults is 1000 and for children is 500) [Rorden 2008].

The diffusivity is computed in one direction at the time for all the directions used in the acquisition protocol (for all the different gradients). DTI images use tensors for expressing the direction for the diffusion. The tensor is defined using three directions that generate eigenvectors and eigenvalues. Working with more diffusion directions, determines better emphasized features, but in this manner, noise can be induced more easily among the features and the trust degree in the extracted data is diminished [Curran 2005].

By using these images the anisotropy and diffusivity values can be computed. The measures for these characteristics are represented by the Fractional Anisotropy (FA) and the Apparent Diffusion Coefficient (ADC). The FA provides the value of the water diffusivity, making the distinction between tissues. The ADC represents the directionality of the diffusion and it reveals the fiber orientation inside the brain. These values are computed for each volumetric image that has been segmented into Grey Matter (GM) , White Matter (WM) and Cerebro-Spinal Fluid (CSF).

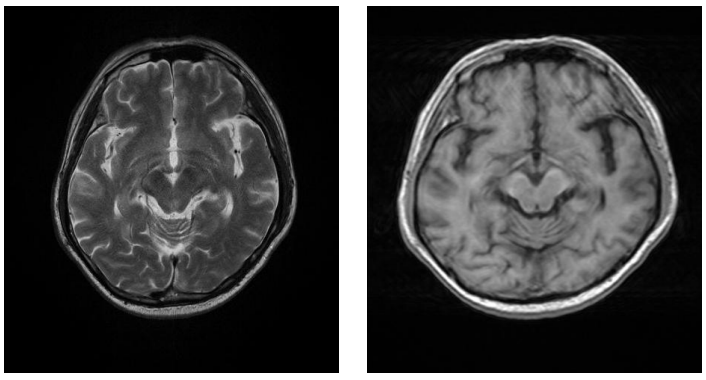

(a) FLAIR (b) T_2

Figure 2.5: Axial slice of 2D FLAIR in 2.5(a) and T_2 in 2.5(b) examples

Analysis and processing for FLAIR imaging (e.g. 2.5(b)) is usually performed for suppressing the CSF in multiple sclerosis (MS) analysis.

T_2 DTI overlay and T_1 imaging sequences have a high level of detail and are usually used by the neurologists in the diagnosis process. The acquisition process in this case is the same one used for the Axial FLAIR images (e.g. 2.5(a)). When collecting the data from the scanner, turning the gradients to their maximum value generates a more accurate image but it can introduce eddy currents as well. These currents manifest as distortions in the image acquired by the scanner [Rorden 2008]. Computing of the FA value must take into account the motion effect induced by these currents and in order to overcome the effect, eddy currents correction function is needed.

As the DTI images are characterized by their water diffusion anisotropy in the tissues and by combining the data from the images taken in several directions (the ones generated by the tensor values) we can compute the FA and ADC and construct the neural fibers. Among the DTIs that are a good source of information, the EPIs with the tensor information provide a good illustration for neuromotor study.

2.3.3.2 Echo-planar images(EPI)

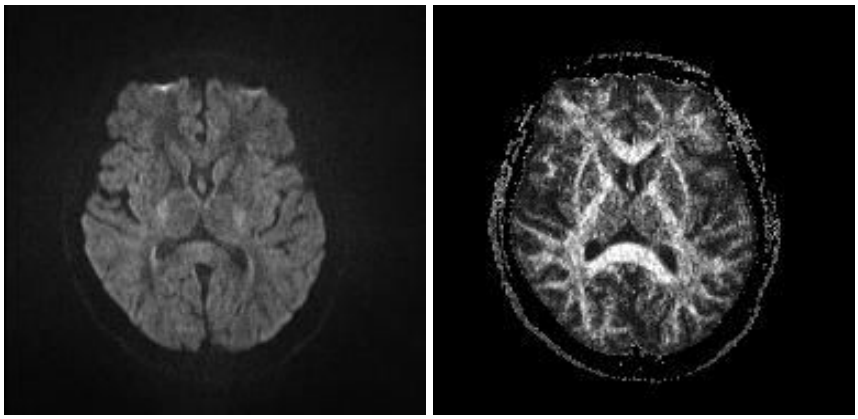

Figure 2.6: EPI and FA example images for the same patient, highlighting the Putamen contour due to the dopamine flow on the FA image.

From the DTI images the EPIs (Fig. 2.3.3.2) are among the ones with the lowest resolution. The advantage of this type of DTI is that they contain the tensor information as matrixes, giving the actual orientation of the water flow defining the brain fibers.

The tensors are obtained as a result of water diffusion on the neuronal fibers and they are stored as matrix representing the diffusion directions. This information is able to provide the diffusion direction and the anisotropy values stored as tensor values. To make use of this information, limiting the value of the anisotropy for noise elimination represents a solution. The tensors are computed using the diffusion directions and the B0 image as ground truth. Serving as directional-related indices, the tensors offer information regarding the angle between the current location of a fiber and the possible evolution of the same fiber.

This type of image is not appropriate for the anatomy extraction and analysis, but the tensor and anisotropy values stored represent the bottom line of fiber reconstruction the source for processed FA and ADC images.

Fractional Anisotropy images (FA) result from the computation of the anisotropy level for each voxel on the EPI image s(Fig. 2.3.3.2). They contain not only the anisotropy

values, but also the color code for it. This type of image represents the diffusion direction inside the fibers. Because of that, the Putamen area, one of the targets for the dopamine flow, is well defined and stands out well contoured with high anatomical detail.

The values computed for FA (equation 2.2) take into account the λ value that represents the eigenvalues determined from the diffusion tensor vectors [Facon 2005]. This value is expressed using the ADC value from equation 2.1.

$$f_{ADC} = \frac{\lambda_x + \lambda_y + \lambda_z}{3} = \lambda \tag{2.1}$$

where $\lambda_x, \lambda_y and \lambda_z$ represent the eigenvalues computed from the x, y and z tensors on these directions.

$$f_{FA} = \sqrt{\frac{3}{2}} \sqrt{\frac{(\lambda_x - \lambda)^2 + (\lambda_y - \lambda)^2 + (\lambda_x - \lambda)^2}{({\lambda_x}^2 + {\lambda_y}^2 + {\lambda_z}^2)}} \tag{2.2}$$

The formulas of these parameters represent standards from the diffusion point of view. By computing the value of each of these parameters at the voxel level, we obtain the FA and ADC sequences (see Fig. 2.3.3.2). In the case of equality on all directions for the value of the FA, a low anisotropy is revealed and if its value is produced by a high level in certain directions, a high anisotropy is present. The movement of the water protons and their diffusivity at the voxel level is determined by the ADC value.

2.4 Conclusion

Imaging biomarkers are usually used as surrogate endpoints and, to date, they have limited utility in clinical trials and practice. Although they are very promising, they do not accommodate the preclinical problems. In this situation, the medical imaging currently does not constitute an alternative to the current clinical procedure. The fact that the imaging biomarkers offer the prospect of more efficient preclinical studies and clinical trials denotes one of the motivations in studying them.

The experts present at the Radiological Society of North America (RSNA) sponsored Imaging Biomarker Roundtable envision that by 2025 imaging biomarkers could be integrated into clinical practice [Radiological Society of Norh America 2009]. Concentrating on prognosis, rather than diagnosis within the imaging biomarkers, this approach designates as one of the needs in the area, together with the need for a standardized system for new imaging biomarker validation and evaluation.

The need for specialized hardware and/or software for image biomarkers management illustrates another point discussed at the 2009 RSNA meeting where the final conclusions included: a collection of imaging biomarkers integrated into clinical practice and trials, new imaging biomarkers, a repository of biomarker images and an infrastructure for both validation of the biomarkers and future development.

We propose using the medical image as biomarker by itself, not as a source to follow on the medical image one of the existing clinical biomarker, but using its own information as a tool or as a comprehensive valorization of the physical or surrogate markers. DTI have not been used even as surrogate markers in PD, just to determine the level of anisotropy.

For an imaging biomarker to be successful it must be linked to the disease that is targeting, to provide an accurate measurement that is reproducible and to be able to be used in clinical trials [Smith 2003]. This represents our next step for proposing the DTI as a PD biomarker: correlation with the disease, measurement of the image provided features and validation on a consistent database.

Chapter 3

Applicability of medical image as biomarker

Contents

Current PD biomarkers make use of the medical image for analyzing detectable symptoms of PD. Analyzing the pathophysiology of the disease, we propose a new approach by exploiting the information from the medical image as PD marker. The current chapter proposes a feasibility study to determine three main aspects:

- Does the medical imaging contain the pathophysiology needed by PD detection ?
- Can the PD physiology be extracted from the medical image level ?
- Is there a correlation between the extracted physiology and the clinical scale ?

The first aspect is linked to the capacity of medical imaging to illustrate the physiology changes specific for PD. Specificities of medical image can provide these aspects. The PD physiology, even if present and targeted by one of the medical image modalities, should be exploitable, as we need these features extracted for analysis. From another standpoint, the physiology, even if extractable from the medical imaging, is relevant only if correlated with the disease severity. This correlation at the feature level is the first hint that the information is capable to express the pathophysiology.

For establishing the possibility to use medical imaging as biomarker, these evaluation steps provide the circumstances for it. All the elements should be applicable independent of the subject and/or specificities of the patient, repeatedly and reliably. Therefore, including a test, unbiased by the specifics of the patients, represents another aspect of the feasibility testing.

3.1 Premises that determine our approach

Considering the existing biomarkers with their capabilities and flaws, introducing a new biomarker requires an analysis of the possibilities and the coverage of the theoretical aspects that back up the study. For PD, the theoretical aspects are linked to the specific pathology and anatomy-physiological aspects surrounding the studies linked to the disorder.

As presented in the PD analysis in the previous chapter, the dopamine lost determines physiological changes after the PD onset. Thus, the study of this physiological change can be used as a marker to determine early clinical diagnostic of the disease. In PD, there is a relatively poor dependency between the degeneration of the dopaminergic nigral cells and the clinical phenotype. This aspect does not permit the direct usage of a dopaminergic measure as biomarker. A measure derived from this degeneration and liked to the symptomatic process can be used in correlation with the clinical diagnosis. *This correlation, between the clinical established diagnosis and the possible biomarker has to be proven first.*

Taking a backward approach and considering the causes of the physiological deterioration and equally the effects that they produce by translation onto specific PD symptoms, we propose the approach presented in figure 3.1. For determining the early development of the pathology, we are analyzing the process that leads to the clinical decision. As the specific symptoms causing the diagnosis are detected on the motor stage, the specific symptomatic area of the pathology is reached once the motor tract is affected. This physiological process starts much earlier as its effect is only detectable when most of the dopamine cells are lost. Detecting the amount of the dopamine lost at the non-symptomatic stage, even on the pre-motor level, should be possible by analyzing the deterioration of the motor tract. Studying this deterioration at the SN tissue level, physiologically affected by the PD, we can bypass the intermediate steps by determining its correlation with the clinical phenotype and provide an earlier diagnosis at this point on the pre-motor stage.

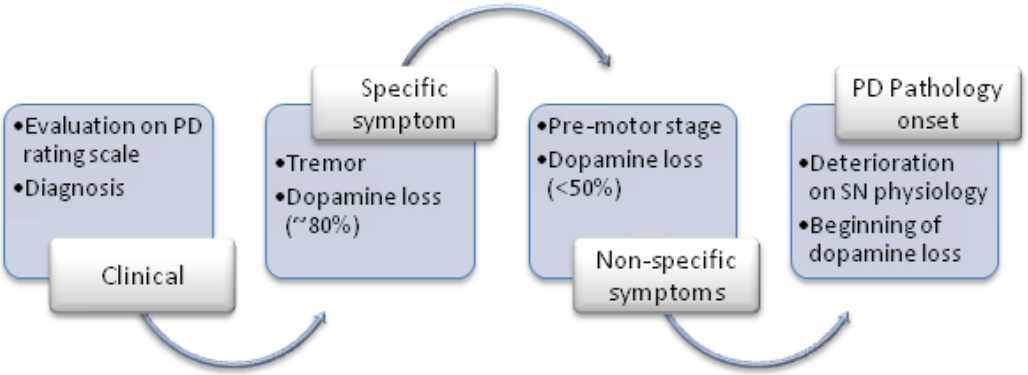

Figure 3.1: Reverse Pathology to Clinical process

Disclosing the PD affected area on the medical image acknowledges it as a biomarker,

as it is not used for a physical biomarker, as a tool, but as information source itself. The pathology determining physiological changes represented at the image level must establish its validity and reliability. The Fractional Anisotropy imaging, one of the DTI imaging techniques, contains the dopamine flow directionality, computed for each visual point- at the pixel level. This imaging technique developed for dopamine study incorporates information on the dopaminergic data comprise by the protocol method. *Finding a correspondence between information from this imaging type and the clinical diagnoses illustrates a manner to determine the feasibility of our study, proving not just that the imaging contains the PD pathophysiology, but also that it is detectable and correlated with the current diagnosis scale.*

The hypothesis that represents the essence of our feasibility study is captured in figure 3.2. The pathological manifestation presented as physiological changes can be recognized as abnormalities at the image level. We contemplate the employment of specific medical images that withhold the essential information regarding the condition of the neuromotor fibers, determining the clinical symptoms. Using this logical path, we integrate the clinical aspect into the physiological change.

Figure 3.2: Hypothesis linking the pathological manifestation with the clinical symptoms

The figure 3.2 is a schematic representation of our proposition for the medical imaging specific manifestation of PD. The physiological functionalities at the tissue and cell level have a correspondence at the symptomatic level and the patient is experiencing the result of the clinical PD manifestation. The deterministic link between the pathology, physiology and clinical aspects for PD is not abrupt and must be taken into account. When studying the possibility for introducing biomarkers, the links between the three stages are targeted.

In performing the feasibility testing we are constructing it on the main element accountable for PD: the dopamine. We envision two levels of information for this key element:

The dopamine content inside the whole brain as the neurotransmitter affects more than the motor tract, its value should affect other neural tracts as well.

Specific value for dopamine on the neuromotor fibers because its downfall determines one of the specific symptoms leading to PD diagnosis.

The distribution of dopamine on the whole brain can be studied using the anisotropy level. Significant changes among PD patients and control cases for the FA and/or the ADC management are translated into practice to provide further study. Focalizing on the source of dopamine, the SN, as it is the first area affected by the PD, we should obtain more accuracy and additional data from the pre-motor stage. Before studying this area we need to establish that the extracted area is relevant for our study.

The relevancy of the SN area is given by significant differences between PD patients and controls, like in the study conducted on the whole image. The differences among patients having different stages of the disease are relevant as well, making the disease grading. A further study determining the existence of a correlation between the relevant established areas with PD, is to conclude the feasibility test. As the purpose is to determine if the image can be used as a biomarker, the correlation study is mandatory to be immune to the demographic parameters and consistent among tests, providing reliability and repeatability.

The ground truth for the correlation test is the H&Y value for each patient obtained by cognitive testing.

As for the medical images chosen for the feasibility testing, they are DTI sequences: the EPI withholding the tensor information, essential for the neuromotor tract and the FA providing the anisotropy with the diffusion directionality. The two techniques, even though both DTIs, are complementary as information. The database with its particularities and image protocol determine the approach and the intended purpose for each imaging type in our study.

3.1.1 Database and image protocol

For all the medical images, the protocol and acquisition parameters determine the image quality and are relevant for the study from both technical and economical points of view. *Medical Images* are digital representation of aspects on human anatomy - body parts, tissues, organs - by using advanced techniques and processes that allow visualization inside the body for clinical purpose [Dictionary 2010].

For the medical standard in DICOM format, there can be several imaging types included in the files (*.img file). These imaging types represent the actual visual information displayed (e.g. MRI, ultrasound, X-ray image, tomography). When we refer to a certain *imaging type*, we actually mean the protocol used (e.g. DTI, fMRI) to capture the image appertaining to a specific imaging modality (e.g. MRI).

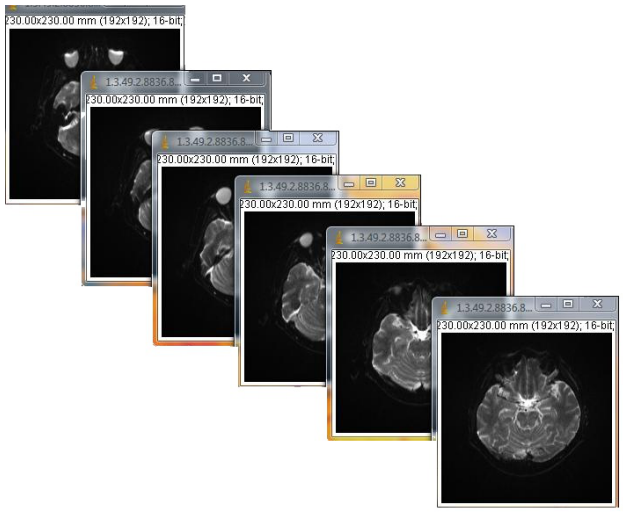

Figure 3.3: Example of consecutive axial views - slices of a stack

A number of 68 patients diagnosed clinically with PD and 75 control cases underwent DTI imaging (TR/TE 4300/90; 12 directions; 4 averages; 4/0 mm sections; 1.2 x 1.2 mm in-plane resolution) after giving informed consent. The heterogeneity of the patients - Asians, Eurasians and Europeans - can also be used to characterize a general trend for PD prognosis. This aspect targets the demographic parameters that have to be indifferent for a biomarker. It should be applicable on any type of image, regardless of the patient. For the EPI images, the DTI images acquired for each gradient direction, we have 351 images (e.g. Fig. 2.4) that represent slices of 4mm of brain axial section taken in 13 directions, represented as 12 tensor values from 3.1 and the B0 image, for each step (one step represents a position on the vertical brain axes). In this case, we have 27 images that constitute a single 3D brain

x	y	z
1.000000	0.414250	-0.414250
1.000000	-0.414250	-0.414250
1.000000	-0.414250	0.414250
1.000000	0.414250	0.414250
0.414250	0.414250	1.000000
0.414250	1.000000	0.414250
0.414250	1.000000	-0.414250
0.414250	0.414250	-1.000000
0.414250	-0.414250	-1.000000
0.414250	-1.000000	-0.414250
0.414250	-1.000000	0.414250
0.414250	-0.414250	1.000000

Table 3.1: Gradient Values used in our protocol for diffusion images

volume - containing all the possible sections in order to show a complete image of the brain volume.

In our study, we are working with medical image sequences or slices - consecutive sectional views (see Fig. 3.3) - stored in a medical standard format, together with the acquisition protocol, the information regarding the patient and the clinical establishment where the acquisition/diagnosis was performed. If for 2D management we are working with pixels, when representing digital images as numeric format, at the volume level we are using *voxels*. A voxel does not possess its position encoded, it is relative to the other voxels, but it contains the information referring to the empty and occupied space in a volume. It possesses sizes that make possible volume estimation. The voxel can be defined as a three dimensional pixel, a volumetric pixel. For a correct 3D representation of the sequence of 2D acquired images, an alignment between the consecutive image slices is needed, in order to obtain smooth and continuous anatomical details.

For each patient, we dispose of 351 EPI images representing 12 diffusion directions and one without diffusion each of them composed of 27 slices. This is the reason why the tensor computation, which takes the 12 directions into account, has a good accuracy.

Due to the complex structure of the medical image encoding encapsulated by the DICOM format we need to take the useful information from the header file. During the processing and analysis level we only make use of the image itself, without the additional information. This is the reason why we transform the image from the DICOM format to Analyze and store it as stacks of images that represent an entire brain volume for each patient and each modality.

3.2 Proposed scientific approach

According to recent research, the areas providing PD pathological and relevant physiological changes revolve around the motor tract and the fact that due to dopamine lost, it is not functioning properly. As presented in figure 3.5, we adopt a bottom-up approach starting from the clinical level and analyzing the pathophysiological changes at the image level to determine if the information from the image can constitute a marker for PD. In this manner, taking into account the three perspectives- clinical, physiology and pathology - we can provide a more accurate view of the disease. The graphic representation starts at the clinical level with the movement disorder, determined by the neuromotor failures,

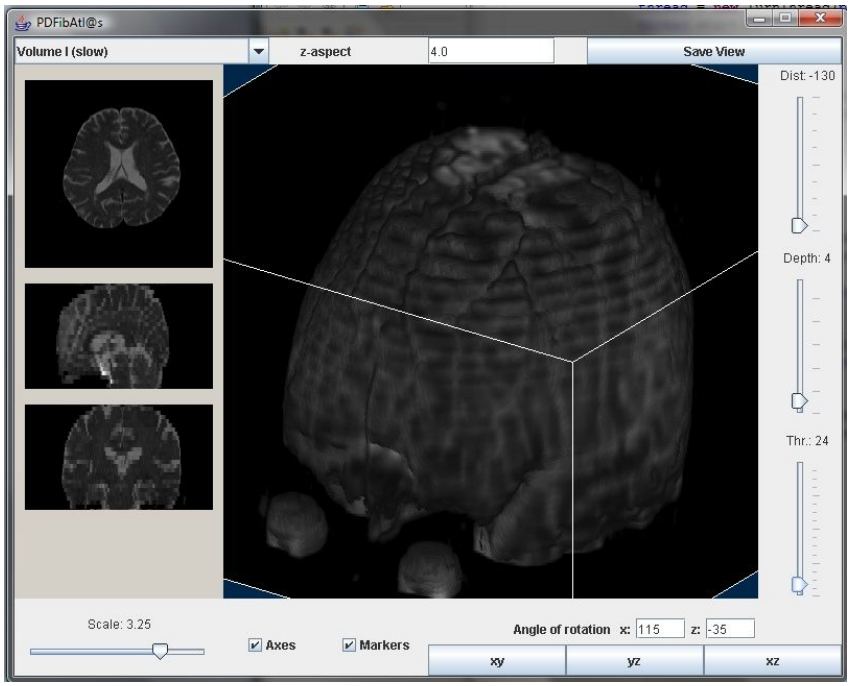

Figure 3.4: 3D Image Stack generated with imageJ

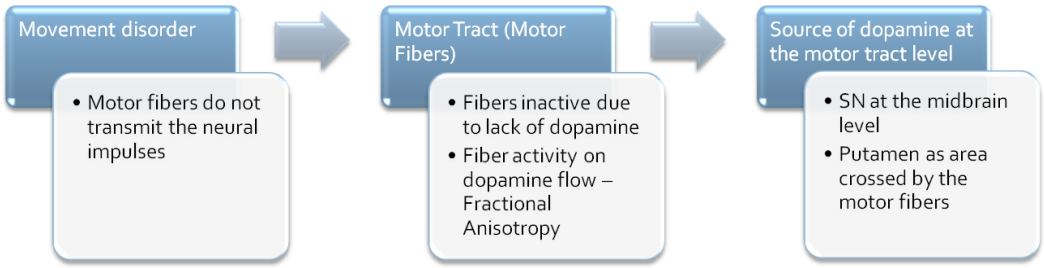

Figure 3.5: Feasibility approach- factors determining our study

which are not just symptoms, but clinical diagnosed PD markers. At the motor level, the physiology determines the fault on transmission at the neural fiber level. The source of these inadvertence is determined by the pathology factors of the disease that reside at the dopamine source, Substantia Nigra (SN) and the area where the neural impulses do not reach anymore, the Putamen.

The main challenges on the scientific demarche is represented by the feasibility studies involving the research for determining that the image is able to provide the needed patho-physiological elements. The way to exploit the extracted information is linked to the fact that the gap between the image level and the PD knowledge must be broken by bringing meaning into the extracted features and introducing value to the visual data.

Taking these aspects into account, there are several elements to be achieved when using the images:

- Finding the clinical aspect needed to be exploited

- Taking the image that best reflects the clinical aspect
- Finding the image feature that contains the physiology that is affected by the clinical feature
- Extracting and Exploiting the image feature
- Finding the interpretation that emulates the pathology changes

As the clinical symptom determining current diagnosis is the trembling, this aspect is also able to make distinction among other neurodegenerative diseases and PD. The motor tract affected by dopamine, determining the clinical symptoms, is best found in Diffusion MRI, as it provides the anisotropy value for the motor fibers functionality.

The reverse engineering at the analysis stage of the features require bridging a new gap at the knowledge level and determining the way the physiological process of PD affects the extracted features so that we can bring the Proof of Concept (POC) to the Proof of Value (POV) level.

3.3 Preparing the Feasibility testing

Taking a small cohort from our database for preliminary tests (21 patients and 25 control cases) we perform several tests. In this case the amount of images is enough for performing a well-documented study. Depending on the DTI type of image, their resolution and their quality changes. The DTI images with high accuracy on the anatomical detail, even if the resolution is not the highest, provide good primary data for segmentation.

Using at first a global approach, we determine if the anisotropy level on the whole brain is correlated or visibly affected by the PD pathology at a measurable level. The fact that the FA imaging conceals the anisotropy information is perceptible as the image is produced by computing the anisotropy values based on the equations 2.2 and 2.1. The question at this point is if the anisotropy information is valuable and can be further used.

Further on we concentrate our study on a more localized area as we study the midbrain. The study of this area containing the source of dopaminergic cells, the SN, represents a higher level of refinement for the tissue physiology. Manually segmenting this area provides the values unaffected by the segmentation process, determining the brute correlation with the disease. The anisotropy values and the directionality are both represented on the FA image. The FA color code stands for the direction of diffusion.

- Red - left right (LR)- Red channel values for the fibers oriented from left to right in the FA color image;
- Green - anterior posterior (AP)- Green channel coding for the fibers oriented from anterior position to posterior in the FA color image;
- Blue - up down (UD)- Blue channel coding modality for fibers going from upwards to downwards inside the head volume in the FA color image;

The fact that the neuromotor tract has, according to the medical knowledge, an Antero-Posterior diffusion orientation, corresponds to the green channel color code on the FA image. This aspect provides an idiosyncrasy for isolating the targeted tract.

For both general and detailed studies we are using volumetric data. On the whole brain approach we align the slices and compute then the anisotropy. For the midbrain study, we perform additional segmentation on the aligned slices before computing the anisotropy. The slice management and volumetric image handling represent the initial steps of both approaches.

3.3.1 Managing the image stacks and slices

There are several stages in managing the volumetric data at the image level. The provided images in DICOM format are pre-processed using spatial normalization [Ashburner 2000] and robust smoothness [Kiebel 1999] implemented in statistical parameter mapping (SPM). Afterwards the resulted data is segmented according to the brain tissue type using the fMRI module that implements the Tairarchi atlas. The white matter (WM) image is further used for the computation of FA and ADC values for each voxel, providing new images.

For statistical studies and inter-patient correlation, we store several information provided by the DICOM image and header file into a MySQL database along with a list of features. From the header file we are interested in extracting the the patient information, angulations and the type of the image that we are handling.
Parsing the images from a folder we are detecting the patient identification number (patient id) and the image type. Once we have the DTI image that we need, we identify the slice number and the direction of diffusion, if required (only for the EPI images), and we can proceed at constructing the volume for the patient that we are dealing with.
All these preliminary steps are performed using imageJ [1] toolbox in Java. We further transform the images from the DICOM standard encryption into Analyze format, because the image is separated by the additional information and for supplementary changes we can manipulate just the image, without the rest of the data. In these conditions, normalization on the images using Statistical Parameter Mapping (SPM) is faster.
Each patient has stored in a separate folder several DTI imaging types. Specific data for each image is stored as well (e.g. image size, type etc). When working with EPI images representing the same axial slice taken using different diffusion direction, determined by the tensor values, we place them on the same stack. For constructing an image volume on a specific direction, we take from each stack the slice belonging to the designated direction. Different directions have different gray levels and are more or less affected by the surrounding noise.

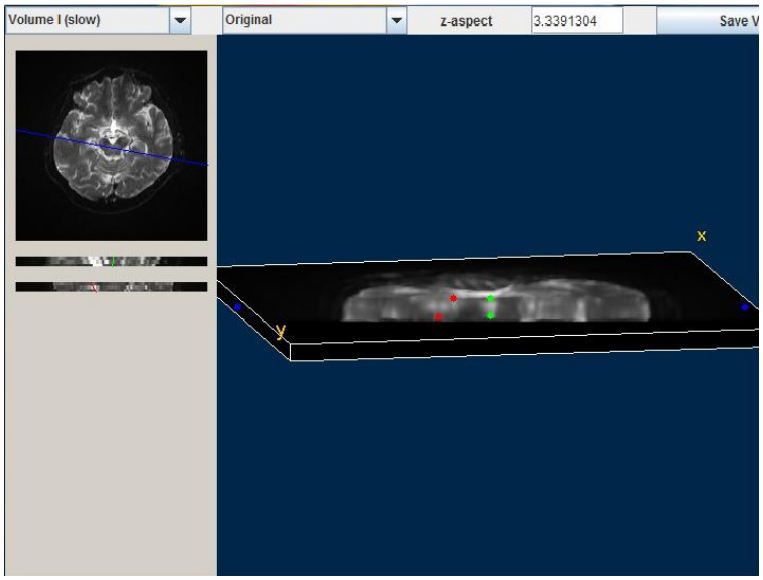

Figure 3.6: Slice view in 3D - voxel level

[1] imageJ - http://rsbweb.nih.gov/ij/

This aspect is present in all the head images and it is due to the fact that the patient can slightly move while breathing and/or trembling. The resulted image is most of the time blurry. To overcome this effect, we apply the spatial normalization and inter-slice alignment for constructing the 3D image.

Each image is additionally preprocessed using the Anisotropic diffusion filter for a better delineation of the anatomical elements. Using the pixel intensity uses a contour plotter function implemented in imageJ to extract the brain from the background image.

The diffusion FA (equation 2.2) and ADC (equation 2.1) values are computed for each image and the mean value for the stack. The value that characterizes the image is the mean value from all the values of the stack. The functions that compute the FA and the ADC values are created in Matlab by Craig Jones [Jones 2008] and use the FA/ADC equations from 2.2 and 2.1. These new sequences developed using either directly the pixel/voxel information, or those produced by the scanner, represent the value of the anisotropy and the diffusivity for a certain patient. The information provided at the image level is low-level and we are extracting it for further usage together with medical knowledge for diagnosis and prognosis.

3.4 Preparing the image for processing

Digital image processing is concerned with working with programs that manage the digital images in order to modify their characteristics. The methods implemented by such a program take as input images and provide the same number of images as output.
The digital image processing domain refers to transforming an image f in another image g by applying a function to it. The first and most used technique is to apply a specific operator ϑ so that:

$$g = \vartheta(f) \text{ [Sonka 2009]} \tag{3.1}$$

In this case, the operator is meant to perform a specific task but to preserve the image information. These operators are part of *mathematical morphology* and are usually used for the preprocessing step of the image systems to remove noise, artifact, to enhance certain aspects as the contours. The image operator ϑ must satisfy two properties: distributivity and translation invariance. These properties guarantee the preservation of the initial image attributes. The distributivity assures that the effect of the operator on the combined image can be deduced from the individual image and the translation invariant offers the same result on a translated image as it does on the original one [Sonka 2009].

Mathematical morphology is used for image processing and analysis as it offers the possibility to represent any translation invariant operator between complete lattices using elementary morphological operators. We are using the morphological operators at the preprocessing level of our approach.

In our system we need several elements of image pre-processing for a good image quality, before processing. This is prevailed with morphological operators, together with segmentation algorithms and de-noises filters. Our main concerns are linked to the movement artifacts from our images that must be eliminated for a proper analysis. When placing the images on a stack, the alignment between the slices is highly needed. This process accommodates the 3D volume with a regulate volume and an adjusted contour for the anatomical volumes.

The medical images represent transversal slices of the head. Depending on the imaging angulation, there are several sectional views that provide human body images: axial view (Fig. 3.7(b)), sagital view (fig. 3.7(a)) and coronal view (Fig. 3.7(c)). The 2D images (ex.

Fig. 3.6) that represent consecutive sectional views compose a 3D image, a volume (ex. Fig. 3.4).

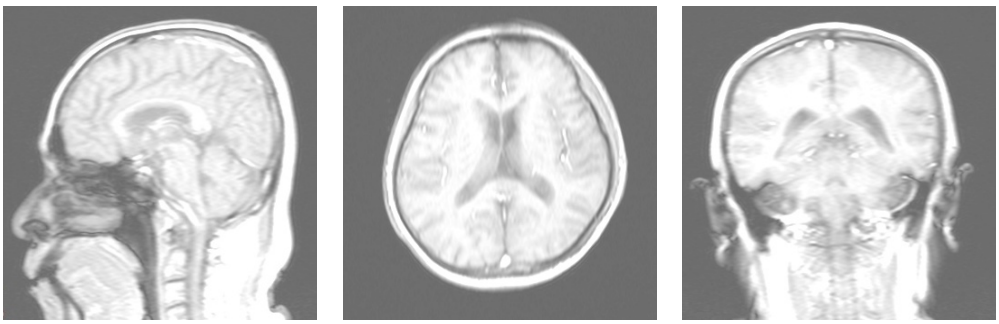

(a) Sagital slice (b) Axial slice (c) Coronal slice

Figure 3.7: Head MRI slice views

For the axial plane, the images that we have in our database are taken in AC/PC plane - Anterior Commissure/Posterior Commissure. This axis is significant from the anatomical point of view and it is used by the radiologist because it is distinguishable in all the MRI images. The sagittal plane and the coronal one are not used by our approach.

3.5 Feasibility study

In this research part of our study we are using existing dedicated systems for medical imaging handling. This provides stability to our methodology as we are not concerned at this point with the technical aspects of the processing. We use the Matlab provided suite for the global test and imageJ for the midbrain analysis.

Statistical Parameter Mapping (SPM) is an academic software toolkit used for analyzing functional imaging data by image processing and analysis [Guillaume 2008]. In our approach, we use several functions provided by SPM. We necessitate segmentation features in order to perform bias correction and spatial normalization at the same time as tissue segmentation. In combination with VBM5, which performs region-wise volumetric comparisons among several subjects, SPM5 requires images that have been spatially normalized. For revealing the physiological elements we require the images to be segmented into different tissue classes. The smoothing process offers us a clearer image which is necessary prior to performing statistical tests [Friston 2000].

Voxel Based Morphometry (VBM) is used in our proceeding at the data processing level. We use VBM5 in our proposition as it complements itself very well with SPM5 toolbox expanding its capabilities. It uses previous segmentation for further analysis [Gaser 2008] performing a voxel comparison for determining the tissue concentration. Its disadvantage is the susceptibly to registration and segmentation errors.

The image must be preprocessed before VBM5 is applied, as it does not work for all medical imaging protocols. This pre-processing is done in our case using SPM5. The functions from the brain extraction module are applied for our images and for normalizing the GM and WM images. With VBM, registering the brain to a template and smoothing the result by applying an average value for each voxel, between itself and its neighbors, overcomes the differences between brain anatomies.

3.5.1 Global image information analysis on the whole brain

The medical imaging processing tools using SPM and VBM run under Matlab 7.0. These toolboxes provide us with the segmented images and the pre and post processing steps corresponding to our study. The script that computes the FA and ADC takes the segmented tissue images, using the B0 value and a threshold of 50 for the diffusion values (the default value), delivers the diffusion tensors values.

The processing level requires several additional parameters that need pre-setting for the SPM function to generate the tissue maps [Yushkenvich 2008] [Fillard 2002]. The Eastern Asian brain maps for the segmentation phase is one of the parameters. We choose this particular map because it is the closest one to the population content in our database, but it is nevertheless restrictive. Regarding the bias regularization, another SPM segmentation parameter, we use the heavy threshold for this purpose, as it eliminates the surrounding noise.
The segmentation process generates grey matter (GM), white matter (WM) and cerebral spinal fluid (CSF)-see Fig. 3.8. The tissue segmentation is evaluated by assessing the result of the segmentation, the segments - the GM, WM and CSF. The volume obtained by putting all the resulted segments together is the stripped brain, without the skull area. We eliminate the skull as it influences the FA and ADC values afterwards.
An optimization for the brain images is represented by the normalization of the image to a standard space. This is completed by matching the grey matter to a reference one and eliminating, in this manner, the skull [Friston 2000].

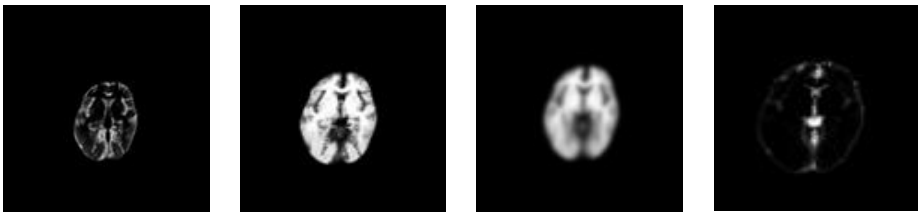

(a) GM (b) WM (c) WM smoothed (d) CSF

Figure 3.8: Images Processed:GM, WM, Smoothed WM and CSF

In figure 3.9, we illustrate the requirements from the VBM functions before beginning the processing procedure [Yaasa 2004]. Using SPM functions attains these requirements. Performing normalization for an image in the warping process, disturbances introduce some differences. Modulation is used for compensating these differences. By performing modulation the amount of grey matter is preserved in the normalized image. (E.g when a lobe has half the volume of the image in the template, then during normalization the volume could be doubled, but the voxels will be affected in this case because their number will be doubled). Using the modulation process the coordinates in the normalized image will be restored to their original values by using the deformation field values [Friston 2000].

For the normalization process, we can use one or more template images. The algorithm minimizes the sum of squares difference between the image and the templates. The first step creates a match between the images of the head with the skull. The next step performs a matching between the brains and registers the result. The registration step uses a Bayesian framework that searches for the solution that maximizes the a-posteriori probability [Friston 2000]. At this point, in the SPM segmentation algorithm, the deformations are estimated for the modulation part.

The registering process for the tissue probability maps and the processed image uses a

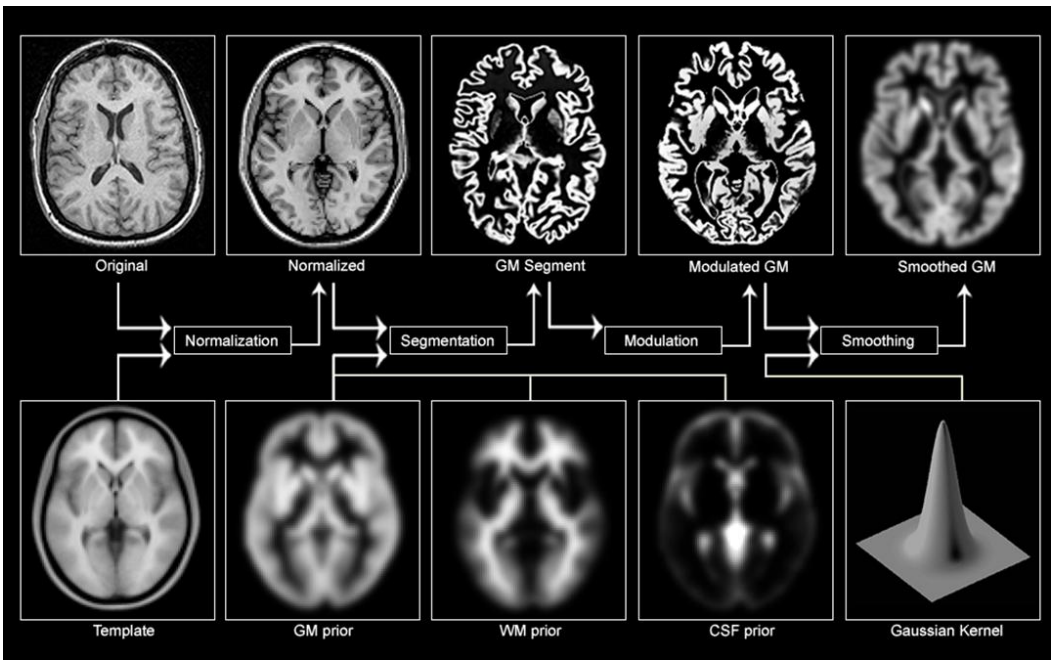

Figure 3.9: VBM Pre-processing requirements [Yaasa 2004]

minimization of the sum of the two terms -the two images. This process is performed by the warping function. For this function, the portability of the data and the parameters are used. We obtain a smoother deformation. Having a smaller value for the cutoff allows more detailed deformations to be modeled, but the processing time is longer [Friston 2000].

We use a smoothing function from the SPM in order to eliminate the noise or deformations acquired during processing. The function performs the smoothing using the Gaussian kernel. Pathology detection with deformation-based morphometry is integrated within the pattern theoretic approaches - deformation maps of the variations in normal anatomies based on continuum mechanics [Thomopoulos 1994].

The segmented images obtained, the brain maps, are used afterwards to characterize each patient from the three perspectives. We are computing the anisotropy values for these types of images. After eddy-currents correction a valid segmentation is possible on T_1 and T_2 images, but we are more interested on the EPI images, as the tensor information is comprise within.

We tested a different DTI image to determine those that offer not just clarity, but meaningfulness for the disease. The information stored by each imaging type has a different meaning. For the FLAIR DTI images we only perform the tissue segmentation and spatial normalization with the Statistical Parameter Mapping (SPM5) and the Voxel Based Morphometry tool (VBM5) on a stack of images constituted by all the 19 slices acquired (see Fig. 2.5(a)). The resulted images constitute a volume image. Afterwards, the diffusivity functions applied on each processed image determine a mean value for all the images that represent the same tissue, characterizing the whole brain. This imaging type is not complete enough for our study, as it does not provide the anisotropy or other fiber related data.

For the EPI images we obtain a value for each tissue type on the 27 images stack. Characterizing the entire volume (see figure 3.4) of the brain, we compute the average values of these functions on all the images. The gray matter (GM) and white matter (WM) segmented images are used afterwards to determine a value to characterize the entire volume. The analysis using VBM5 is done next when the FA and ADC values are computed

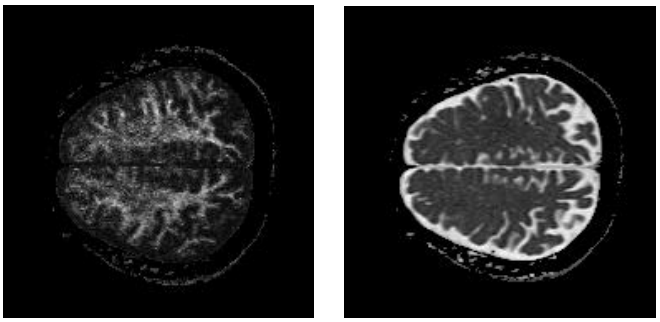

(a) FA image (b) ADC image generated

Figure 3.10: FA 3.10(a) and ADC 3.10(b) example of generated images

as well. An angular correlation is used to overcome different intensities inside the slices due to the diffusion and to achieve similar image brightness for all slices. Even with additional optimization on the obtained images, the final result does not provide the same quality as the one generated directly by the scanner.

Even with the additional algorithms including spatial normalization and Bayesian coefficients for maintaining the deformation ration at the anatomical level, the processed images have a low resolution. After the atlas-based segmentation into gray matter (GM), white matter(WM) and cerebro-spinal fluid (CSF), we store these images. The stacks generated at this level are then transformed into Analyze format for further analysis.

3.5.1.1 FA and ADC computation

After tissue segmentation performed on the brain image the current working images are the white matter (WM), the gray matter (GM) and the cerebral spinal fluid (CSF) for all the types of images used. The images containing WM and the smooth modulated images with WM are then used for FA and ADC computation (Fig. 3.10).

FA is a useful measure in the DTI images as it reveals the connectivity at the brain level. Again, for all types of images the values are taken and for each patient an average is computed for expressing the values at the volume level. The values used for providing the images in figure 3.10 are computed using the equations 2.2 and 2.1 on each slice of the volume. The mean value obtained from all the slices for the FA and ADC represents the information that we are studying for determining the anisotropy and diffusivity.

The image analysis is using two parameters: FA and ADC. The obtained values must be close to the value of 1 [Chan 2007]. For our images, we obtain an anisotropy average of 0.56 for each slice image and of 0.52 for the whole brain on the GM images. For the CSF images we have a lower value, as expected, and for WM slightly lower values than for the GM.

Augmenting these values demands changes in the processing and the pre-processing as well. These results depend on the data processing but also on the diffusion values and the tensor directions. When performed on more diffusion directions, we obtain higher stacks and better accuracy as well.

For evaluating the analysis we are using the H&Y scale (see annex D) where the Parkinson patients are annotated on a scale from 1 to 5, according to the severity of the disease. We are trying to achieve the same classification using the FA and ADC values like the one in the H&Y scale, making the difference between the affected cases and the healthy

ones by computing the values for the parameters on the patients as well as on the control images. Different severity degree for the disease, expressed just like in the H&Y scale, can be determined by the analysis functions.

3.5.2 Localized study on the midbrain anatomical area

Analyzing the green channel from the FA color images to determine if the fibers running in the AP direction are similar for all the cases or if there are degradations for the PD cases. Segmentation of the midbrain area does not aim on accuracy, but on limiting the image informational volume from the whole brain, to a smaller area of interest. Therefore, we segment the midbrain manually by determining a box-sized volume that includes the needed anatomical area. This process does not introduce additional noise or artifacts during the image handling, permitting an independent analysis of the brute value of the anisotropy. This value serves further to determine if a more precise automatic detection affects the information by inducing artifacts or eliminating part of the relevant data.
The easiest way to analyze the green channel is to generate the histogram for the area. The histogram represents the number of pixels that have a certain intensity: $N(b_i)$

$$P(b_i) = \frac{N(b_i)}{N} \tag{3.2}$$

where N represents the total number of pixels.

Based on the fact that the neuromotor tract, according to the brain pathology, follows the anterior -posterior direction, we perform a color analysis on the volume of the midbrain roughly extracted, in order to see whether the fibers starting from this area oriented in AP direction have a correlation with the H&Y scale.

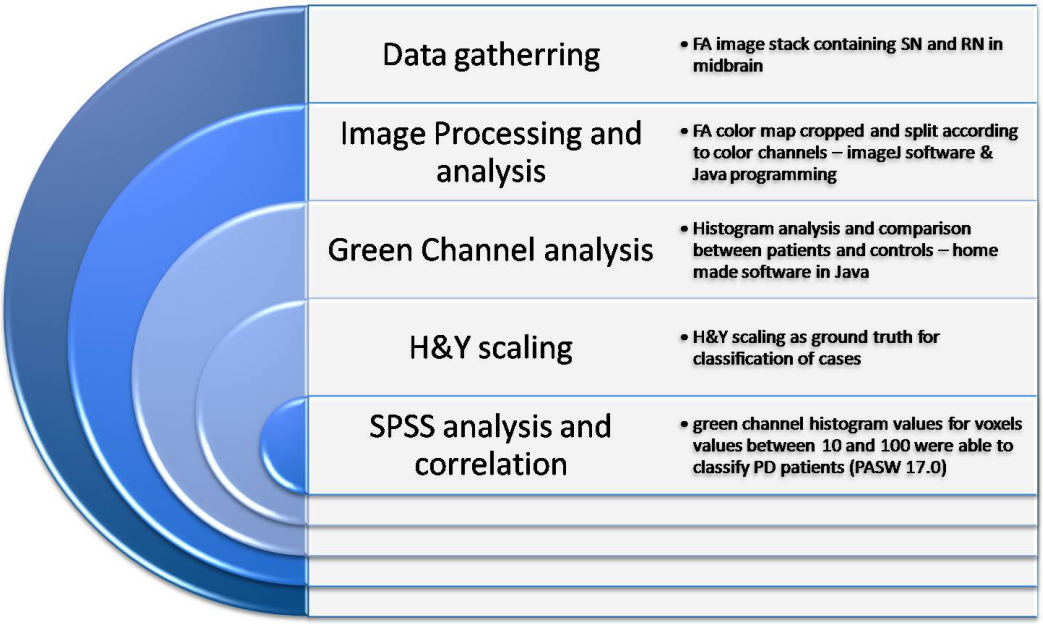

Figure 3.11: Green channel analysis

Figure 3.11 represents the main aspects in the analysis of the green channel. We make the rough detection of the midbrain area and compose the volume of interest on the EPI image. Placing the determined volume on the FA image for the green channel extraction, we perform an alignment between the two image types. Once we split the obtained FA volume

Test nr	H&Y [avg]	Age		Male/all	
		Patients	Controls	Pat	Control
1	2.312	64.5	59.37	11/16	6/16
2	2.375	63.31	60.93	9/16	9/16
3	2.375	64.06	58.5	8/16	7/16
4	2.467	62.75	61.5	9/16	8/16

Table 3.2: Test batches characteristics [Teodorescu 2009b]

on the three-color channels, we consider just the green one for generating the histogram and extracting the values for the intensity range of interest. This range is chosen in a way that we can exclude the noise. We estimate it in between 10 and 100 units. The histogram-ranged values are then correlated using PASW 18.0 (Predictive Analytics SoftWare, formerly SPSS-Statistical Package for the Social Sciences) tool with the H&Y values.

This analysis offers the opportunity to see if the PD and the correlation between the disease and the level of green affect fibers starting from the midbrain area. This level of green represents the anisotropy level and this particular area is one of the PD affected ones. Correlated with PD, as the motor tract represents most of the fibers going in AP direction, represents a correlation between the physiology and the clinical level. In this case the anisotropy level, if correlated with the H&Y scale represents an indicator of the disease at the midbrain level. Therefore, we are able to determine that the starting point for the fibers we need to grow is relevant for our study.

3.5.3 Test parameters and characteristics

Testing procedures must assure that they are sensitive to our parameters and robust to other exterior factors. Thus, we construct several testing batches by varying parameters that we need our test to be robust to. We apply this procedure for the demographical parameters, as shown in table 3.2. In order to evaluate the different stages for data processing, we introduce several testing groups - testing batches - constituted by random cases so that we can evaluate the robustness.

We prepare four test batches from the 42 patients available - 21 PD cases and 21 controls. Age variation can affect the disease by introducing brain atrophy and making the neural fibers harder to detect. This is the reason why we introduce this factor as a parameter in our tests. The patient's gender can affect the detection as the female have smaller skulls. The detection and segmentation of the images is then more difficult. Together with these parameters, the H&Y value represented as the severity degree of the disease could affect the anisotropy.

The test groups are chosen so that one of the demographic parameters varies and the others are correlated among patients and controls. Big differences on the results from one test to another reveal the sensitivity of the test to the demographic parameters. A consistent test for all the test batches is not sensitive to the variation parameters (see table 3.2). If the testing procedure has similar results on all the test groups, we can further analyze the results of that particular test, depending on its interpretation and input data.

3.5.3.1 Green Channel analysis on the midbrain area

For the green channel study, we dispose of a batch of 42 cases (21 patients and 21 control cases). From this batch, we take out randomly 5 cases from the patients and 5 from the

Test nr	Independent Sample T-Test		Correlate Bivariate		ANOVA	
	Left	Right	Left	Right	Left	Right
1	24.4	74.0	13	8	0.872	0.937
2	12.2	69.3	7	8	0.906	1
3	75.5	65.3	3	6	0.937	1
4	83.6	71.4	7	7	0.937	0.906

Table 3.3: Study on Green channel on the left and right side [Teodorescu 2009b]

controls in order to eliminate the subjectivity - the influence of the demographics - from our study (table 3.2).

The T-Test is applied on the histogram obtained from the midbrain area by eliminating the noise. This procedure aims at detecting a correlation between the value of the histograms and the H&Y values. The histograms represent the anisotropy value on the AP direction in the midbrain area, which should indicate the motor fibers and in PD could be characteristic for the progression of the disease. Examining this correlation, we vary the age difference between the patients and controls and the number of male subjects in the testing batch, as well as the mean value on the H&Y scale.

The results on the green channel study performed on the patients with the characteristics from table 3.2 are presented in Table 3.3. This table contains several T-Test methods and their results regarding the correlation between the green channel histogram values and the H&Y values.

The Independent Sample T-Test detects a large variation between the values of P, which can be explained only by the variation of demographic characteristics of the patients. We consider this type of study to be affected by demographic characteristics, especially on the left side (e.g 12% - 83 %). Similar range of variation is obtained on the Bivariate test, visible on the left side as well. The ANOVA test is the most consistent one and has good results, being reliable and adequate for our purpose. This initial approach representing the feasibility study with the associated results, have been presented on the RSNA conference [Teodorescu 2009b] from the clinical point of view. This study confirmed that there is a correlation among the anisotropy on the AP direction and the H&Y severity scale. We interpret this correlation as a link between the fibers staring from the midbrain and the H&Y scale. The fibers at the midbrain level that are affected according to the PD severity, represented by the H&Y scale, are with no doubt the motor ones. Therefore the motor fibers starting from the midbrain are indicators of the PD severity and have AP directionality. The ANOVA test provided a good correlation, but not applicable for quantization of the disease.

3.5.4 Feasibility conclusions

The global testing evaluates the FA and ADC values on the entire brain volume. The mean value on each patient does not offer an average able to distinguish between the PD and the control patients, therefore we need to further focalize our study.

The FA and ADC images obtained computing the corresponding values reveal a good image of the dopamine paths. The Putamen is better defined on the FA image and a more insightful study on this area is possible. We will use the image without skull, as it interferes with the management of the information, as shown in the global image testing. Managing

the whole brain, there are several aspects that arise from our study for further processing:

- Removing the skull as the bone tissue interferes as intensity with the tissue voxels, introducing additional noise
- Removing the noise in the image surrounding the skull - the artifact
- Focusing the research to a volume of interest: at the hemisphere level or midbrain level

PD affects both brain hemispheres, but is more obvious in the left side of the brain, therefore an analysis on this side should be more relevant. For the whole brain analysis, the anisotropy information exists at the image level, but as the volume includes several neural tracts, a more focused study should perform better.

At the patient level, preparing for the feature extraction algorithms we needed landmarks applicable to all patients for guiding our algorithms without any interference from the patient variability. These elements, together with the hemisphere detection algorithms, set up the elements for the automatic detection of the location where we need to apply the feature extraction algorithms.

From *the study of the green channel* the AP positioning of the fibers reveal a pattern that follows the disease severity that indicates that the dopamine flows in this direction, validating the medical premises and the fact that it can be followed on the image. Studying the flow at the midbrain level by using the FA values from the image highlights the fibers that we need for study. The aspects revealed by the localized study on the source of dopamine provide another perspective, backing up part of our premises:

- The dopamine affected by the PD pathology is represented by the FA
- The FA image is capable to provide accurate information on the PD pathological state
- The information at the FA level is correlated with the PD severity evaluated with cognitive testing

Analyzing the two feasibility studies providing a general view and a PD targeted one, if using the whole brain proved to be inefficient for emphasizing the abnormalities, when zooming in the affected area, we obtain a correlation with the PD. The predisposition of the study inclines to the local approach, where the non-specific PD areas are eliminated and in the remaining information, the PD affected pathology represents a higher percentage. In these conditions a more accurate segmentation of the midbrain should determine a higher or stronger correlation with the disease.

The final conclusion for the feasibility study is that DTI medical image not only incorporates the information needed for PD pathology, but that this information is exploitable. These aspects determine the liability to use DTI imaging as biomarker as it is able to provide information that reflects the PD pathology. This type of biomarker offers proprieties from the clinical end-point marking as it is further tested on diagnosis process. The results provided by these studies and the methods for testing provide a comparison value for further tests determining additional inferences.

3.6 From feasibility to information processing

Considering all the elements highlighted by the feasibility testing, the conclusions and the difficulties encountered at the medical image management, the transition from theory to

the technical aspect we make next the transition to processing. This implies several perspectives: manipulating the specific medical image standard with the exclusive information provided by it, removing the unwanted data and extracting the parameters for processing and estimation, as well as eliminating the specific variations introduced by an automated system handling different patients. If for the first perspective we are able to estimate and elaborate a method for managing the standard and extract the medical information, for the second perspectives, we are able to define algorithms and methods only after analyzing the requirements.

Using a specialized library providing the elementary digital image processing and analysis functions is justified as it offers medical image reading and writing, basic filters and plug-ins. It enables us to use algorithms already implemented and to begin our processing at a higher level of data management. The *ImageJ* [2] represents our choice as it is a useful open source Java based library conceived for medical image processing and analysis that offers the possibility to develop a reusable module application integrable in the library as a plug-in. It also has the advantage that developers using this library are continuously updating it by offering their contribution as plug-ins. The entire functionality is encapsulated in *ij.jar* for easy integration and usage. In this manner the newest algorithms can be tested with the available images and further development can be made without rewriting the basic existing functionalities. Besides, it offers the possibility to test several methods before deciding on a certain algorithm or approach by directly analyzing the results.

For each image type, we are targeting the PD related features, specific elements that are better portrayed in that particular DTI imaging type. Managing different imaging types determines different techniques for pre-processing and analysis.

For the DICOM management, we use a Java program with imageJ features, able to extract and store the information from the headers to MySQL tables. Beside the patient identification number, the header file provides information of the slice number and the image type stored and the diffusion direction for the EPIs. The slice number is used for volume construction, together with the diffusion direction.

Once this first aspect of the automatization for the images is solved, we determine the unwanted data inside each DTI image type, based on the experience from the feasibility testing. An analysis of the DTI images that we will further use defines several aspects taken into consideration:

- Eliminating the skull from all the images
- Eliminating the surrounding noise
- Treating in an automatized manner all the patients

Eliminating the skull is a requirement detected on the global testing because it affects the FA and ADC values, as the intensities of the pixels for the bone tissue are similar to those representing the WM. The surrounding noise represents pixels that have the same effect as the skull. In regard to the patients, their heterogeneity is benefic for validating our study, but an automatic approach needs to consider all the variations that generate dissimilarities that can affect the research and management of the images. In this area there are several aspects as well:

- The demographic aspect
- The position in the image for each patient

[2] ImageJ website -http://rsb.info.nih.gov/ij/ - last accessed on June 2010

- The orientation of the brain for each patient

In view of the demographic aspect we have constructed the feasibility testing method, but this aspect on an automatic approach poses the same problems: different brain sizes dependent on the patient's sex and/or age, different brain atrophy determined by the geriatric factors in elderly patients and different brain shape susceptible to the patient's race. These elements together with the positioning and orientation inside the image constitute new tasks for the pre-processing level of our study.

3.6.1 Skull removal

Examining the performance of the methods used in the feasibility study we determine the elements needed for managing our imaging for an optimal result. The methods used for global feasibility testing have been applied to the EPIs, as they are the ones providing the elements for the fiber growth. The FA images require this procedure as well, not only for skull removal, but for eliminating the noise as well. The atlas-based skull removal method offered by SPM and the entropy based one (MedINRIA) performed better on the feasibility stage, than the atlas method provided by Slicer, which was slow on our images.

Before applying the skull removal method on the images we use a contrast enhancement of 0.5% for a better volume delineation. The angle for the enhancement is limited in our case at 60 degrees minimum, to avoid highlighting the noise.

Using the atlas based approach (SPM) , the segmentation detects the skull using its position as the tissue surrounding the brain. With this approach due to the EPI image quality, some of the other types of tissue patches were removed or not correctly identified. This tissue is mainly the CSF, because it is placed next to the skull, but the result was also influenced by the patient variability.

The algorithm based on the voxel entropy (MedINRIA) [Fillard 2007] is affected by the exterior elements such as noise. This sensitivity did not provide a dependable result on our images.

Our own method is based on the positioning of the skull with regard to the rest of the tissue in the image. It uses KMeans classification for the tissue to detect the bone entropy corresponding to its tissue. It detects the position of the voxel cluster large enough to represent the skull and positioned on the exterior of the other large clusters. The KMeans method introduced in our approach is implemented in Java and was available as a plug-in in imageJ[3]. The FA image provides the size for the skull cluster. We used a four-class disposition to distinguish between the bone tissue, the GM, the WM and the CSF. The algorithm was not sensitive to the exterior noise, as we have applied previously a noise removal filter provided by the same library. All the values for the pixels outside the skull perimeter were considered as noise and faded into background.

After applying the removal algorithm the brain tissue constitutes the only information in the image. Estimation, analysis and processing on these images consider just the brain tissue state.

[3]KMeans in imageJ: http://ij-plugins.sourceforge.net/plugins/clustering/index.html - last accessed on June 2010

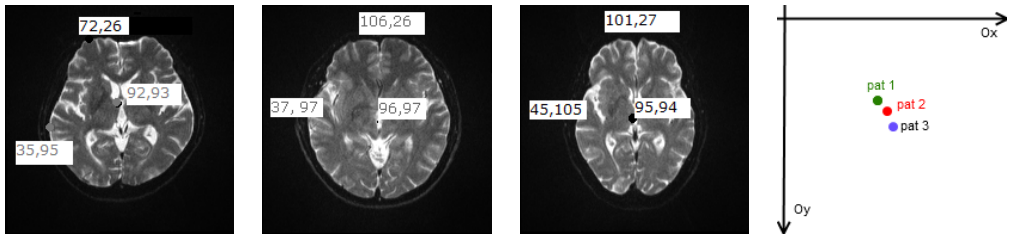

(a) Patient 1 position (b) Patient 2 position (c) Patient 3 position (d) Position of patients on the image

Figure 3.12: Variation in patient position inside the image

3.6.2 Inter-Patient variability

The automatization of the marker and accurate testing are dependable of the unitary management of the patients. The inter-patient variability treats the differences between patients and presents solutions for dealing in the same manner with all the images, independent of the patient that it belongs to. For proposing a solution for the variability, the variable involved has to be identified first. In this case, the variations are the result of the demographic differences and of the patient's positioning on the image.

The *demographic differences* are the main source for the inter-patient variability. These demographic differences consist in differences among patients due to sex, age or race. The difference resulting in the female skull being smaller than the male is due to the sex difference. The race difference is manifested as different shapes of the skull among Europeans, Asians and Africans. Another demographic factor is the age factor determining elderly patients that suffer from brain atrophy to poses different brain shapes and shifting of the anatomical structures. In these cases there are also anatomical regions that can be affected by other diseases or geriatric conditions. All the demographic factors determine different width and height of the brain volume resulted from differences for the brain shapes among patients.

The *positioning of the patients inside the image* determines different positioning for the algorithms handling the brain information. Figure 3.12 represents different patients and their positioning on the image coordinates (sub-fig.3.12(d)).

Another aspect regarding the inter-patient variability is represented by the differences among the volumes of interest, determined by different volumes of certain anatomical structures. The midbrain area is one of our volumes of interest and this structure is not immune to the inter-patient variability factor linked to its shape and volume. Figure 3.13 illustrates the differences among patients regarding the midbrain area shape and size, as well as its positioning relative to the whole brain volume.

The same differences are present for the Putamen as well, another volume of interest for PD pathology.

3.6.3 Intra-Patient variability

The differentiate development of the two hemispheres determines discrepancies on their volume and shape. This diverse development of the hemispheres is translated also onto the corresponding anatomical structures. These structures complementary to each hemisphere present different development in volume and shape. The variability from this standpoint is illustrated in figure 3.14.

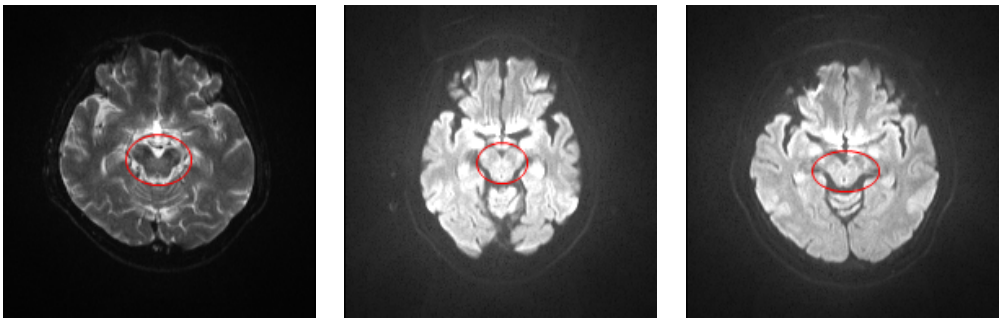

(a) Highlighted midbrain for patient 1 (b) Highlighted midbrain for patient 2 (c) Highlighted midbrain for patient 3

Figure 3.13: Differences in shape for the volumes of interest among different patients - highlighted midbrain area on EPI B0 axial slices.

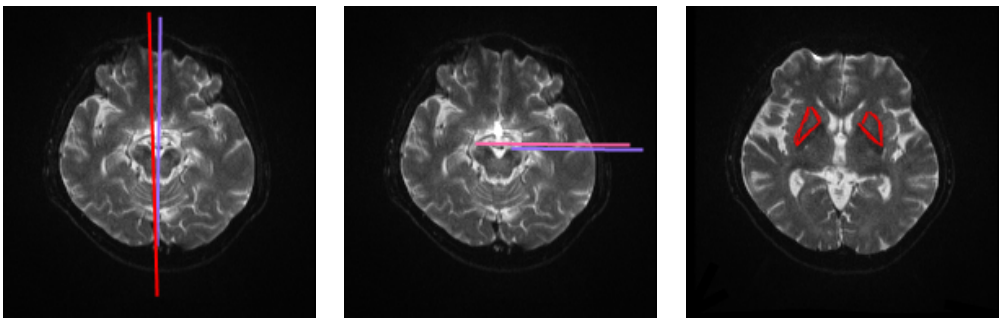

(a) Patient orientation on the image (b) Differences in midbrain shape and size form one hemisphere to the other (c) Differences in putamen size and shape between the two hemispheres

Figure 3.14: Orientation of the patient in the image in 3.14(a) and differences in shape for the volumes of interest for the same patient in 3.14(b) and 3.14(c)

PD pathology reveals distinctions on the manifestation of the disease for the two sides. Our study considers this aspect separating the two hemispheres and performing independently for each of them.

3.6.4 Using geometrical elements for solving the patient variability

For the patient variability we define a system of references based on the image landmarks, consistent for all patients. We consider introducing several geometry-related parameters able to determine the relative position of the brain and its anatomical structures in the image.

Having only the brain structure represented the whole image enables us to set landmarks based on the whole volume estimation, so that we can eliminate at least a part of the patient variability. We are retrieving *the center of mass* for the brain using an imageJ plug-in algorithm -object counter[4]. This evaluation of the position of an object on an image can be performed at 2D or 3D level corresponding to one slice or several. This landmark is

[4]imageJ plug-in Object Counter : http://rsbweb.nih.gov/ij/plugins/track/objects.html - last accessed on June 2010

able to facilitate an alignment among the patients and to define a central axis through each brain volume. The center of mass represents the solution for the relative positioning of the segmentation methods inside the brain volume. It is useful when determining the slice that comprises the anatomical region of interest placed higher or lower on the central axis of the brain volume.

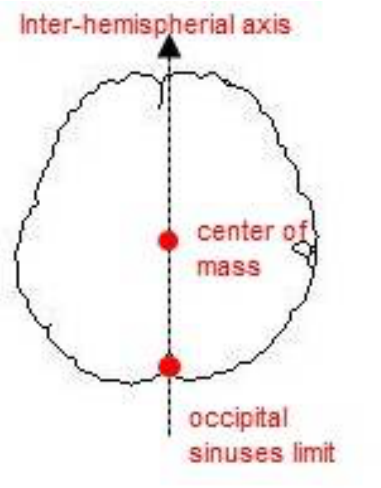

Figure 3.15: Brain edges detected for variability function evaluation

For determining the positioning inside the brain structure for each patient we need additional information regarding the orientation. This aspect is determined using the inter-hemispherial axis representing the axis delineating the two hemispheres of the brain for each slice.

3.6.5 Hemisphere detection

For an uniform handling of the patients, beside the center of mass at the volume level we need a definition for a plan view, a plan that integrates the center of the brain, making the distinction between the two hemispheres. Detecting this plan requires the outer boundary of the brain (Fig. 3.15). We analyze this contour as a variation function determining the maximum inflexion point on the function corresponding to the occipital sinuses at the base of the Occipital Bone of the skull.

This distinctive mark, together with the center of mass of the brain, determines a sagittal plan between the two hemispheres. In 2D, on an axial slice, the mark of the occipital bone and the center of mass determine a horizontal axis indicating the orientation of the brain in the image. This axis serves as inter-hemispherial limitation.

3.7 Conclusion and challenges

As the feasibility study revealed, the *midbrain area* anisotropy indicates a correlation with the PD severity. The pathology for the midbrain area determines significant physiological changes, detectable at the image level. This anatomical region is therefore one of the image volume of interest used for the neuromotor tract study. The study of this tract is possible only if fiber detection is possible.

The diffusion directionality, chosen and validated by the feasibility testing on the green channel, revealed significant information stored by the neural fibers situates on AP direction. The fact that the anisotropy level represents this information highlights the influence of PD on the neuromotor fibers. For an accurate extraction of the fiber tract needed for further study a second volume of interest is required. This necessity resides at the midbrain area, as several other neural tracts traverse it. The FA image that contains the anisotropy and the directionality cannot be used as guide in tractography because the tensor information resides inside the EPI. In this case we need as second volume of interest a structure traversed by the neuromotor tract and positioned on the AP direction from the midbrain standpoint. The PD pathology studies reveal that *the Putamen* area is one of the structures that meets our requirements and manifested sensitivity to PD. This area represents in our study the

second volume of interest.

Automatic patient management does not include variances due to the demographic elements and inter/intra-patient differences. The geometrical landmarks and the inter-hemispherial axis are our proposed solutions for these variances. An adaptive approach on the detection for the volumes of interest completes the intra-patient variability elimination.

The detection of the volumes of interest should be performed on the image where the neuromotor fibers are grown. The EPI nomenclature includes the tensor information used in tractography. This process determines the neural fibers by using the diffusivity directions. Our targets are the fibers from the neuromotor tract, starting from the midbrain area and passing through the Putamen. The midbrain can be detected on the EPI image, but not the Putamen. For the second volume of interest the FA image offers better information. In this situation the tractography requires a pre-registration process for the Putamen on the EPI volume.

Chapter 4

DTI information processing and analysis

Contents

Having already the context provided by the feasibility test and based on the existing scientific research, medical imaging, specifically DTI, is able to provide consistent information related to PD. The medical imaging information is also in concordance with the PD progression. Based on the theoretical premises studied in the previous chapter as feasibility tasks and considering the conclusions, a reliable study linked to clinical testing requires an automatic system. The aim at this point in our research is *to create a system totally automatic that can evaluate the PD severity based on the DTI imaging information* and we present in this chapter the methods for processing and analysis.

In these conditions, the premises for our approach reside in the previous chapters. As presented by the feasibility study, the SN found in the segmented midbrain area has an anisotropy value that is correlated with the H&Y values. A more accurate detection of the midbrain area, achieved by automatic segmentation, should provide better correlation. The correspondence illustrated by the anisotropy level, determined by the dopamine circulation on the neuromotor tract, is the targeted feature in our research for the image processing level. The module represents the entire information transition process from figure 4.1. There are several levels of management for the information enabling the medical image to be used as biomarker.

The first two steps in our approach have been resolved by the methods presented in the previous chapter, as they arise from the feasibility study determining the specific algorithms

Figure 4.1: Main steps from raw data to prognosis

for implementation. The third and forth step define the medical image information management as they represents the image processing methods and feature extraction. The methods developed for information management influence the final result of our study. These features should offer a correlation with the disease at least as good as the one determined at the midbrain level.

The processes performed by the algorithms from the pre-processing level to the analysis level can be situated both on medical image processing and image analysis domains. During *digital image processing*, we alter the images during the method development, as required by our algorithms, but specific processing elements are used by the algorithms in the pre-processing level. Managing medical image information for feature extraction can be included in the *Image Analysis* process. The algorithms performing image analysis are concerned with extracting information linked to the context of the image [Burger 2008]. The methods using these algorithms take as input images, but they generate as output either an image or numerical data. The methods from figure 4.1 can be included among image processing and/or image analysis algorithms.

The discriminative biomarker of our study is represented by the EPI and the FA imaging, as resulted from the feasibility analysis. We start by using EPI images, where using an automatic segmentation algorithm we extract the midbrain area. The FA Image stacks are used for automatically segmenting the Putamen. The registration is required for placing the segmented Putamen on the EPI stack for tractography. This process for determining the neuromotor tract uses the detected volumes of interest on the EPI, where the diffusion tensor are..

Prior to the detection of the volume of interest, there are several elements that need to be integrated in our automatic system providing the processing with the images and additional information for handling. The geometry elements, determined in the previous chapter, are used by the processing methods. Our automatization process using the DTI image starts by using the already available elements:

- EPI/FA images without skull
- The inter-hemisferial axis
- The center of mass of the brain X_c, Y_c, Z_c
- The position of the patient on the image (O_x,O_y,O_z)

The pre-processing level had to overcome the **low resolution** of the images. The same problem can affect the automatization of the detection process applied for the volumes of interest using the relative position of the anatomical structures. As reference point for this case we can use the center of mass of the brain (X_c, Y_c, Z_c), as its position is not influenced by the patient variability.

Another problem that we have to surmount is the human intervention by the segmentation algorithms. The segmentation methods have to detect the anatomical region of

interest on the axial slices. The volume representing the anatomical structure is obtained like the brain volume by generating the stack. Each axial slice provides a sectional view of a particular section of the brain, comprising different parts of the volumes of interest. Among the slices constituting the brain volume for segmentation we need the particular one (or several) containing the required anatomical structure. This specific slice represents for the segmentation algorithm the *slice of interest (SOI)*. In order to start the algorithms at the right place on the right slice, the position of this slice must be determined first. This position represents the placement of the axial plane (O_x and O_y axis inside the volume) relative to the coronal(O_x and O_z axis of the volume) and the sagittal (O_y and O_z axis of the volume) plane views on the O_z axis of the brain volume.

The detection on the central axis of the brain for the slice of interest represents the **algorithm for placement inside the brain volume**.

Inside each slice the brain anatomy consists of several structures. Finding the needed structure starts with determining its position on the 2D slice. This algorithm performs the **placement inside the slice** with identification of the right place for the volume detection.

Developing the proceedings presented in figure 4.1 we illustrate in figure 4.2 the refinement progression used for the information. This entire implementation of the automatic system representing the proceedings in this figure constitutes our prototype named PDFibAt@ls. The figure represents the information refinement hierarchical evolution, starting at the DICOM standard and finishing by providing the clinical PD value of severity. The midbrain and the Putamen segmentation require specific automatic algorithms at the processing level in the informational context. Our study is based on their accuracy at the anatomical level. In the processing procedures we use image processing and analysis algorithms for accurately determining the required information from the EPI images and further use it for fiber detection. The registration process is making the transition at the feature level. The information analysis at the feature level performs the tractography on the EPIs and extracts the neuromotor tract. By analyzing the fibers at the knowledge level, we determine the correlation of these features with the PD severity to distinguish the link with the disease and their relevance for our study.

There are several steps to be followed in transforming the information from the visual level into quantitative information. The pre-processing level prepares the image for the algorithms that extract specific information concerning the anatomy and pathology of the subject.

4.1 Context for DTI information processing

There are systems using DTI images in analysis and processing, providing different features and data for the user. Analyzing the performances of these methods on our database we are able to determine the capabilities of similar systems. We can evaluate the new prototype PDFibAtl@s including our methods by comparing it to the results obtained with the other systems. At the method level, the analysis provides the strengths and the weakness determining additional challenges four our information processing level.

All the systems presented are freeware and are specifically dedicated to DTI medical image usage. Additional systems have been tested, but the images either did not provide any result or the program closed during processing or even stopped the machine while processing the data. The systems presented here provided the best results for our images.

They are tested from several perspectives, corresponding to our steps, in the DTI information management steps:

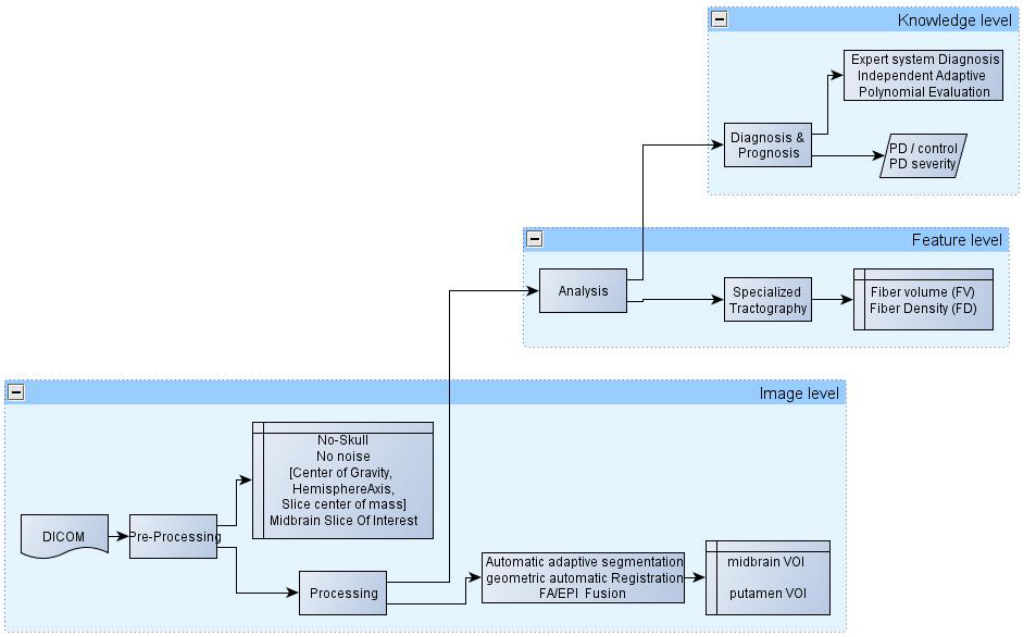

Figure 4.2: Proposed approach for image processing and analysis, the main informational level stages on our study.

- Management of DTI images (12 diffusion directions)
- Segmentation procedures
- Registration capabilities
- Tracking algorithms using one or two regions of interest

A global evaluation of the systems demands all the perspectives to be considered and additional validation from the neurologist based on the results. Local evaluation refers to an analysis of the methods implemented by the systems. A general presentation of the main capabilities of the systems precedes the presentation of the local evaluation in the context of each required task in our informational context.

The **MedINRIA** system[1] represents a French project by INRIA laboratory in Sophia Antipolis and provides a series of applications for medical image processing and visualization. As underlined by the Asclepios site, the main interest points provided by this software are the Log Euclidian metrics - metric for tensor estimation, HARDI - high angular resolution diffusion imaging, fiber tracking, block matching, diffeomorphic demons- defined in registration and DT-RefinD- registration technique [Vercaunteren 2008b].

The project is structured in independent modules, implementing different algorithms, that offer just specific features when needed: the DTI Track module or the tensor viewer module, the Fusion module for registration and another module only for DICOM management and preparing the image stack for the DTI Track module.

[1] MedINRIA - http://www-sop.inria.fr/asclepios/software/MedINRIA/ - last accessed on May 2010

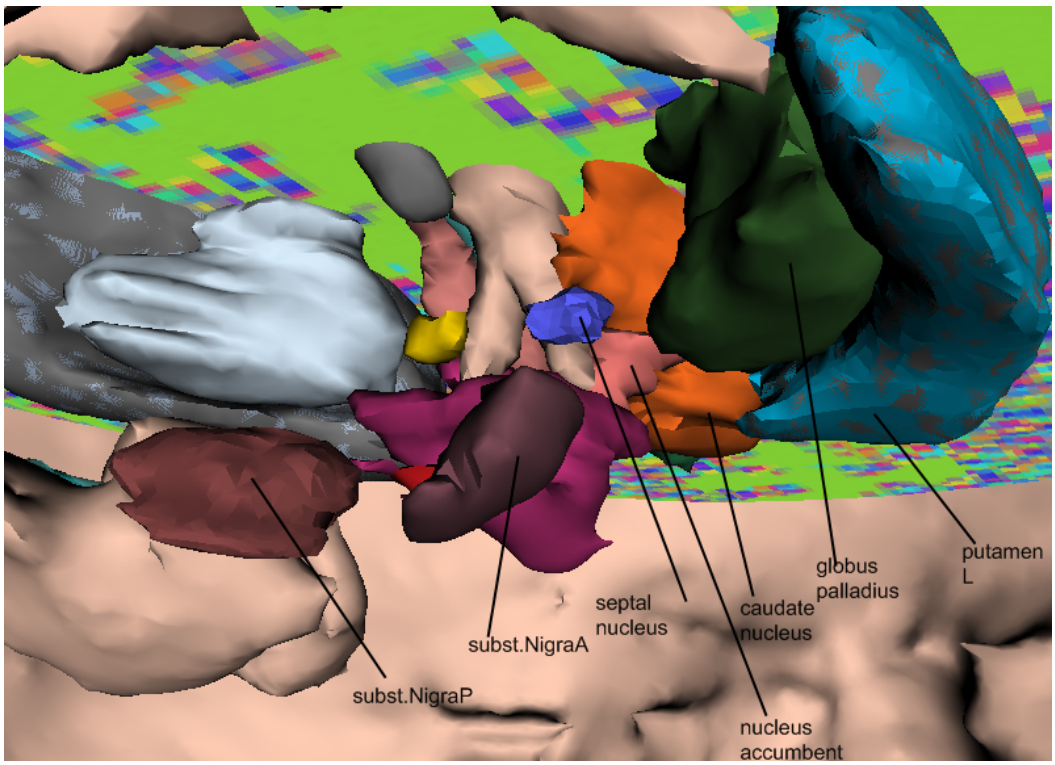

Figure 4.3: Result image when using the 3D Slicer Atlas

The entire project is implemented using ITK[2] for image processing and VTK[3] for visualization capabilities. The DTI Tracker was one of the tested modules for its method in fiber tractography, together with the Image Fusion module, the one providing several methods for image registration.

3D Slicer is provided by the MIT AI Lab with the Surgical Planning Lab at Birmingham and Women's Hospital, as presented on the home page[4]. The project represents a collection of algorithms and applications dedicated to medical imaging. The DTI management offers a 3D image viewer and tracking algorithms, as well as registration methods [Talos 2003]. The Slicer provides also an atlas for segmentation of the brain, specialized for DTI images (Fig. 4.3).

The system is developed in Visual C, using visualization libraries and advanced computing algorithms like VMTK (vascular modeling toolkit).

Matlab based systems (SPM and VBM) - Statistical Parametric Mapping (SPM)-used in our feasibility testing due to the multitude of functions and dedicated methods is a plug-in software that extends statistical processes dedicated to the functional imaging data. The software package performs brain image processing and analysis[5]. This plug-in software is designed for the Matlab environment. The version of SPM5 accepts DTI images

[2]ITK - imaging toolkit `http://www.itk.org` -last accessed on May 2010
[3]VTK - visualization toolkit `http://www.wxwidgets.org` - last accessed on May 2010
[4]Slicer - `http://www.slicer.org/` - last accessed on May 2010
[5]SPM site -`http://www.fil.ion.ucl.ac.uk/spm/` - last accessed on May 2010

for processing providing alignment and pre-processing methods using the fMRI dedicated module.

The Voxel Based Morphometry (VBM)[6] represents another module that can be integrated in Matlab with SPM, as a plug-in in SPM5. This module is able to make segmentation in WM and GM based on voxel-wise comparison.

The TrackVis [7] with the dedicated Diffusion Tracking module uses linear least- squares fitting method and offers Q-Ball/Hardi reconstruction [Wang 2007]. It uses standard FACT for fiber tracking, but we test the Runge-Kutta method as we are using a similar method in our approach.

These methods are implemented in C and the visual elements together with the image processing are created using the VTK library. The Diffusion tracking module performs the image processing taking the DICOM files and delivering the computed fiber tracts. The TrackVis module offers visualization for the fibers and the possibility to segment the images and extract bundles of interest from the computed tracts.

4.2 Segmentation methods for brain images

The aim of segmenting images is to classify sections of pixels based on their intensities, defining regions of pixels with the same intensities and/or similar intensity. These regions have a certain homogeneity that is characterized based on a scale or on the fractal features. They can also be defined by their boundaries or their interior. When defined by their boundaries, a contour-based approach tests is needed to determine whether each pixel appertains or not to the specified contour. When based on region definition, we usually need several features that cooperate for its definition: compactness, projections, moments, texture and co-occurrence matrix [Sonka 2009].

Analyzing the co-occurrence matrix, we can define a histogram so that the features designated for the morphological characterization are also applicable for classification of the pixels. In this case, the energy is used as a direct measure of homogeneity and the entropy as an inverse measure. The maximum probability and the contrast utilized as a measure of local image variation, permit the texture to be classified. The correlation inside the matrix can differentiate among regions of pixels at the histogram level.

When analyzing the voxels for classification, many approaches could be chosen, depending on the final goal of the process: for a pathologist, a classification might be needed to distinguish between sizes of cells, whereas for a radiologist, it is more useful to know if the textures in certain regions are similar. The choice of features used for classification can be made depending on the final purpose. These features are introduced in a classifier and produce the class decision. For a robust classification, knowledge of the medical area can be used, if available. In this case, we can define a parametric classifier that decides the final clusters, based on additional knowledge [Bankman 2009].

We can use the discriminatory power of the features for classification, but we need classifier-independent feature analysis (CIFA) [Sonka 2009]. Feature analysis used for classification purpose usually treats the discriminatory power from the classifier point of view - classifier oriented - by choosing the classifier typology and just then the classes are determined by running the classifier with the selected features. The accuracy of the classification

[6] Voxel based morphometry (VBM) -http://en.wikipedia.org/wiki/Voxel-based_morphometry - last accessed on May 2010

[7] Diffuion toolkit -dtk - http://www.trackvis.org/dtk/

represents, in this case, the discriminatory level of the used feature. When choosing a data-oriented approach, the features are ranked using inter-class specificity. CIFA is specific to diagnosis problems as its purpose is to optimize the classification performance. This is possible by performing a feature analysis based on the structure of the features extracted, determining thresholds based on the discriminatory power of the features and using these thresholds for a more accurate classification.

Computing the relative feature importance (RFI) offers the possibility to rank the features according to their usefulness and to include, at the same time, the medical knowledge in the ranking process as a diagnosis criterion for classification. The algorithm proposed in [Sonka 2009], estimates the separation between classes using each new feature. In this case, the weighted absolute weight size (WAWS) defines the limits between classes using eigenvectors and eigenvalues. For estimation on the RFI, in order to choose a metric distance, accurate KNN is usually used. Also, a weighting factor after estimation of these features can be attached so that the features lead towards a correct diagnosis.

In our study intra-patient variability can affect the segmentation results and RFI is able to remove this factor. A knowledge-based segmentation takes into account the features, their spatial constraints and the anatomical elements. For a low-level segmentation, the spatial constraints are included in the algorithm, with the ROI specificity set as boundaries. Using active contours implies fuzzy logic application for high-level segmentation. In this case, for more accuracy on active contours, internal and external constrained forces and additional knowledge are introduced. For the same purpose - more accuracy for edges and regions - some rules can be introduced based on the medical knowledge based on the intensity or the spatial structure values. Uncertainty can be taken into account not only with fuzzy logic, but also by modeling and classifying the anatomical variability, with multiple subject analysis and evaluation of spatial distribution in normal anatomy. Our requirements for integrating the variability and achieving a fully automatic management of the DTI information, incline towards segmentation based on active contours to overcome the intra-patient variability.

4.2.1 Segmentation context

There are several manners for managing tissue classification to determine the delineation of anatomical structures or for organ limitations. The atlas-based approach represents one of these modalities. It uses a pattern that can be applied on any brain to determine the position of anatomical structures inside the brain and extract them. There are several brain patterns used in segmentation algorithms. The inconvenience of this approach is represented by the fact that these algorithms do not take into account the patient variability. It has to provide an atlas for all the demographic type of patients (Asians, Europeans, African). Also, a registration between the atlas and the image is needed for a correct coincidental placement.

Another approach integrates the intuitive way for detecting the main tissue types: bone (skull), WM, GM, CSF. This technique analyzes the pixel intensities and is able to determine the similarities that constitute the same type of tissue. The technique is dependent on the image quality and the threshold set by the user to make the difference between tissue types, managing the sensitivity in this way. Computing the entropy values and setting up a threshold for the main tissue type defines the classification. This method parses the images and places the pixels according to the threshold and the entropy values. The sensitivity represents the main challenge of this approach.

This segmentation method proposed by SPM is able to determine all the main brain

anatomical structures, but it does not automatically overcome the inter/intra-patient variability. The intervention of the user is needed. The tissue segmentation used in our feasibility study is not applicable for detecting volumes of interest.

The systems that we are testing have different approaches for the segmentation. MedINRIA provides a manual segmentation for the regions of interest. The same accuracy, using the manual approach as well, is provided by the TrackVis module. 3D Slicer and SPM provide atlas-based approaches. 3D Slicer does not manage to finish the computation for our images and the SPM results are blurry and inaccurate.

4.2.1.1 Atlas-based segmentation

The brain atlases describe a representation of the brain, with anatomical elements and their spatial relationships, the proportionality between these structures. They are used in registration, warping strategies and annotation systems. There are specialized atlases for the brain, but there are also limitations due to the demographic parameters and the imaging clarity. One of the most used atlases is the Talairarchi Brain Atlas, integrated in several systems (SPM is using this atlas). There are also deformable brain atlases, where the anatomic variability is managed by spatial normalization schemes. The drawback of these atlases is represented by the fact that not all the brain structures can be captured and molded by these algorithms. When talking about the brain, the variability is manifested on every metric.

We use the fixed atlas approach on the images from the SPM segmentation module. Typically, the brain atlases are used for highlighting and/or extracting the volumes of interest. The fixed atlas approach is not applicable in our case, due to the fact that we have a brain database from Singapore, containing not only Caucasians, but also Asians. In this case, a mapping of the brain is not accurate enough. A specific atlas that contains automatically detectable anatomical volumes, represents a tool that can be applied to any type of patient, offering the necessary malleability.

Another use for the atlas is to determine the position and the placement of different anatomical structures inside the brain. In segmentation, finding the VOI inside the image stack, as well as its placement at the image level, is usually done by the user or is based on the atlas geography. In our case, we are making this step automatic, by introducing several placement algorithms before the segmentation stage starts, without using any atlas in determining these positions.

Based on the tests effectuated using our images on the existing modules implementing different segmentation methods, the most accurate one is the manual segmentation, but it does not represent a possibility for our prototype. We need a fully automatic approach with methods for placement and preparation. The atlas based algorithm is not accurate and does not take into account the variability at the patient level or the differences among images, but the relative positioning inside the image is known.

4.3 Our DTI image segmentation approach

An automatic segmentation process taking into account the variability poses two problems: finding the targeted volume and extracting the correct volume. As we are not using an atlas based approach, the targeted volume is achieved by medical knowledge and using geometrical landmarks. For the extraction process, we define an adaptive method that has to overcome the patient variability.

The segmentation process is part of the mathematical morphology as well, as it labels areas in an image according to their intensities. The watershed-based segmentation, applied

on overlapping and non-overlapping particles, represents one of the reference algorithms together with the gray-based algorithm. For our imaging types, since we have a complex color image, we use KMeans segmentation for differentiating the brain tissue and we work on the map image stack.

4.3.1 Preparing the stack for segmentation

There are several aspects before detecting the volume of interest. As anatomical structures have specific locations, just like the placing of the heart inside the thoracic cavity is on the left side, the anatomical brain structures have specific locations inside the brain as well. This is the reason why we first need to find the reference marks, in order to treat all the brain volumes using the same approach. We consider the relative positioning to a standard point. We have chosen this point to be the center of mass of the brain, represented by the image axes with the variables (X_c, Y_c, Z_c). The detection of this point is detailed in the previous chapter. The approximated placement of the algorithm depends on the center of mass of the brain volume determining the algorithm for the **placement inside the brain volume**, which is further tuned for a better detection. This tuning is relative to the positioning of the patient inside the image, part of the inter-patient variability parameters (see section 3.6.2). The head placement higher or lower on the image stack, determines a placement higher or lower for the slice of interest on the central axis of the brain.

Detecting the slice of interest (SOI) starts from the center of mass of the brain. Considering the placement of the anatomical regions (volumes of interest), we can approximate the position of the required slice. For the midbrain, we consider the slice of interest 8 mm lower than the center of mass and for the Putamen area, 2 slices higher than one that includes the center of mass. Due to this manner of placing the slice of interest according to the center of mass, there are several patients that do not perform well. These are the patients that, in the volume acquired in our images, do not have the entire brain volume and the content is shifted more towards the neck. In this way, the patients do not possess the needed slices containing the upper part of the brain (e.g.the hand commissure- often used as a landmark in alignment and/or registration might not be present for all the cases).

This approach used for detecting the slice of interest was not very helpful due to the differentiated brain volume content on the image stacks. Some of the patients are placed higher or lower on the sagittal plane. The center of mass in this case is positioned relative to the object inside the image, which can contain the entire brain or just a part of it. For the cases with smaller brain volume, the stacks include the entire brain, for the others this is not possible. In order to establish the position and the content of the brain volume, we select the first and the last axial slice in the stack and we extract the volume for each of the objects from these slices. We establish thresholds for approximating the position of the midbrain relative to the determined center of mass of the object in the stack, representing the brain section. The evaluation of the threshold is estimated in equation 4.1.

$$P_{slice} = \frac{Vol_{Zslice}}{Vol_{Fslice}} * \frac{100}{ST} \tag{4.1}$$

where Vol_{Zslice} and Vol_{Fslice} represent the volumes of the objects in the slice with the determined center of mass, respectively the first slice on the stack; ST is the slice thickness (4 mm) and the values for this parameter place the midbrain by using the thresholds:

- Slice 0 if $P_{slice}<60$
- Slice 1 if $60<P_{slice}<70$
- Slice 2 if $70<P_{slice}<85$

- Slice 3 if $85 < P_{slice} < 100$

These threshold values represent the statistical established studies with regard to the midbrain position and its placement relative to the percentage determined. If the stack is not correct - if it does not contain the minimum slices for the midbrain and the Putamen detection - we transmit an error value for the slice of interest (-1). Once this position is determined, the Putamen algorithm starts with two slices above the midbrain slice - one slice completes the midbrain volume and the second one includes the AC/PC line. We adjust the Putamen slice if the detected volume is too small (20 pixels) or if it is placed too near to the midline. If this is the case, it means that the brain is placed higher on the central axis and we will find the Putamen one slice above the one we have placed our algorithm.

In order to start the tracking process at the tissue level, the position of the region of interest on the slice must be determined first. We need to find the placement of the anatomical region inside the axial image for which we extract the volume : **placement inside the slice**, with storage of its position for further usage on other slices in completing the volume detection.

Detection for *the starting point of the volume of interest in the midbrain area* is done similarly to the detection of the slice of interest and it is combined with the hemispheres separation. The actual algorithm that designates the hemispheres limitations defining the inter-hemispherial axis is presented in the previous chapter. The limit is used for the algorithms determining the volumes of interest for providing a better image processing time by considering only one hemisphere at the time. The algorithm for finding the midbrain structure starts from the center of mass of the brain section inside the slice of interest and following the inter-hemispherial axis tests for a gray matter region on a segmented tissue cluster map.

Detecting the starting point for the Putamen detection algorithm is different from the one used for the midbrain, as the Putamen is not placed on the inter-hemispherial axis and does not have a geometrically detectable point next to it or a standard distance from one of the landmarks. We are working on the FA image as it contains the anisotropy that follows the dopamine flow and makes the Putamen more distinguishable than on the other type of images. Our algorithm is based on the placement of the two areas relatively to the center of mass of the image. As this is a more complex matter there are several steps performed for achieving an adequate positioning inside the image and eliminating the inter-patient variability:

- Classification of images (SOI) based on the head shape
- Segmentation on tissue type based on the voxel intensity
- Validation of the Putamen region based on the placement of the center of mass

The first step represents a rough categorization of the head based estimations. Defining three main classes based on the position of the center of mass with regard to the image center we estimate the patient positioning. The second step is meant to distinguish the tissue type and ease the search for the Putamen. This segmentation is performed using the KMeans[8] plug-in based on an existing approach [Jain 1988]. The same segmentation method is used for detecting the position of the midbrain when following the inter-hemispherial axis. The number of clusters used for this method is based on the tissue types that the image contains. The tolerance is set as the default value together with the randomization seed. The image

[8] IJ Plugins: Clustering http://ij-plugins.sourceforge.net/plugins/clustering/index.html - last accessed on June 2010

containing all these clusters represents the map for the algorithm used for detecting the volume of interest. Based on the map image and the medical knowledge, our algorithm starts from the center of mass and follows the inter-hemisphere axis. Depending on the category established at the first step, the algorithm chooses the proper height relatively to the image axis for hemisphere exploration on the left and the right side. Parsing two tissue types and reaching the CSF, represent the indicator that the next to this tissue resides the Putamen. On this tissue, we can apply the active volume tracking algorithm.

4.3.2 Volume Segmentation Algorithms - Active volume segmentation

The process of active volume determination is performed for each axial section, at the slice level. The volume at the stack level is determined by using additionally the preparation algorithms. At the slice level, after determining the starting point for the active tracking algorithm on the SOI, we move on to the active detection process defined by growing the considered region. This detection is performed on the map images generated by the KMeans method. The threshold for the growing algorithms is represented by voxels appertaining on another tissue type, different from the one we are exploring. Depending on the anatomical region detected and the explored hemisphere, the detection algorithms limitations differ. Nevertheless, after this exploration is finished, we apply the same approach on the next slice having as staring point (seed) the center of mass of the previously detected region. At the end of the process, we compose the extracted volumes by making a stack from the extracted ROIs.

Considering a generalization on the active volume-tracking algorithm, there are several main steps to be followed:

- Seed placement inside the ROI
- Considering new points for the ROI extension
- Comparison with the voxels in the ROI and threshold elements
- Validation of the considered voxel as part of the ROI

These steps are further adapted and refined to fit our image resolution and the determined anatomical shapes.

The algorithm for **detecting the volume of interest representing the midbrain structure** possesses two detection steps: the definition and detection of the region of interest and the volume detection. For the region of interest, we use a snake-based algorithm applied on the segmented image map obtained with KMeans in imageJ. This map image can detect the surrounding CSF delineating the midbrain. On the gray matter class obtained in this manner, we perform the snake-based algorithm that is set to start from the center of mass of the object in the slice of interest and depending on the side of the brain that we are exploring, our algorithm selects each pixel and compares it with the anterior validated one. This exploration step ends when there is a difference between the new pixel and the previous one or when reaching the midline representing the inter-hemispherial axis. After finishing the region growing algorithm on one slice, we explore the slice above it in a similar manner. As we know from the study presented in [Starr 2009], almost 80% of the SN is found in one slice (4 mm) and we want to make sure that our volume of interest contains this anatomical region. In this situation, we take the two slices that most probably contain the SN in the midbrain segmentation.

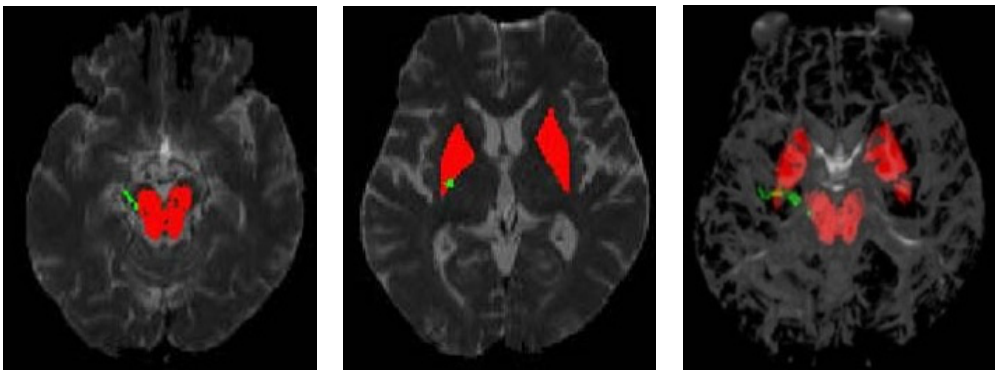

(a) EPI with detected midbrain and fibers

(b) EPI with detected Putamen and fibers

(c) 3D image of fibers detected passing through VOIs

Figure 4.4: EPI with detected VOIs in 4.4(a), 4.4(b) and 4.4(c) with 3D fibers on an example

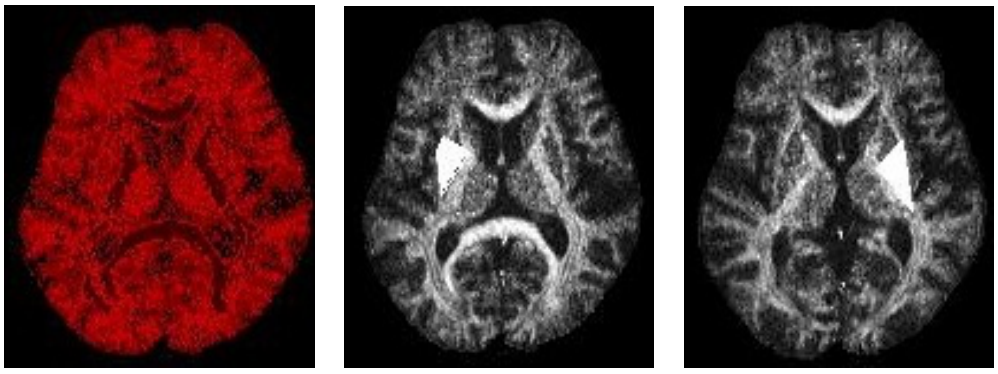

(a) FA image clustered

(b) FA image with detected Putamen on the left side

(c) FA image with detected Putamen on the right side

Figure 4.5: FA image with Putamen detected[Sabau 2010]

In figure 4.4(a), we illustrate the detected volume of the midbrain for both sides of the brain hemispheres and the fibers projected on the EPI. In figure 4.4(b), after manual segmentation of the Putamen volume on the FA images and registration on the EPI for both sides, we use it for fibers detection. In figure 4.4(c) we display a 3D view of the fibers passing through the detected volumes of interest. **For the Putamen volume detection**, we take into account the shape of this specific anatomical region and we construct a totally different algorithm from the one used for the midbrain. This method must overcome several obstacles: the placement of the Putamen that is not necessarily at the same level on both sides, its size differing from one hemisphere to the other, as well as its shape. As the FA image offers a better contour of the Putamen than the other type of DTI images due to the dopamine flow, we perform the detection on this type of image. The KMeans image map is applied on the FA image on the same manner like the one used for the EPIs.

The Putamen shape on the slice of interest - the slice above the one containing the AC/PC line- is triangular, whereas the slice above this one is more quadrilateral. This is the reason why if we want a high accuracy, we have two approaches for the algorithms used on the Putamen tracing. One of these algorithms starts from a triangle placed at the seed's place. This triangle moves its vertices only on the class of voxels appertaining to

the ones of the seed. It stops when reaching another class (3-5 consecutive voxels different from the ones constituting the VOI). The same manner of operating is applied for the other approach, except the fact that it starts from a quadrilateral shape, moving at each step four vertices. We adjust the obtained shape by comparing the left and right side limits and the positioning of the VOIs in each hemisphere.

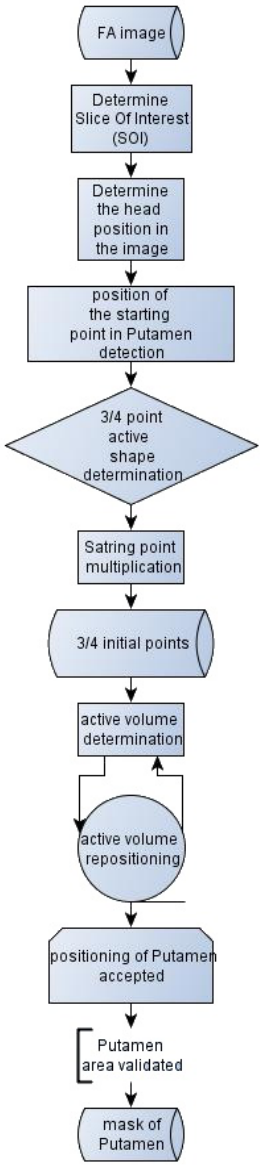

Figure 4.6: Putamen detection on the FA image

As shown in the flowchart from figure 4.6, after the positioning at the volume level on the slice of interest, the algorithm has to determine the relative position of the head inside the image. Depending on that position, we choose the starting point for the active volume detection. Once the starting point positioned, we choose the suitable algorithm for the shape extraction. We apply the triangular shape growing method for the right side and the quadrilateral one for the left side and the upper slices of the detected volume. These algorithms divide the starting point into three, respectively four points (fig. 4.10). The three-point algorithm follows the triangular shape of the Putamen, which is more obvious on the slice with the AC/PC line. The choice was made by statistically determining the difference between the two algorithms and the manually segmented images that represent the ideal segmentation shape.

Both algorithms consider the extension of the region of interest by taking each pixel next to the ones that represent the initial detected cluster. If the pixel appertains to the cluster of the initial points, it becomes one of the shape defining points - the edge of the triangle for the three points segmentation algorithm, or the edge for the quadrilateral algorithm. The active volume determination stops when other clusters are encountered.

The detected area is placed by balancing the one determined for the other hemisphere. After positioning the two determined areas, the algorithm is repeated for the upper slice to complete the volume extraction. The seed for this slice is considered the center of mass of the determined region from the initial slice. The slices with the determined regions are transformed in mask images that are further transformed according to the parameters acquired from the registration algorithm. The registration is the consequence of the fact that the Putamen segmentation is performed using the FA image stack. This volume of interest is intended for usage on the EPI stack on the tractography algorithm. A registration among the EPI and the mask stack of the detected Putamen is needed.

4.4 Registration for the volume of interest

The registration is imperative for our overall approach, as we need the Putamen detected volume for tractography. By placing the detected area from the FA image on the EPI stack, we are performing a transfer of information from one DTI type to another one.

Presenting a short context of the registration methods with emphasis on the elements corresponding to our needs, we are determining the most suitable approach together with the necessary elements for it.

4.4.1 Registration context

The registration process performs matching or bringing the modalities to spatial alignment by finding the optimal geometrical transformation between corresponding image data. *For any registration algorithm there are four basic steps representing the activities included in the method: choosing the fixed image and the transformed one, choosing the landmarks, evaluation of the differences between the two images and the transformation of the movable image*[Clatz 2009]. Depending on the way these steps are performed, the registration algorithms can be evaluated. There are several classification methods, depending on the basic activity considered.

- **Landmarks**: Landmark-based (Finite Element Method(FEM) registration) vs. non-parametric registration(Fluid registration, Elastic registration)
- **Differences**: Geometry-based (affine registration, BSpline based registrations: NURBS) vs. Intensity-based (Standard Intensity Based Registration (SIB))
- **Transformation**: Rigid (Affine registration, Iconic registration) vs. Non-Rigid(Fluid registration, Diffeomorphic registration)

There are registration methods that can be included in two or all the three defined categories, as they use algorithms from several categories. The elements defining each category are linked to the first registration defining steps. On a registration algorithm the three categories are combined for a successful approach. Considering each category apart, we illustrate the elements by defining the linking to the registration activities.

The *landmark-based registration* uses specific parameters as landmarks. Hard landmarks (prospective) or soft landmarks (retrospective) with respect to the imaging process designate the types of parameters requires by this registration methodology. The *non-parametric image registration* techniques are based on force computation to solve the differences until the two images converge [Gholinpour 2007].

Based on the method for determining the differences between the two images, the two possible approaches consider either geometrical positioning of the pixels/voxels or their intensity value, where the appropriate distance can improve the registration [Theverovskiy 2006]. There are several ways to choose the appropriate distance in this case: based on the intensity differences, on the correlation or on mutual information. All these cases define an optimal linear registration. The standard intensity based (SIB) registration uses the intensity similarities to quantify the quality of the registration. The Iconic Feature Based (IFB) registration has elements of both methods using the geometric approach for distance evaluation on the corresponding features, however the correspondence is based on the pixel intensities [Thomopoulos 1994] [Cachier 2003a] [Cachier 2003b].

The third criterion for classification is represented by the transformation method. The rigid transformation method defines a mechanism that does not change the volume or the relative positioning for the image content. The non-rigid transformation uses physical transformation altering the image composition [Maintz 2000]. *Feature-based registration* or geometric registration extracts the feature points and, computing the displacement between these points, is able to fit a transformation with or without regularization. The *intensity-based registration* prepares the transformation for optimizing the similarity by directly minimizing its value. These methods affect the voxel values by changing the image

gray level without prior segmentation [Wirijadi 2001] [Zitova 2003]. The dispersion in the distribution of the image gray values is evaluated by the *entropy* measure.

Depending on the image represented and the purpose of the transformed image, there are several registration methods that take for each step one of the two possible approaches. One of these cases is the Finite Element Method (FEM), included in the ITK library. This method is based on BSplines and computes the displacement between the images using a grid evaluation [Klein 2007] [Sidka 2008]. This grid defines a mesh that can be considered adaptive, uniform or even anatomy-based. Using physical transformation (Triangular, hexahedral, tetrahedral, etc) the moving image is deformed to the model [Park 2004] [Pluim 2000] [Dinov 2002]. This approach is linked to the specifications given for the geometry and the behavior of the elements, as well as the boundary conditions. As such in this case, the registration is a landmark–geometry–non-rigid one.

For a landmark-intensity non-rigid registration example, we can name the diffusion registration method. It is defined by a gradient-based regularization used for a finite difference approximation in the partial difference equation. Starting from this approach, Thirion in 1995 [Tharin 2007][Vaillancourt 2009] defined a performing non-rigid registration based on "demons"- diffusion functions. The main challenge and the key in this approach is the placement of each "demon" in the image domain [Vercaunteren 2008b]. The "demons" are functions that decide the movement of particles on the template image so that the disparity is minimal [Yeo 2009]. This approach is recommended on large dimensional image data, but measuring smoothness by oscillation of gradients and the fact that it does not represent the actual physical image characteristics represent drawbacks [Vercaunteren 2008a].

From the non-rigid registration methods the elastic and fluid registration methods are delineating, using basic physical laws on the intensities places them under the intensity-based methods and the initial checkpoints define them as landmark-based classification. The elastic registration is justified by the deformation of a body or the tissue [Bagci 2007] [Pew-Thian 2009]. Tensors are used to limit the boundaries for the shape matching. The fluid registration compared with the elastic registration uses the basic fluid mechanics for regularization [van Heckle 2007]. These techniques are not recommended for hand and brain images registration, as these tissues do not deform following the mechanics included in these techniques [Gilles 2008]. If the fluid and diffusion registration depend on pre-registered checkpoints (landmark-based) in the image domain, the curvature registration does not need these parameters. This type of registration does not depend on the initial points and data (non-parametric), but it changes the shape of the image elements.

A transformation that includes translation, rotation, scaling and other affine transforms represents a linear transformation and does not affect the image information. This transformation defines an *affine registration*[Modersitzki 2004]. When using the local affine transformation guided by a global affine transformation with mutual information and anatomical mask, the *piecewise affine registration* is performed [Theverovskiy 2006]. Completing this approach by using common information generated by mutual information-based thin-plate spline determines a *piecewise affine initialized spline-based registration*[Clatz 2009]. The landmark and intensity based registration methods are part of the non-rigid category of algorithms.

4.4.1.1 Challenges for registration

The main *problems in registration* are encountered at the beginning, when analyzing the data that the registration is meant to align. Aligning images from the same modality or different ones determine different approach for measuring the distance and for the transformation techniques. The same elements differ also for intra or inter-patient registration,

where the patient variability affects the transformation [Modersitzki 2004]. Depending on the components displayed by the medical image, limitations are introduced for the transformation approach.

All the registration algorithms generally have the main stages corresponding to the three activities specific for the method:

Feature Detection choosing the boundaries, the contour lines and intersections; distinctive objects spread on the image; common to the two images; not sensitive to image deformation

Feature Matching correspondence points between features; similarity measures are used combined with spatial relationship among features;

Transform Model Estimation estimates the alignment of the two images; differences between images have to be removed by registration;

Image Transformation mapping functions and transformations with interpolation techniques; the trade-off between the accuracy of the interpolation and the computational complexity

In the context of the current DTI image registration methods , the Fusion Image module (MedINRIA system) offers a manual method, the automatic affine registration and the diffeomorphic registration. Each patient must first be processed using the DICOM dedicated image handler, the Image Viewer. This module provides the image format needed by the Fusion Image module. There is no inconvenience with this aspect, just adding time for processing and an extra step. The diffeomorphic demon registration changed the pixel values on the target image [Vercaunteren 2008b]. It provided a morphed image as result of the combined pixel values of both target and source image [Ceritoglu 2009]. For some patients the resulting image was ambiguous and the anatomical detail was not good enough even for manual ROI detection. The manual rigid registration performed the best from all the proposed methods in this module. Its accuracy is nevertheless highly dependable on the precision of the used when introducing the landmarks. These registration methods do not perform with the accuracy needed by our study. This precision is linked to the correct fiber detection and any inadvertence at the registration level represents a major drawback [Curran 2005].

An atlas based registration is tested on the EPI images using SPM5 [Guillaume 2008]. The images are mapped on an atlas and depending on the position of the main anatomical structures with regard to the ones in the atlas where the transformation is applied [Chetelat 2005]. The problem for our images was the final result as the images were folded on the results and we could not use them further. This registration method includes an anti-folding method, K-fold cross-validation but this method is conceived for the fMRI images, not for DTIs.

Complementary to deformation based morphometry (DBM) and tensor based morphometry (TBM), the Voxel Based Morphometry method is tested [Yaasa 2004]. In DBM the group difference is established using local deformation, whereas in TBM the tensor information provides the local displacement. In VBM the differences in the local concentration of volume, depending on the tissue type detected at the voxel level, determine the registration landmarks [Ashburner 2000] [Klein 2009] [O'Donnell 2009]. Completing this method with a voxel-wise statistical analysis for exact determination of the landmarks provides a better accuracy [Beyer 2007] [Feldmann 2008]. The warping transformation represents the final step providing the transformed image.

Another registration method based on the regions of interest used as landmarks is the one provided by the 3D Slicer [Talos 2003]. This approach is similar with the manual approach because the user chooses manually the corresponding regions and annotates them. This technique is strongly influenced by the checkpoints and the accuracy of the evaluation for these checkpoints. The method offered results only for a few patients, as it was not able to complete the process for most of the volumes provided.

The rigid registration automatic method by TurboReg [9] was not developed for head images and it did not provide the required results. The 3D Slicer [Ceritoglu 2009] provided good results when using the manual registration method. However, this method was not only time consuming, but also from the resources point of view disappointing as it stopped the machine each time, even before completing the computation.

4.4.2 The fitting registration for placing the Putamen

The challenges for completing the registration reside in *finding the best correlation landmarks in both images, finding a suitable spatial transformation and, for our type of images, preserving the tensor direction* [Clatz 2009]. In our case, we perform intra-subject registration, as we match images belonging to the same subject. Our registration is *a rigid one*, as it contains only translations and rotations, affine transformation, and it is fully automatic. Mapping the homologous features by using geometrical distances defines *a geometry-based registration*. This is the case for our approach as well.

The elements that distinguish a good geometry-based registration method are related to:

- Choice of landmarks and the precision
- Determining the transactional values

For the fist element, we verify the placement of the volume of interest relative to the center of mass of the brain, as well as the position of external limits of the brain volume related to the same point. In order to determine the directionality of the image we use the inter-hemispherial axis and its orientation. It provides the angulations for the horizontal and vertical plane used in rotation and displacement parameters. All the transformations are performed on the mask image extracted from the FA stack, keeping the EPI as model.

Analyzing the technique used there are elements from the iconic registration method as well [Cachier 2003b]. These elements are the anisotropy value used for defining the volume that is registered. As we are not using this information directly for the transformation of the image, our registration is more geometrical [Gholinpour 2007] [Maintz 2000].

The presented landmarks are determined on both FA and EPI image and the differences among them are computed for determining the transitional values. These values are the ones from matrix 4.2.

$$\begin{bmatrix} x' & y' & z' & 1 \end{bmatrix} = \begin{bmatrix} cos\theta_x & sin\theta_x & 0 & d_x \\ -sin\theta_y & cos\theta_y & 0 & d_y \\ 0 & 0 & 1 & d_z \\ 0 & 0 & 0 & 1 \end{bmatrix} \begin{bmatrix} x \\ y \\ z \\ 1 \end{bmatrix} \tag{4.2}$$

Representing the transformation applied on the FA image has to perform several actions: rotation, translation and skewness. The rotation angle for the transformation is computed by taking into account the inter-hemispherial axis. The θ_x value is the angle between the axis and the O_x axis of the image and the θ_y is the angle between the same axis and the

[9] TurboReg - http://bigwww.epfl.ch/thevenaz/turboreg/- last accessed on November 2009

O_y of the image. We compute this angle for each image type and the difference between these angles represents the transformation values. For defining the angulation presented in equation 4.3 respectively 4.4, we consider the geometrical display from figure 4.7.

$$sin\alpha_x = \frac{SP_y}{I_1SP} \tag{4.3}$$

$$sin\alpha_y = \frac{SP_x}{I_2SP} \tag{4.4}$$

where SP is the starting point of the hemisphere axis given by the inflexion point (occipital sinuses at the base of the Occipital Bone of the skull) placed on the lower part of the brain (posterior area of the brain) and the SP_x and SP_y are the projections of the SP point on the O_x respectively O_y axis; I_1 is the intersection between the axis and O_x and I_2 is the intersection between the axis and O_y.

We compute the α angle for the FA image and the β angle for the EPI image. The θ angle is the difference between α and β and we use it for the rotation. The translation value from the transformation matrix (d_x, d_y and d_z) represents the difference between the centers of mass in the two types of images. Another aspect of the transformation is represented by

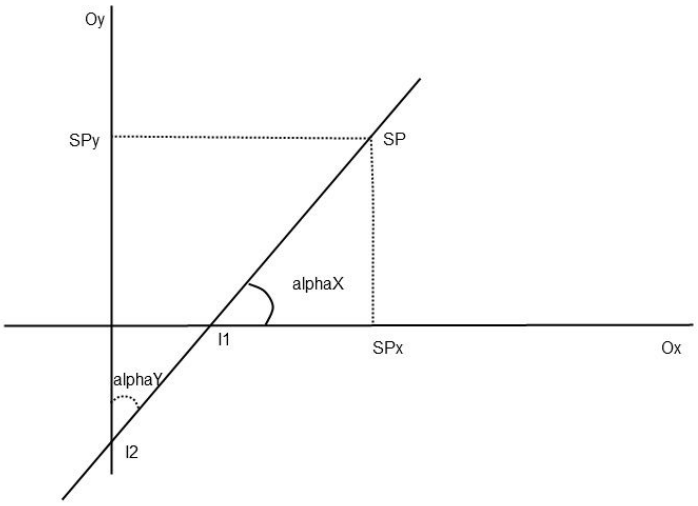

Figure 4.7: Geometrical view of the registration parameters

the axis orientation. The difference between the orientations of the axis determines us to flip the transformed image. This orientation is the result of the axis definition, as it uses as starting point (SP) and the center of mass is afterwards used on the image axes. Different orientation of the axis determines a flipping of the image in horizontal and/or vertical plane.

Because the FA images are generated on the AC/PC plane as well as the EPIs, there could not be any skewness problems or resizing aspects.

4.4.2.1 Feature Fusion

Fusing two images refers to the process of morphing them or warping them, at the image level. Both these techniques represent registration methods used, but they alter one of the images by incorporating the information from the other image [Singh 2009] [Awate 2008] [Kor 2004]. In our case, we are talking about fusion from another point of view, as we do

not want to change the image, we put together information extracted from the image with different meaning, complementing each other.

The mean diffusivity represents the knowledge encapsulated in the diffusion tensors from the EPI images. It reveals the displacement of the molecules together with the overall presence of obstacles represented by the brain anatomical structures. The degree of anisotropy represents the expression of the molecular displacement in space and together with the orientation of the anatomical structures is found in the FA images. For an accurate determination of the fiber tract trajectories, we need all these information. The tensors from the EPIs cannot be moved, as they represent important data with stored values for each voxel. The FA image by using the anisotropy guides and helps the detecting of the Putamen with a high degree of accuracy for the segmentation process. This aspect justifies extracting the information from the FA level and infusing it to the image used for fiber tracking.

Putting together information from different sources enhances common characteristics and adds the specific elements from each source. In our case, we fuse information by putting together the displacement of the diffused water molecules representing the anisotropy with the tensor information and the anatomical regions. We fuse the information in by using the detected Putamen mask from the FA image and placing it with the tensor information inside the EPI. We fuse the two images without blending them [Zitova 2003] or warping them [Gholinpour 2007], just taking the needed information from one image and inserting it into the other one by registration [Maintz 2000] [Wirijadi 2001]. In this manner, after the images are segmented the information from the FA image is registered to the EPI and further used for extraction and validation purposes. The information about the diffusion reveals the trajectories of the neural fibers and this information at the tissue level is stored on the architecture of each voxel of the EPI.

4.5 Image Analysis included by the Tractography

The tractography algorithms are used to evaluate the water diffusion represented by the tensor information in the EPI images. The angulation information is used to determine the direction of diffusion for the neural fiber reconstruction. These algorithms are defined for WM fiber tracking, where all the fibers dispose of the same diffusion direction. Although this is not the case for us, as we are working in the GM, we use the same approach on our images.

There are two main procedures for the DTI tractography architecture: *deterministic and probabilistic*. The deterministic approach connects neighbor voxels starting form an initial set of points until the angulation or the FA values reach the previously set threshold values. Probabilistic tractography considers uncertainty of the fiber orientation and uses probabilistic density functions to determine the fibers. Using DTIs both methods are able to detect the fibers even in the case of fiber disruption and/or reductions. For a deterministic approach the initial points need to be known and there is certain sensitivity in the estimation of the principal direction of the diffusion. The probabilistic approach needs more computational time due to the probability functions, but its results are more accurate for the partial regions.

Another classification considers the method used for determining the next step while tracking the fibers. From this standpoint, the approaches can be classified in *local and global*. Local tractography uses a seed voxel or a ROI as starting point for fiber initialization. This tracking algorithm takes small steps deciding each time on the direction for the fiber. In the deterministic approach, only one possible direction is provided as next step, whereas on the probabilistic approach there are several possibilities for the next step. The downside when

using the local tractography is the fact that there is no target region defined and extracting a specific bundle of interest in these conditions is challenging. The global approach in following the tracts starts by setting up the source seed voxel or ROI and a similar one for the target. Using the deterministic method for choosing the diffusion direction provides only one possible path and the probabilistic method provides more paths again, depending on the probability distributions. The global tractography is constrained to a specific connection and symmetry between the source and the target [Yendiki 2010].

Based on these approaches new methods of tractography have been developed by including other parameters when tracking the neural fibers. Descoteaux et al. in [Descoteaux 2007] use the sharp fiber orientation distribution function (ODF) for a reconstruction from Q-Ball Imaging. This type of imaging uses probability distributions instead of tensors. Fillard et al. [Fillard 2009] propose the use of spins with potential energy to trace the fibers on global tractography - the spin glass tractography method (SGT).

Our approach already has the initial volumes of interest used in a global approach. The method is set on detecting just the fibers starting at the midbrain VOI and reaching the Putamen VOI: the strationigral tract. To determine the fact that our images are able to provide the fibers, we try several tractography methods.

4.5.1 Tractography context

The DTI tracker from MedINRIA system performs fiber tracking for the entire brain. Providing a VOI, this module can extract just the bundle that passes through that specific region/volume. We cannot select a specific fiber direction for tractography. Unfortunately, the module does not permit using two regions/volumes for refining the bundle of interest. This is the main reason why the local tractography is not accurate enough for selecting the neuromotor tract. The method tested by using Log-Euclidian metrics on a deterministic approach (MedINRIA) is not adequate in our case as it cannot accurately select the bundle of interest. The method using the midbrain detected volume provides more than 100 fibers, which is inconsistent with the medical knowledge. The neuromotor tract determined is wrongly placed on the volume of interest, not only on the SN area indicated by the neurologist. The number of diffusion directions slowed down the entire process.

The second order Runge-Kutta method included in the tracking from the Diffusion Toolkit in the TrackVis [10] system was studied as well. This algorithm is a probabilistic method as it offers for each voxel multiple diffusion directions. We tested this method on our images by applying a global tractography and defining the ROIs manually in TrackVis. The tractography generates, like the DTI Tracker (MedINRIA), all the fibers, but the choice of the bundle of interest can be refined by using two or more regions of interest (see fig. 4.8). Even if this is a fast method and very close to what we need as final result from the tractography, the generated fibers include noise. The number of fibers is correct and the noise is represented as fibers that cross both volumes of interest, but not all of them are placed in the SN area from the midbrain. Another global probabilistic tractography is proposed by FreeSurfer [11]: TRActs Constrained by UnderLying Anatomy (TRACULA). The preliminary testing before release on this method uses 60 gradient directions and DWI images of 2x2x2 mm or T_1 images of 1x1x1 mm [Yendiki 2010]. We did not test this software as it has not been released yet.

In our case a global approach is much needed, as an algorithm that economizes time is desirable. The growing step is evaluating just the tensors from a defined VOI and starts

[10] TrackVis - http://www.trackvis.org/-last accessed on July 2010
[11] FreeSurfer - http://surfer.nmr.mgh.harvard.edu/-last accessed on July 2010

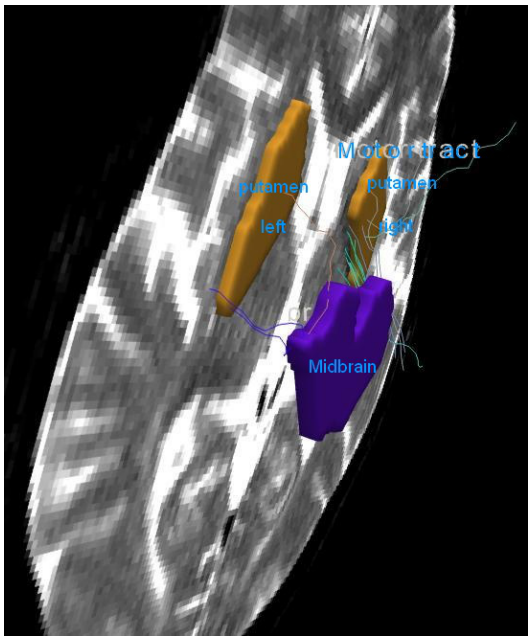

Figure 4.8: The motor tract detected on TrackVis

the growing towards the other determined VOI. In this manner, we will grow just the fibers that are interesting for us and we will validate only those that reach the second VOI.

4.5.2 Our tractography approach

The initial method introduced by Basser in [Basser 2000] takes into account the diffusivity directions and the values of the tensors. Le Bihan in [Le Bihan 2001] takes into account the anisotropy characteristics at the tissue level and determines a better detection of the fibers. We choose this classical approach because it represents a fundamental way of tracking the fibers, which we can further develop and modify according to our needs. Our approach is a global deterministic tractography as it uses the neighbor voxels when tracking the fibers, providing the seeds as volumes of interest. We are using the thresholds of 0.1 for the FA value and 0.6 for the angulations, like in the original approach.

Before developing the methods to detect and to select the neural fibers, understanding the fibers functionality is mandatory. A physiological definition of them is necessary as well. From the anatomical point of view, the gray matter (GM) represents the dendrites of the neurons and the white matter (WM) corresponds to the axons of the neurons. Neural fibers represent the link between the axon of a neuron with the dendrite of another neuron. The anisotropy enhances the neural flow passing through the axons. The effect of diffusion on the MRI signal is attenuated (A) depending on the tissue type encountered by the water molecules.

$$A = exp(-bD) \text{ [Le Bihan 2001]} \tag{4.5}$$

It all depends on the diffusion coefficient b and the tensor D that characterizes the mobility on each direction of the water molecules [Basser 2000].

$$\underline{D} = \begin{bmatrix} D_{xx} & D_{xy} & D_{xz} \\ D_{yx} & D_{yy} & D_{yz} \\ D_{zx} & D_{zy} & D_{zz} \end{bmatrix} \text{ [Le Bihan 2001]} \tag{4.6}$$

A, the attenuation, represents the effect of diffusion depending on the tensors and the b coefficient as shown in equation 4.5 and can be expressed as by the equation 4.7.

$$A = exp(-\sum_{i=x,y,z}\sum_{j=x,y,z} \underline{b}_{ij}\underline{D}_{ij}) \text{ [Le Bihan 2001]} \tag{4.7}$$

For the DTI images, we must first estimate the values for D_{ij} using multiple linear registration from equation 4.7 and the diffusion tensor computation for the degree of anisotropy from each voxel. This process followed by the determination of the main direction of the diffusivity for each voxel completes the preparation for each voxel's diffusion value.

Once this step completed, the trace of the fibers can be studied. For this purpose, the diffusion is represented as ellipsoids at 3D level. The tracking based on the diffusion tensor values is computed using equation 4.8.

$$Tr(\underline{D}) = D_{xx} + D_{yy} + D_{zz} \text{ [Basser 2000]} \tag{4.8}$$

For estimation of the fiber trajectories on the 3D space curve, the Feret equation describes it and, using a tangent vector associated with the tangent eigenvalue, we obtain an estimation of the tensor.

$$t(s) = \varepsilon_1(r(s)) \text{ [Basser 2000]} \tag{4.9}$$

where $t(s)$ is the trajectory of the curve s determined by the arc $r(s)$ and represented by the normalized eigenvector ε_1 associated with the tangent eigenvalue. Finding a solution for $r(s)$ can be achieved by using the Euler method, the Runge Kutta or the Gear's method. Gear's method is preferred in [Basser 2000] and we follow the same approach.

Retaining this approach, we are determining the fibers passing through the midbrain area, the first volume of interest, and arriving to the Putamen volume on both sides of the brain hemispheres. The approach used by our system is presented as data flow in figure 4.9.

The midbrain area, where the SN resides, is a gray matter volume. The process of growing the fibers starting from the EPI means actually taking the tensor information and, based on the anisotropy value, choosing the starting point of the fibers. In the white matter area, the placement of the fibers is more obvious because the axons represent this area and the neural flow is very intense. That is the reason why it is very challenging to make the fiber recognition and to grow them starting from the midbrain area, where the predominance of the tissue is the GM.

For our system, we consider the approach presented by Basser in [Basser 2000] and for the tensors approach we use the approach proposed by Bihan in [Le Bihan 2001]. In the first approach, the algorithm is based on the Fernet equation for the description of the evolution of a fiber tract. This approach is specific to white matter, as the axons form the white matter. The midbrain area is gray matter. The number of axons in this area is much less than in the white matter and the fibers are not aligned as the ones in the white matter. We apply this algorithm in order to see if there are relevant fibers linking the two VOIs that we can determine (Fig. 4.4(c)). We use these VOIs to choose the bundle of interest and separate the fibers that we need from the ones that are not part of the motor tract. Although we grow all the fibers from the midbrain, we validate only the ones starting from the midbrain area that also reach the Putamen area. Fibers are not validated if they are too small, with anisotropy higher than 0.1, or those that do not have the AP directionality and/or angulations that exceeds 0.6 degrees. The threshold values are the same used in [Basser 2000] [Le Bihan 2001] [Karagulle Kenedi 2007]. In this manner taking a global tractography approach the fibers can be determined, without needing the SN clearly defined.

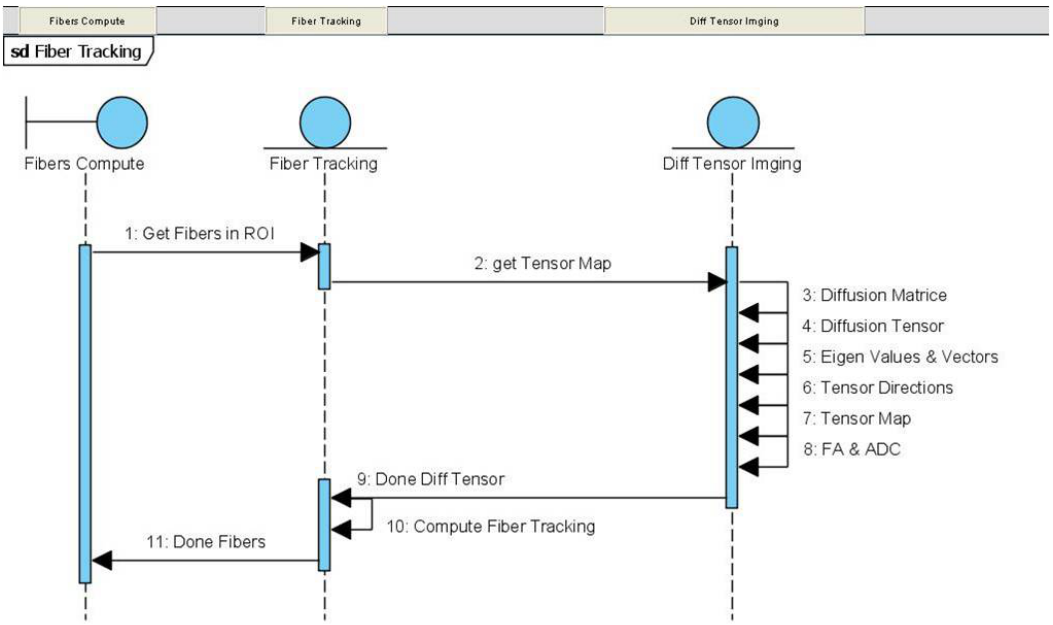

Figure 4.9: Algorithm used for fiber tracking

The detected fibers have to be evaluated using a measurable value to define them as features. The transition from the image level to the feature level for the DTI provided information is determined by evaluating the fibers. For this purpose we define the metrics from equation 4.10 and 4.11.

$$FD = \frac{F_{Nr}}{Vol_{Brain}};\ FD_{rel} = \frac{F_{Nr}}{Vol_{VOI}} \tag{4.10}$$

where FD represents the fiber density computed as the number of fibers - F_{Nr} - in the volume of the entire brain - Vol_{Brain} and FD_{rel} represents the fiber density relative to the volume of interest- Vol_{VOI}. Computing the fiber volume and the brain volume an analysis is possible to detect the geriatric effects on the brain and on the neural fibers al well.

$$FV = F_{Nr} * V_{height} * V_{width} * V_{depth} * F_{leng} \tag{4.11}$$

where FV represents the fiber volume computed as the product of fiber number (F_{Nr}), fiber length (F_{leng}) - constant as the fibers must pass through both regions of interest and the voxel dimensions: $V_{width}, V_{height}, V_{depth}$.

According to the medical manifestation of the disease, the fiber density and volume should be diminished for the PD patients, compared with the control cases. The degradation of the fibers should also be correlated in direct relation with the severity of the disease specified by the H&Y scale. Before reaching the evaluation and diagnosis part for our algorithm, we present our work at the on the processing level, where we extract the basic image features.

4.6 Medical Imaging Processing Contributions

Reaching for a fully automatic medical imaging processing and analysis system, we created algorithms for positioning the slice of interest as containing the brain volume, in order

Pat.ID	Left area of Putamen	Right area of Putamen	Relative error for left Putamen detection [%]	Relative error for right Putamen detection [%]
1	77.491	33.005	33.33	26.10
3	24.395	10.045	58.02	77.50
7	61.706	58.836	6.17	30.61
9	64.576	70.316	11.11	57.43
27	50.225	77.491	13.58	73.49
132	66.011	24.395	13.56	45.38
168	66.011	21.525	13.56	51.80
177	54.530	61.706	6.17	38.15

Table 4.1: Preliminary results on Putamen detection [Sabau 2010]

to detect the relative position of the anatomical region to be segmented. These intuitive algorithms based on the anatomy of the brain and the tissue intensity is applicable for other volumes of interest.

4.6.1 Evaluation of the segmentation algorithms

There are several characteristics when analyzing the result of a region-based segmentation. Comparing an image segmentation result to the ground truth-represented by the manual detected region performed by a specialist-represents one way of evaluating the automatic segmentation. Another way would be to estimate the overlap difference between the ground truth image and the segmented one. There can be over-segmentation or under-segmentation when the two images overlap and one of them is bigger than the other one. When there is a ground truth region that the segmentation does not contain, we are dealing with a missed region. A noise region manifests as a region identified in the segmented image, but not contained in the noise region.

Midbrain automatic detection is preformed on the EPI stack with no diffusion direction (B0 image). The algorithm providing the segmentation is applied on the test set with the manually determined Putamen (42 subjects) and the results are studied by our specialist. Validating the algorithm actually means verifying if it managed to segment the whole midbrain and just this part, without taking part of the surrounding tissue or the CSF (see fig. 4.4(a)). This is the criterion followed by the neurologist in validating the algorithm.

For the **Putamen detection** the evaluation is performed by comparing the manually segmented images with the automatically detected ones. Performing a logical AND operation at the image level between the two Putamen slices at the pixel level. We are using the imageJ Image Calculator on the segmented volumes. We compute the number of the non-black pixels at the same position on both images. The difference area gives the error rate of our segmentation algorithm. As shown in table 4.1, the area difference between the two methods determines the values found in column two and three of the table and determines the results in column four and five of the table. Also a validation done by our neurologist is necessary for this step. For the registration performed on the detected volume, we use medical knowledge for validation and visual evaluation.

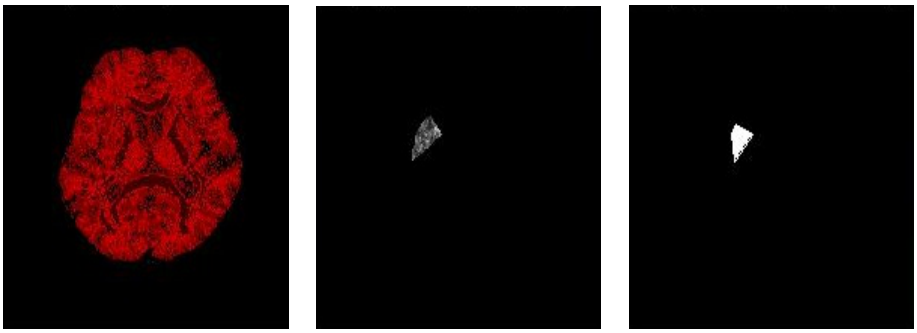

(a) FA image clustered (b) FA extracted Putamen manually extracted on left side (c) FA extracted Putamen automatically detected on left side

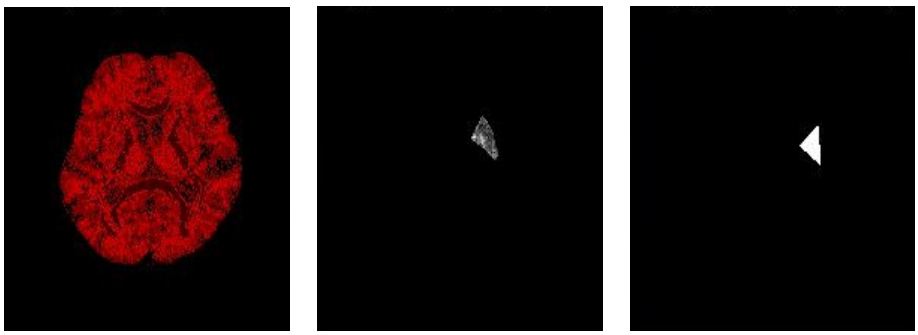

(d) FA image clustered (e) FA extracted Putamen manually extracted on right hemisphere (f) FA extracted Putamen automatically detected for the right hemisphere

Figure 4.10: Putamen segmentation

4.6.2 Evaluation of the registration method

The registration has the purpose of aligning two images so that they overlap. We need it for aligning the segmented volume of the Putamen from the FA stack with the one in the EPI stack. As presented in the context examination of this process, other algorithms do not deliver satisfactory results from the medical point of view four our images. This is the reason why we propose a specific approach, by automatizing the entire process.

In our method, the registration process with the acquired parameters is fully automatic. It uses the EPI stack with no diffusion and the FA one. The results can be visually verified as we are applying the transformation on the Putamen mask. We transpose the image on the EPI for using it as target in the tractography process.

4.6.3 Tractography evaluation

The motor tract is automatically detected in our case by growing the fibers between the two volumes of interest: midbrain area and the Putamen. This is consistent with a global tractography method. After computing the FD and FV on each side of the brain, we study the effects of PD on each extracted bundle of interest. We perform the T-Test determining the correlation between FD/FV and H&Y scale. As the FD is dependent on the FV, the two parameters have the same variation. For the medical relevance of the correlating between the H&Y parameter and the fibers, we test the measures provided

using WinSPC (Statistical Process control Software). For the simple correlation purpose, we analyze Pearson's parameter (see Table 4.2 column 2 and 4). We have chosen for testing in this case the ANOVA method: one way ANOVA, General linear model ANOVA (MANOVA) and we test the equal variation on density considering the Lavene parameter. Using the same test as the one from the feasibility study ensures immunity to the external parameters and offers the possibility to determine if the level of correlation determined for the raw data is the same or better at the feature level.

This evaluation is performed when developing the method and the statistical tests are applied using *the test batch from the feasibility study to determine the influence of our methods on the correlation*. When we perform the global testing taking into account 80% of our data, we obtain p=0.05 for the group homogeneity on the H&Y assigned cases, classified using the measured fibers from the left side of the brain. On the ANOVA test for the same cases, the significance is 83% with an N=35 subjects randomly taken by the software from the total of 42.

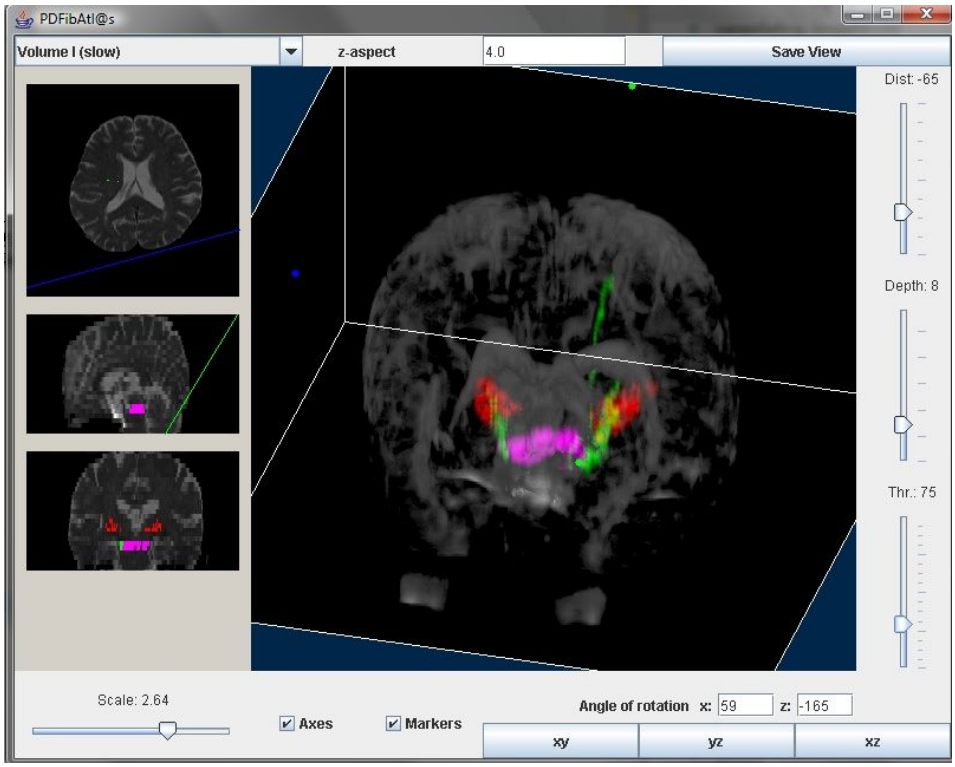

Figure 4.11: 3D View of the grown fibers from PDFibAtl@s

Taking a closer look on the testing batches, we can follow the variation of the relevance degree depending on the demographic elements and with regard to the test taken, just like we did in the feasibility testing. A significant value for correlation is given when the value of Pearson variable is lower than 0.01. In table 4.2 we perform the testing for correlation between the H&Y value and the FV. Our conclusion after this test is that the influence of the testing batch taken into account, affects the results. For the test batch 3 on the left side, we have both variables indicating a very strong correlation, while the other test vary and appear not to be significant.

Test nr	Left Side		Right Side	
	Pearson	P-value	Pearson	P-value
T1	0.041	0.825	-0.096	0.599
T2	0.107	0.555	0.023	0.898
T3	0.010	0.955	-0.037	0.841
T4	0.108	0.555	-0.101	0.581
Total	0.054	0.735	-0.098	0.541

Table 4.2: Simple correlation between the fiber volume (FV) and H&Y values[Teodorescu 2010]

Test nr	One-way ANOVA				MANOVA	
	FV		FD		FD	
	Left	Right	Left	Right	Left	Right
T1	0.00	0.00	0.00	0.00	0.105	0.515
T2	0.00	0.00	0.00	0.00	0.638	0.067
T3	0.00	0.00	0.00	0.00	0.138	0.404
T4	0.00	0.00	0.00	0.00	0.329	0.404
Total	0.00	0.00	0.00	0.00	0.149	0.629

Table 4.3: ANOVA testing [Teodorescu 2010]

The same testing method Luke the one validated by the feasibility study is used *for the fibers* as well. This validated method proved to be unbiased by the influence of the demographic parameters or by the processing methods. The physiological elements represented at the image level could also influence these results. This time, the test batches consider *the correlation and the regression coefficients*. We can distinguish a difference between the two hemispheres of the brain on the results tables. The variations among the testing batches are the result of the inter/intra patient variability. The One-way ANOVA test is used to compare three or more unmatched groups and that is the reason we test our results using this method (first 4 columns in table 4.3). MANOVA results are presented in columns 6 and 7 from the same table. On the ANOVA One-way test, the value considered significant is 0.00. In table 4.3, *we can conclude that this test shows a strong significance on all the testing batches, more than we have obtained from the feasibility testing where the correlation was not always complete and variate (86-100 %)*, while the MANOVA and the Lavene variable do not show any significance. In some of the cases, the equal variation of density could not be computed due to lack of a certain type of cases (Table 4.4), while the Lavene parameter is significant only for the whole database on the left side. *These T-test show the medical relevance of our system, but from the technical point of view, we have to evaluate the robustness of the algorithms and their speed, as well as their accuracy compared with the manual detection and extraction. Even if the correlation for all the patients is 83%, less than the one determined by the feasibility testing, taking the same batch of subjects and performing the ANOVA test delivers a correlation for each of the tests equal or higher than the one determined during feasibility.* We perform the same test using the defined test batches to determine if the automatic segmentation or the tractography affected the nature, the quality or the quantity of information. These aspects could be altered by the new measures introduced at the fiber level as well.

These are the premises that are further used on the analysis and prognosis module.

Test nr	Test variation of density P-value		Lavene	
	Left	Right	Left	Right
T1	0.499	-	-	-
T2	0.932	0.855	1.33	0.04
T3	0.888	-	-	0.57
T4	0.733	-	-	0.721
Total	0.742	0.542	0.000	0.921

Table 4.4: Variation of density [Teodorescu 2010]

Chapter 5

Diagnosis and Prognosis

Contents

In the context of the neuromotor fibers extracted for analysis and using the measures we defined for these features, we require algorithms for interpreting these features. The correlation between the measures and the disease severity validate the relevance of the features regarding the disease. The informational transfer from the anisotropy level, tested by the feasibility, reaches the fiber level, tested after the tractography. The DTI information has been transferred from the visual raw level to the numerical feature one by bridging the gap from the pathophysiology towards the clinical stage. This stage can be reached only after the physiology represented by the extracted features can be interpreted using medical knowledge. The process of transferring the information from the pathophysiology level to the clinical one and reaching the diagnosis stage with the data provided includes medical knowledge. Classification methods for different stages of PD using medical knowledge are required for feature interpretation. This process can be introduced among the transactional science methods for transforming the information from the visual level to the knowledge level.

As presented in figure 5.1, the information analysis stage in our study starts by using the features extracted after the image processing level. Reaching the knowledge level by interpreting the features implies the use of analysis algorithms. Incorporating the anatomical knowledge to the attributes from the pathology level provides a larger view for the extracted image features, offering the possibility to be interpreted in the context of diagnosis and prognosis. The overall system becomes then a Computer Aided Diagnosis (CAD) system. In our approach, as in the prototype elaborated from it, managing the features extracted from the image level and transposing them to the diagnosis and prognosis level is needed to reach the clinical stage. Overcoming different levels of data abstraction we are able to solve the semantic gap, at the information level and at the knowledge level, the gap between the pathophysiology and clinical stage.
As we need interpretation for the specific features and we have established that it is linked to the medical knowledge, the *Computer Vision* domain is appropriate. This domain is linked to the two previous domains used for managing the digital images in general and applied in our approach for medical images as well. Computer Vision algorithms interpret the

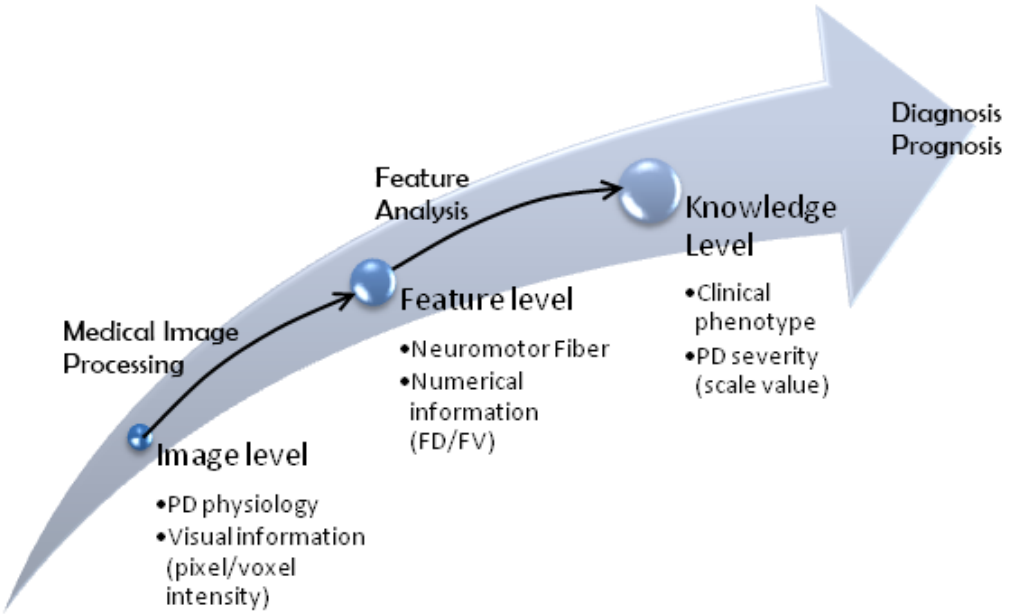

Figure 5.1: Information migration and transformation processes

images and provide the diagnosis at the end. Elements from this domain are recommended for the analysis stage.

In this chapter, we present the use of fuzzy logic to make the transfer of information from the extracted and processed features of the motor fibers to the PD diagnosis. Several aspects need to be considered therefore at the analysis and interpretation stage:

- The difference between the control patients and the PD cases
- The differences among PD patients having different disease ratings

In any analysis method, the features are first classified to determine the manifold display. A neural network structure constructed as a graph can be used to define concepts or classify features. Using similarity and medical knowledge a rule-based classification could determine the place of a feature among the others. The established correlation with the disease severity determines the number of classes. The characteristics for the features in each class define the classification criteria. The first criterion has to make the difference between the control cases and the PD affected patients. Another level of classification with medical knowledge, specific PD pathology, has to be able to determine the PD severity.

In the context of CAD and studying the general architecture of such a system, we analyze the steps necessary to use the features extracted to determine if they can be used. For this purpose, we are studying the features homogeneity and their classification according to the disease severity, but also the scale that the features have to be placed on.

5.1 Computer Aided Diagnosis (CAD) context

The results obtained by the processing level provide the input data for this module. The correlation tests performed at each stage validated the link between the features variation and the severity of the disease. Defining this link represents the challenge for this stage of

the study. The diagnosis criterions and their applicability help us to integrate the medical knowledge by using rules. We analyze the H&Y scale and since there is a correlation between the features extracted and this scale, we transform the statistical correlation by implementing the rules. This link can be made visible by attaching a variation function onto the features so that the evaluation of the function determines the disease severity. Following the function variation and estimating the value of the features for cases that are uncertain, could reveal the early cases of PD.

Diagnosis aims at making specific identification of a problem - a disease, whereas prognosis follows the problem evolution to reveal the early cases [Bankman 2009], reaching towards the source of the problem. While diagnosis is concentrated on the whole picture at a given time/snap - the raw images features analysis, the prognosis requires more granularity and reaches on to the detail, as it discovers and correlates the variation of the parameters for early diagnosis purposes. In our case, the diagnosis determines if a case belongs to the PD affected or the control subjects and if affected, it has to determine the degree of severity for the disease.

As presented in figure 5.2, there are several stages when defining a Computer Aided Diagnosis (CAD) system. In our case, the first stages performing image pre-processing and feature extraction have already been treated in the previous chapters and we need a clustering phase at this stage, with the pre-normalization of the extracted features, to provide the diagnosis.
Different combination of features provide different classification performances and for a robust classification, fewer parameters are recommended [Sonka 2009]. As clinically PD is manifested more visible on the left side of the brain, the features extracted on this side will have a higher trust degree in our CAD. Jain et al. [Jain 1997] provide a large categorization for feature selection as deterministic methods: stepwise feature selection, stochastic methods and genetic algorithm feature section, optimal methods with exhaustive search of all possible feature combination.
The *stepwise feature selection* is based on successive inclusion of features in the classification algorithm. Each new feature should improve the classification result. In our case, we have only the fibers and the VOIs and we include the fibers first in the classification process and then the volumes for a more refined selection.
Genetic algorithms are based on the idea of evolution in nature. The solution for these algorithms must be a string and there has to be a fitness function for correspondence between the input string and the output one. This variant of classification is not applicable for our case, as we have no strings. The classifiers that usually apply for the image based CAD are the *pattern classifiers*. The initial image is processed and features that represent the pattern are extracted and fed to the classifier that returns the proper decision class.
When using a classifier, a training stage defines the known classes. The linear discriminant analysis and the classification trees can also be applied to medical image analysis. The *linear discriminant analysis* makes the difference between two classes using a linear decision boundary [Sonka 2009]. This approach is not applicable to our data set. The *artificial neural networks (ANN)* perform like the linear discriminants, but they use nonlinear approach. It highlights the underlying density functions of the classes without assuming any rigid form of limitation. For using this approach we must first determine the densities and their attached functions. Another approach on the classifiers part is the *Bayes decision rule* or Bayes optimal discriminant function. It incorporates a priori information into the determination of the classifier parameters for an optimal discriminant function that follows the Bayes function.
A *Rule based system* of detection also includes the medical information. The result is not represented by a decision variable in this case. The *Multi objective genetic algorithms*

(MOGA) addresses the difficulties of the optimized rule-based schemes by maximizing or minimizing the n component of an objective vector function - optimization of the Receiver Operating Characteristic (ROC) curve.

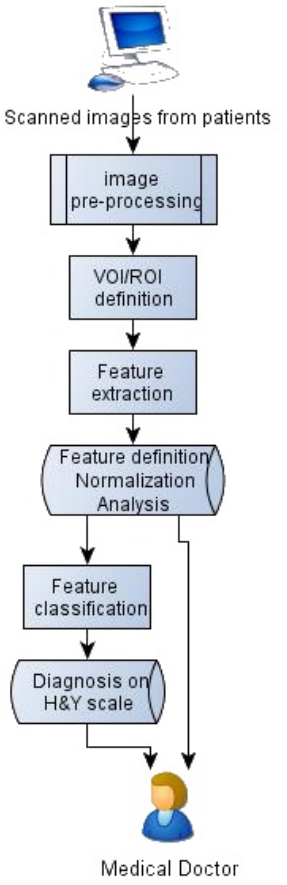

Figure 5.2: Computer Aided Diagnosis System

In the situation of totally chaotic dispersion of the features, fuzzy sets are needed. The *non-probabilistic uncertainties defined as fuzzy sets determine an approach based on fuzzy models.* A fuzzy inference system, or fuzzy model, can adapt itself using numerical data. A fuzzy inference system has learning capability and using this aspect the link between the fuzzy controllers and the methodologies for neural networks is possible using the *Adaptive Network-Based Fuzzy Inference Systems (ANFIS).* These networks have the overall input-output behavior influenced by a set of parameters. These parameters define functions that determine *adaptive nodes* at the network level. Applying the learning techniques from the neural networks to the fuzzy sets determines an ANFIS structure. A typical ANFIS system possess five layers [Jyh-Shing Roger 1995]:

- Input layer- determines using a function the premise parameters
- The rule strengths
- Normalized firing strengths - weights definition
- Consequent parameters - determined using the weights and the variation functions
- Output - decisional output based on the computed consequence parameters

In our case, the fuzzy sets represent the values extracted after the tractography. These sets are defined on intervals and determine *If-Then rules.* Together with these rules, the database (fuzzy sets) and a reasoning mechanism determine a *fuzzy inference system.* At the reasoning part, we have to take into account the inference model [Jyh-Shing Roger 1995].

Following an ANFIS [Bonissone 1997] architecture, we can combine the fuzzy control offered by the medical background and the statistical analysis using neural networks. The fuzzy features represent the a priori knowledge as a set of constraints - rules. Using Fuzzy Modeling (Fuzzy Inference Systems), we can take a subjective or an objective approach. We have tested the objective approach that uses a clustering algorithm and fuzzy system identification to determine the fuzzy rules. This approach did not perform well on our data. In this situation, we determined the intervals for the rules manually for the first learning set. One of the applications of ANFIS is presented as a modality to interpret past data and predict behavior. In our approach, we test a Fuzzy Control (FC). For the FC technology we use rule inference where we make the difference between different disease stages. We adapted this approach, but as the neural networks separately did not perform well, we use adaptive interpolation functions.

As shown in figure 5.3, the features extracted require a pre-processing level - a normalization process for the data set - preparing them for the inference model. We can choose between the Mamdani and the Takagi-Surgeno-Kang (TSK) inference method

[Roussinov 2001]. In Mamdani systems, each rule has a fuzzy set attached, whereas in TSK, each rule has a linear function on the input set of points. While the first model generates as result sets of points, the second one provides one or more real functions. The fuzzy sets resulting from the first method need an additional defuzzyfication step [Gabrys 2005]. Choosing the inference model is not a problem as we need functions as output and we can eliminate an additional step. The TSK model is the one we are implementing.

Before defining the rules, a classification of the input data is necessary following the output data structure. We define the classes that are represented by the feature points and using the TSK inference method we define a rule-based system for diagnosis. This system is able to provide, based on the features extracted, the corresponding PD values. The problem with this system is that it can only detect what it has learned, so if we do not have early cases of PD it will not be able to diagnose that level. This is where the prognosis functions come into place, as they evaluate the patients using variation functions and following their progression we can extrapolate for new cases and place them on the PD scale.

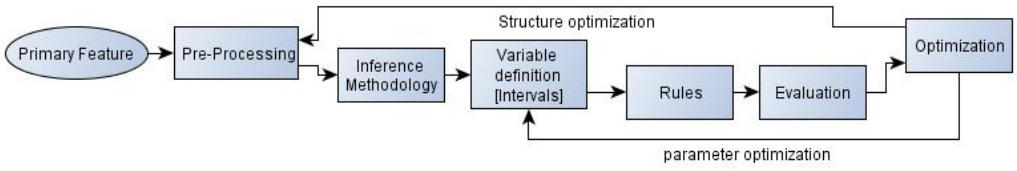

Figure 5.3: Fuzzy Expert System Flowchart

Once the fuzzy inference system is defined, we can apply different learning techniques to link the neural network to the defined system - *neuro-fuzzy modeling*. There are several architectures and learning procedures for adaptive networks. The most popular ones are the *back-propagation neural network (BPNN)* and the *radial basis function network (RBFN)* . The BPNN has the property of learning by propagating the information from the network output to its input. This determines an error rate that permits an adaptive approach on the learning process. The learning rules can be adapted to the data and use different computation methods (e.g. LSE - least squares estimation or a combination of gradients and LSE). The RBFN method uses Gaussian functions to compute the radial basis functions. This adaptive system represents a hybrid learning method.

In our approach, we follow the ANFIS layers, from the input data to the results, adapting the system to our needs. The ground truth is represented by the Hoehn & Yahr (H&Y) value provided by the medical experts. Our system extracts the features and by estimating them has to be able to provide a diagnosis on the same scale. For the database provided by Singapore General Hospital the H&Y values for each patient is known. This represents the ground truth for our evaluation. It is placed on a scale from 1 to 5, but for certain cases, when the neurologists were not absolutely sure of the disease severity, there are ".5" values (e.g. 1.5 when the disease does not have certain cognitive aspects that most of the patients that possess the ones that are placed at level 2 on the scale).

5.1.1 Hoehn & Yahr correlated scale

PD severity is most commonly described on a clinical basis using either the Hoehn and Yahr (H&Y) staging system, or the Unified Parkinson's Disease Rating Scale (UPDRS). One of the standard staging systems used worldwide is the H&Y scale, provided by our neurologists as a basis or a ground truth.

Value	H&Y standard scale	H&Y modified scale (currently employed by SGH)
1	Unilateral involvement only usually with minimal or no functional disability	Unilateral involvement only
1.5		Unilateral and axial involvement
2	Bilateral or midline involvement without impairment of balance	Bilateral involvement without impairment of balance
2.5		Mild bilateral disease with recovery on pull test
3	Bilateral disease: mild to moderate disability with impaired postural reflexes; physically independent	Mild to moderate bilateral disease; some postural instability; physically independent
4	Severely disabling disease; still able to walk or stand unassisted	Severe disability; still able to walk or stand unassisted
5	Confinement to bed or wheelchair unless aided	Wheelchair bound or bedridden unless aided

Table 5.1: H&Y scale differences

Table 5.1 shows the original Hoehn and Yahr scale, that includes stages 1 through 5, but due to ambiguity at level 2, there are two other stages included on the scale: the 1.5 and 2.5. Stage 1 and Stage 5 are rarely diagnosed and this is the reason why for our database we do not provide subjects for these stages of the disease. Stage 1 on the scale represents the mild PD cases, the early stage of the disease. The detection for this stage is not possible yet using the cognitive tests. For stage 4 and 5 the patients suffer from movement disorders so the images, even if they are taken, do not offer valid information. This is the reason why most of the diagnosed patients are those in stage 2 and 3. We are using the original scale for our system for starters, as differences between stages 1, 1.5 and 2 have not sufficient discrepancy. Our entire system makes the distinction for the features on each hemisphere and as the differences between the old scale and the new one are based on analyzing the differences among the two hemisphere, we are provided with the material for such an analysis.

5.1.2 Feature analysis premises

In numerical analysis, the interpolation methods are associated to a method of creating new data points within the range of a discrete set of known data points. The features representing the points will be incorporated by the function variation. Parsing the data points by curve fitting or regression could constitute approaches applicable four our data. There are several parsing methods, but only several interpolation techniques offer the variation required by the required dispersion. A linear interpolation or a piecewise one would not be able to parse the data, as the features represented are dispersed. We implement a combination of spline and polynomial interpolation techniques.

Defining the input data and determining a function to normalize these data represent the first stage for an ANFIS system. We perform these steps by determining the features correlated with the diagnosis and then by clustering them.

5.1.2.1 Feature Clustering

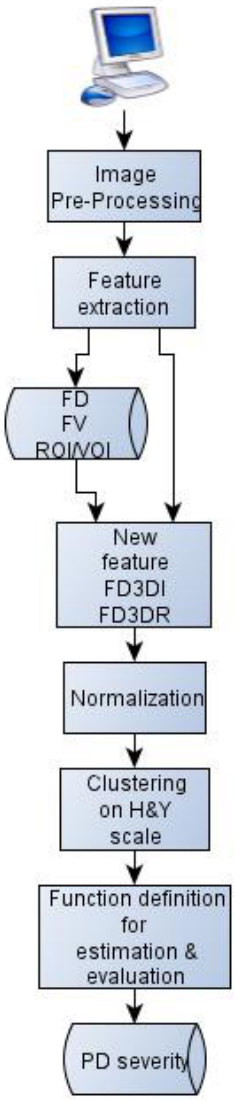

Figure 5.4: Diagnosis based on features -our CAD system

During the clustering process, we analyze the features extracted and their correlation with the stages that represent clusters. The Statistical Parameter System (SPSS) is used for estimation and pre-evaluation as presented in table 4.2. Preparing the data for the clustering includes normalization of data and new definition of features for a global overview. *For a characterization of a case using all the features, we introduce new metrics based on the fibers and the hemisphere attendance.* In this manner, we evaluate a case globally and at the local level, including the specificity as well. The features extracted and evaluated with the FD and FV measures are completed by the FD_3D measure from equation 5.1.

$$FD_{3D} = \frac{Nr_F * V}{Vol_{Brain}} \tag{5.1}$$

We define the fiber density on 3D for each side of the brain considering the number of fibers detected on the hemisphere that we are analyzing Nr_F; the voxel size V and the brain volume of the patient Vol_{Brain}.

Once we have the features defined, computed and then normalized, the learning stage for the clustering includes intervals of variation for each feature. These intervals are defined using fuzzy classes. We thus have in this case the five severity stages and for the control cases class 0 value. As we have patients for training only for PD stages 2 and 3, the other levels of PD are defined using the variation functions from the prognosis definition. After the interval definition, the rules supporting the intervals on each feature are implemented, including the medical knowledge.

In adaptive systems used for this purpose, the learning rules are more complex using together with a basic learning rule, a batch - off-line learning - and a pattern - on-line learning - rules.

For the classification methods,*the problem of supervised and unsupervised approach is an important aspect.* This aspect places the features either into predefined classes, or into unknown ones - the number of classes being unknown. As we want to place the diagnosis onto the same scale used by the medical doctors, we already know the number of classes for our diagnosis so the supervised approach is more appropriate. Among the methods used in the supervised classification, statistical classification is our choice due to the fuzziness of our data and the overlap of the clusters. As table 5.2 illustrates we take the normalized data and make intervals depending on the H&Y values. We use these intervals for training purpose in the rule-based diagnosis. Each interval determines a fuzzy set that has a rule attached for defining the link between the values and the H&Y level.

Variable	Stage on H&Y scale		
	0	2	3
FD	0.0351 - 0.0353 0.0413 - 0.0417 0.0413 - 0.0417 0.068 - 0.081 0.96 - 0.106 0.180 - 0.187 0.279 - 0.302 0.372 - 0.575	0.0328 - 0.035 0.0353 - 0.0413 0.0417 - 0.048 0.050 - 0.068 0.163 - 0.180 0.187 - 0.272 0.318 - 0.372 0.607 - 0.855	0.081 - 0.096 0.122 - 0.163 0.272 - 0.279 0.302 - 0.318 0.575 - 0.607
$FD_{3D}L$	0.00270 - 0.00272 0.00318 - 0.00371 0.0052 - 0.0062 0.0068 - 0.0072 0.0076 - 0.0081 0.0138 - 0.0144 0.0215 - 0.0233 0.0249 - 0.0353	0.0025 - 0.0027 0.00272 - 0.00318 0.00371 - 0.0052 0.0081 - 0.00941 0.0130 - 0.0138 0.0144 - 0.0210 0.0245 - 0.0249 0.0445 - 0.047	0.0062 - 0.0068 0.0072 - 0.007 0.0094 - 0.0130 0.0210 - 0.0216 0.0233 - 0.0245 0.0353 - 0.0445
$R1_{vol}$	7808 - 8064 8192 - 8448 8832 - 9056 9184 - 9664 10944 - 10976 11040 - 11584 12192 - 13024 13728 - 14112 17312 - 25888	8064 - 8192 8448 - 8832 9120 - 9184 10240 - 10496 10752 - 10944 11584 - 12192 13024 - 13728 14112 - 15808 25888 - 50000	9056 - 9120 9664 - 10240 10496 - 10752 10976 - 11040 15808 - 17312
Vol_{avg}	8432 - 8688 9040 - 9056 9344 - 9504 9536 - 10048 10560 - 10592 11360 - 11456 11872 - 11920 12176 - 12640 13248 - 14448 17536 - 26816	8348 - 8432 8688 - 9050 9056 - 9120 9504 - 9536 10352 - 10560 11248 - 11360 11536 - 11872 11920 - 12176 12640 - 13248 14448 - 16800 26816 - 50000	8244 - 8368 9120 - 9344 10048 - 10352 11456 - 11536 16800 - 17536

Table 5.2: Data Intervals corresponding to the H&Y stages of Parkinson's Disease.[Pataca 2010]

5.2 Relationship between features and H&Y scale

Applying predicates on IF-THEN rules is challenging from the point of view of electing the rules, but at the same time, at this level we can include medical knowledge for the decision process- diagnosis must be based on medical knowledge. There are though two steps in a rule-based system:

- Clustering the features
- Define the input-output relationships

For the first step, using subtractive clustering can merge automatic clustering with fuzzy inference systems. The potential for each data point can be determined by computing the distance between the new points with regard to the others. The greatest potential value provides the cluster center. The systems characteristic behavior can be estimated by a fuzzy rule after each cluster.

The approach has the advantage of using a priori knowledge and integrating complementary information by the extracted features. It is also used in expert systems as it permits interpretation of the features. The fuzzy sets at this level are better used in labeling, although it can include uncertainty and object recognition in a procedural form. Using neural networks even if it is less restrictive than linear discriminant analysis (LDA), it does not perform very well for our data, as it is not so exact and not sensitive enough to small differences on the input data (Fig.5.4).

In an ANFIS architecture, the next step is represented by the rule strengths definition. We define a set of rules based on the detected clusters and include the medical knowledge as well. *We decide to use the rule-based approach, as the medical knowledge can be included, different features can be considered at different stages of analysis and we can refine it.* As presented in the tractography study at the evaluation stage, there is a clear correlation between the fiber parameters on the left hemisphere of the brain and the disease severity. There are cases that do not register any fibers detected due to the image quality or to the tracking method, but in those cases we consider the midbrain detected volume and/or the right side detected fibers, if there are fibers detected on this side. These features are used when a case can be placed in more than one class - for tangent clusters.

The definition of the rules for diagnosis includes not only medical knowledge, but overcomes inter-patient variability. It considers the hemisphere studied in the density of the fibers, the volume of interest where the dopamine flow starts and the 3D density of the fibers. As presented in equation 5.2, after defining the clusters using the fiber density- HY_{FD}- and based on the midbrain volume- $HY_{VOI_{Vol}}$ - we evaluate the threshold and place a new case depending on these features. When conflicts appear and a decision between clusters is not obvious, an additional feature is used for diagnosis. If we do not have a positive positioning of the case on the feature axis, than the VOI is not correctly determined due to image quality or insufficient slices for the volume. These conflicts generate the set of rules that we use for the expert system that determines a classification of the cases, depending on the disease severity. The fiber density (FD) values are classified on the H&Y scale in the first row of the table 5.2. These classified FD values from the table are used next for defining the rules in equation 5.2. These rules determine the H&Y value based on the intervals in table 5.2 and considering the correlation between the features in the table and the severity scale.

When the left side fiber density does not provide a reliable value for diagnosis, the right side bundle of fibers is taken into account and if the fibers are not detectable, the volumes of interest are taken as measures for diagnosis. Testing the rules from equation 5.2 we obtain

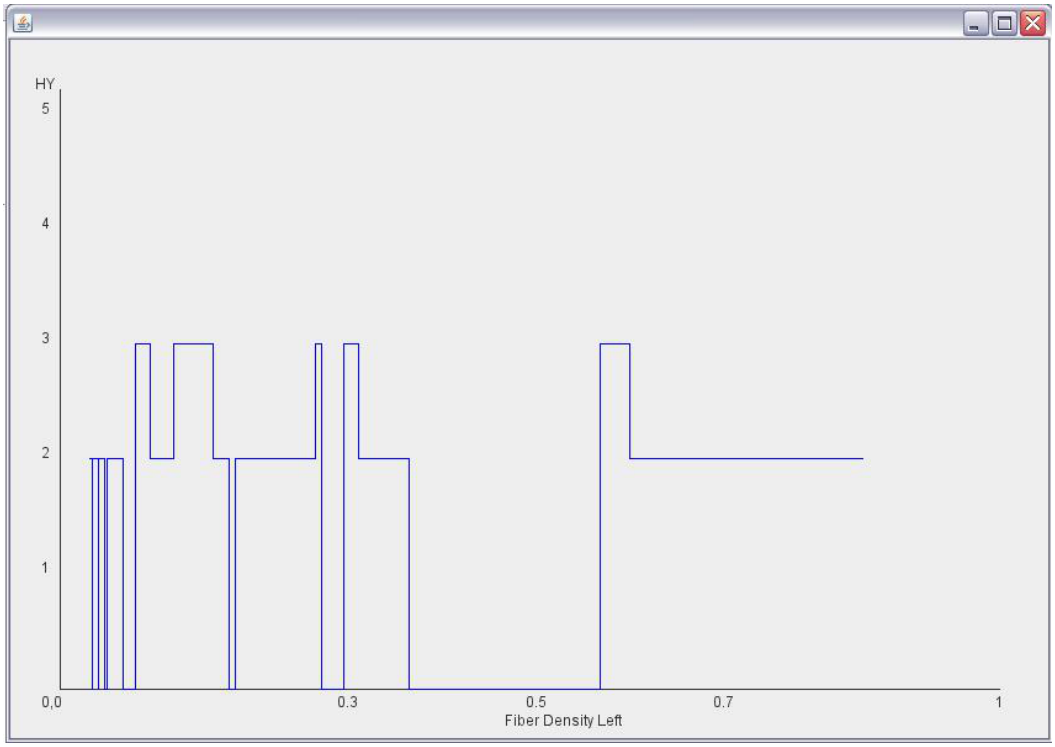

Figure 5.5: Classification with *FiberDensity* values on the left side [Pataca 2010]

the variation function for the FD according to the severity of PD represented in figure 5.5.

$$
\begin{aligned}
&If(HY_{FD} = HY_{VOI_{Vol}} \wedge HY_{FD} \neq -1)\ then\ HY = HY_{FD}\\
&If(HY_{FD} = -1 \wedge HY_{VOI_{Vol}} \neq -1)\ then\ HY = HY_{VOI_{Vol}}\\
&If(HY_{FD} \neq -1 \wedge HY_{VOI_{Vol}} = -1)\ then\ HY = HY_{FD}\\
&If(HY_{FD} \neq -1 \wedge HY_{VOI_{Vol}} \neq -1) \wedge (HY_{FD} \neq HY_{VOI_{Vol}}))\ then\\
&\quad If(FD_{3D} \neq 0)\ then\ HY = 2\\
&\quad else\ HY = 0\\
&If(HY_{FD} = -1 \wedge HY_{VOI_{Vol}} = -1) then\ The\ image\ is\ invalid!
\end{aligned}
\tag{5.2}
$$

Using this set of rules only the difference between the control and the PD cases is possible. On the PD scale, only cases rated stage 2 and 3 can be classified. For new cases, as well as for deviation study on the features, we take the clusters and determine their differences.

In our first approach, when considering neural networks for clustering, the features do not offer a clear boundary among classes defining the disease severity stages. *The diagnosis obtained in this manner is not reliable, due to the dispersedly placed cases and the overlapping nature of the intervals* appertaining to distinctive classes of PD severity. We have tested a simple KMeans approach, knowing the number of classes we need. The results were not nearly as good as those obtained with the rule-based system and fuzzy approach.

5.3 Prognosis method

From diagnosis to prognosis, there is apparently only one step. *While the diagnosis based on the rules is matching the patients to the classes that it was trained to recognize, the prognosis can place patients on severity degree levels that are not learned by the system.*

The diagnosis performs estimation for the patient by placing the feature in one of the classes corresponding to a PD stage or in the control class. The prognosis offers the value of the correlation between the disease and the affected features.

Prognosis systems learn from the formerly acquired data and by analyzing and studying it, a pattern is revealed and used for new cases. Prediction systems using artificial intelligence can be based on neural networks, on fuzzy logic, on genetic algorithms or on expert systems. As previously presented, the interference among different PD levels at the feature level does not provide a clear boundary for classification using neural networks. From the neural networks methods for prognosis, we tested the KMeans and KNN approaches but they did not provide satisfactory results on our data. The overlapping of different feature groups at the class level represents a fuzzy dispersion on the features spaces, but the fuzzy systems need additional knowledge as well. In this context, we consider the results from the rule-based diagnosis system and we continue using the ANFIS architectural method.

At this stage, the learning and classes are already defined and *we intend to find a function by using interpolation among the existing points*, representing the PD pathology on the scale severity. By extrapolation, it could provide the ability to determine the evolution tendency for the features and to determine the early cases of the disease. The ANFIS architecture at this point possesses the functions for determining the consequence parameters that provide the final decisional value. In our case, we define the interpolation functions for this purpose. The intervals with their limitations can be considered as weights in defining the interpolation functions for the ANFIS approach. Like the RBFN model, in this case the weights represent the medical constraints, encapsulated in the intervals, and the variation functions are referred in our case by the interpolation functions. The function determined in this manner should be used for extrapolation onto disease areas that are not detectable at this moment. *The function describes the disease variation based on features and for any new patient, a correct placing of the case on the PD scale.*

For defining the interpolation method, there are several steps that must to be taken:

- New data points within the existing range of acquired data
- Meshing the points
- Using the mesh determines the function that approximates the real data variation

The interpolation methods are based on the shape of the mesh function, which can be: linear, polynomial or spline. Analyzing our data set, a linear approach is not possible due to the dispersed points on the plot. A polynomial approach is challenging at the parameter level and for the final complexity, but we consider it. The liberty in the parameter choice and the adaptability provided in this case represent arguments requested by our data. The cubic spline interpolation method has weights attached to each flat surface to guide the bending of the variation function, but the challenge at this point is to find the correct variations among the weights. This approach requests additional algorithms for weight estimation.

With regard to the polynomial approach, the Lagrange function can determine the parameters and can be easily adapted on any number of features. This represents a desirable choice because for each new input, the basis polynomials can be recalculated and we improve our prediction with each step of the way. The weights offer a good perspective in improving the polynomial functions and define the spline as Lagrange functions.

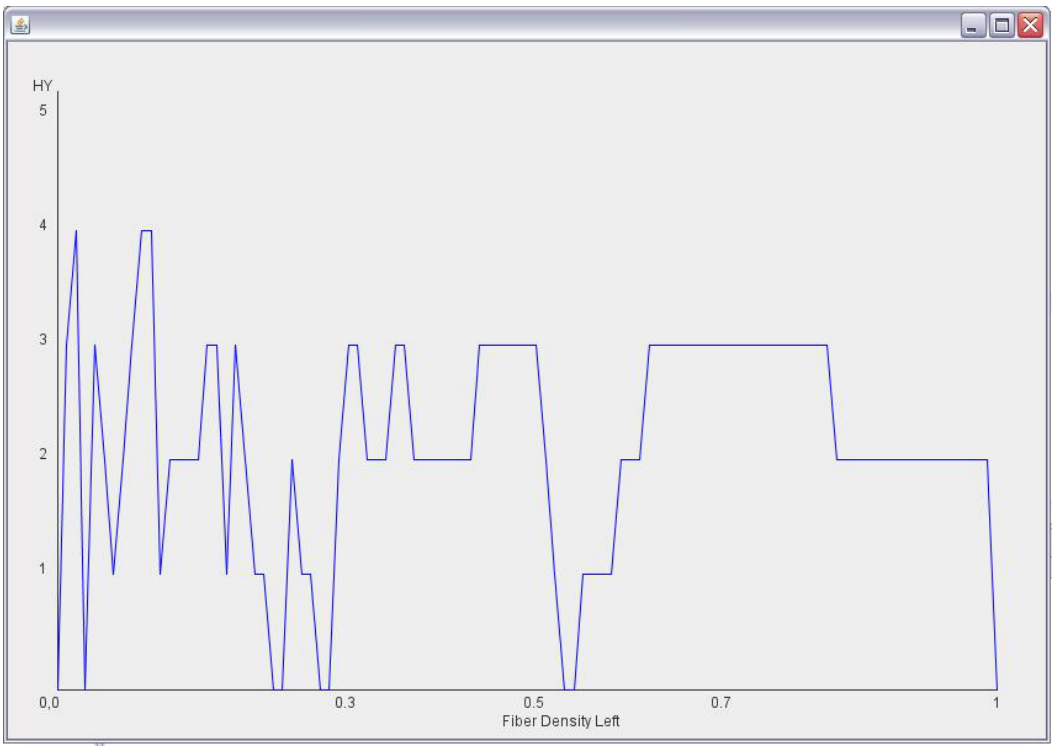

Figure 5.6: The prognosis function variation based on the Fuzzy Adaptive Evaluation (FAE) method

5.3.1 Function definition

A combination of functions is used for estimation purposes. *We aim at placing any new case at the correct level of the disease severity on the patho-clinical space.* This space is defined by the fiber measures encapsulating the pathophysiology and the clinical diagnosis, represented by the H&Y scale. *The feature points used for defining the functions in the patho-clinical space are the manually segmented Putamen patients.* We have chosen these patients as they represent the ideal segmentation and we need accuracy for the function definition. *Each patient represents a point on the patho-clinical space with the placement given by the couple (FD, H&Y).*

The Lagrange polynomials provide us with the coefficients for the spline functions used for interpolation. These methods are quick and easy to implement, but not very precise. We gain precision by dividing the data set. If we use all the 41 points for defining a Lagrange function, we obtain a 40-degree function. We require the function to pass trough all those feature points.

For a definition of a polynomial using the Lagrange approach, we need the coefficients determined by using equation 5.3. For this function, the points (x_i,y_j) represent the features extracted in table 5.2 at the image level.

$$L(x) = \sum_{i=0}^{n} y_i * \prod_{j=0, j\neq i}^{n} \frac{x - x_j}{x_i - x_j} \tag{5.3}$$

The 40 degree polynomial that obtains the coefficients using equation 5.3 is hard to handle. When introducing new cases, the function becomes very complicated and it takes a lot of

time for evaluation. The accuracy is affected as well. By dividing the feature points from the patho-clinical space into sets defined by a function for each set, we gain accuracy. A two point set definition determines a linear function and we already know that the variation is nonlinear; therefore, we start from three set points. A five-degree polynomial function becomes too complicated so the highest degree of polynomial representation on an interval is a four-degree polynomial function.

$$\begin{aligned} C_2 &= \frac{y_1}{(x_1-x_2)(x_1-x_3)} + \frac{y_2}{(x_2-x_1)(x_2-x_3)} + \frac{y_3}{(x_3-x_1)(x_3-x_2)} \\ C_1 &= -(y_1 \frac{x_2+x_3}{(x_1-x_2)(x_1-x_3)} + y_2 \frac{x_1+x_3}{(x_2-x_1)(x_2-x_3)} + y_3 \frac{x_1+x_2}{(x_3-x_1)(x_3-x_2)}) \\ C_0 &= y_1 \frac{x_2x_3}{(x_1-x_2)(x_1-x_3)} + y_2 \frac{x_1x_3}{(x_2-x_1)(x_2-x_3)} + y_3 \frac{x_1x_2}{(x_3-x_1)(x_3-x_2)} \end{aligned} \tag{5.4}$$

The prediction function is dependent on the PD stage determining differences for each set of points. Sub-functions defined for each subset of values corresponding to the severity degree represent solutions. As presented in equation 5.4 we define the parameters for the second degree polynomial function for each set of points.

The polynomial function that uses the parameters defined in equation 5.4 is the second degree Lagrange. Due to the fact that the scale is limited on the upper values at level five, and on the lower boundary at level zero, we apply the same limitations to our functions.

For the forth degree polynomial representation we determine the coefficients as presented in equation 5.5 but for this case, on the last interval, we have points that are far apart for each other. The testing on the whole database will reveal if we need the tree-points sets or five-points sets.

$$\begin{aligned} C_4 &= \sum_{i=0}^{4} y_i \prod_{j=0, j\neq i}^{4} \frac{1}{x_i-x_j} \\ C_3 &= \sum_{i=0}^{4} y_i \left(\frac{\sum_{j=0, j\neq i}^{4} -x_j}{\prod_{k=0, k\neq i}^{4} (x_i-x_k)}\right) \\ C_2 &= \sum_{i=0}^{4} y_i \left(\frac{\sum_{j=0, j\neq i}^{4} x_ix_j}{\prod_{k=0, k\neq i}^{4} (x_i-x_k)}\right) \\ C_1 &= \sum_{i=0}^{4} y_i \left(-\frac{\sum_{j=0, j\neq i}^{4} x_i \left(\sum_{m=0, m\neq j}^{4} x_m * \sum_{n=m+1}^{4} x_n\right)}{\prod_{k=0, k\neq i}^{4} (x_i-x_k)}\right) \\ C_0 &= \sum_{i=0}^{4} y_i \left(\frac{\prod_{j=0, j\neq i}^{4} x_j}{\prod_{k=1, k\neq i}^{4} (x_i-x_k)}\right) \end{aligned} \tag{5.5}$$

There are intervals where a certain polynomial function works better than another one - constraints determined by the intervals that represent the weights. This is the case with the last points on the forth degree polynomial approach, as the second degree polynomial performs better in this case. This is the reason why we need to consider not only the interval where the new points are placed when extrapolating the polynomial functions, but also the surrounding intervals and their own functions.

In the four-degree interpolation function, for the last interval, there are not enough points for the interpolation. For this function, a simple linear function follows much better the interpolation points.

5.3.2 Our analysis approach

When we provide a new case for analysis, we use the fiber features for placing it on an interval, determining the next closest values on left and right sides of the new point. Defin-

ing the interval where the new value needs to be placed, we determine the H&Y values corresponding to the interval and the mean value of the same interval. The three H&Y values provide the data for the rule-based diagnosis system. This system provides the final value for the new case.

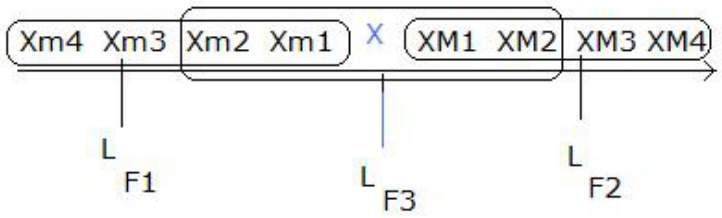

Figure 5.7: Independent Adaptive Polynomial Evaluation (IAPE)

When a new point is to be evaluated and its H&Y value determined, we have several steps to perform. We perform this estimation using the "ideal" set of points. The position of the new point (X) among the others is determined by finding the neighbor points, the one placed higher (X_M) and lower (X_m) on the feature axis- figure 5.7. For determining the H&Y value for the new feature X, we estimate it using the surrounding points. We start by determining the polynomial function using the next four points smaller than X: L_{F1}, those higher than it: L_{F2} and those that are centered in X: L_{F3}. If at least two of these three functions have as result the same H&Y value for X, then we save this value as HY_1. Otherwise we determine the functions using just the three points - second-degree polynomial functions. We can only be stopped by the linear functions that ultimately will produce the value for HY_1. A second value, HY_2, represents the H&Y value for X determined using the linear function that passes through the points associated with the X_M and X_m values. The final value is given by HY_1 if the difference between this value and HY_2 is not higher than three levels on the scale, otherwise the mean value between the two HY is the final estimated value for the disease severity. This algorithm describes an Independent Adaptive Polynomial Evaluation (IAPE) method as it is applied both on PD and controls determining a polynomial adapted to the feature data provided. The method is a hybrid ANFIS approach as it uses as back-propagation the difference between polynomials at each stage but it is also similar to the RBF by using the Lagrange polynomials.

An extension of this approach, adapted for PD cases, is called PD Adaptive polynomial evaluation method (PD-APE). The estimation function is used basically for the PD patients, adding the condition that if HY_1 or HY_2 generate as result the 0 value, the other value is to be taken as a result. This condition does not affect the results of the overall performance. The variation function incorporating this condition performs the best accuracy. From the ANFIS point of view, this method takes into the second layer the firing strength given by the PD correlation.

Determining the control and the PD cases first and then applying the function that provides the best interpolation for the set of points, represents a fuzzy adaptive method for prognosis. This variation function uses for the control cases the second-degree polynomial method and for the patient cases the PD adaptive polynomial evaluation method.

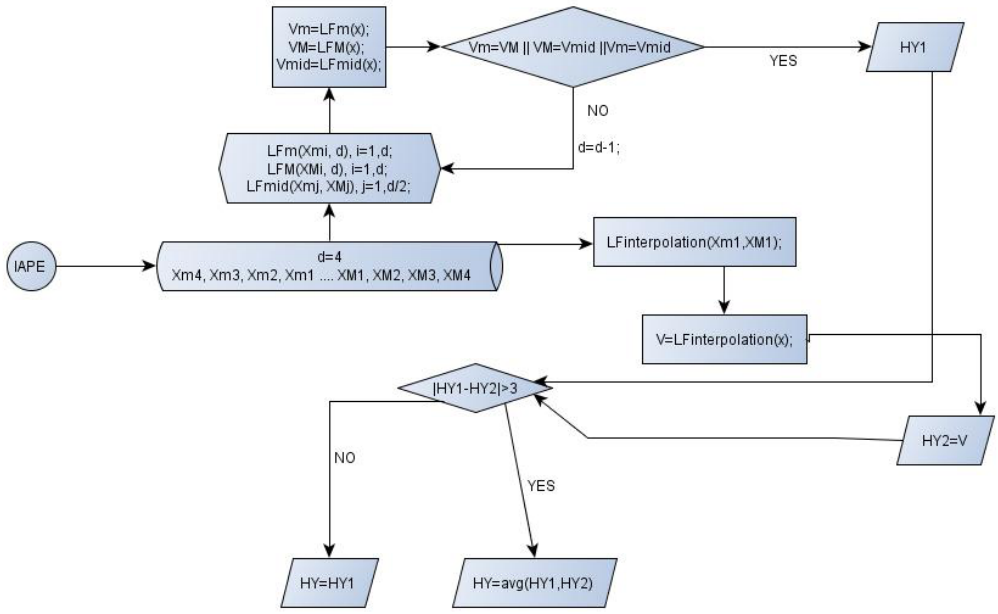

Figure 5.8: Data flow on Independent Adaptive Polynomial Evaluation (IAPE)

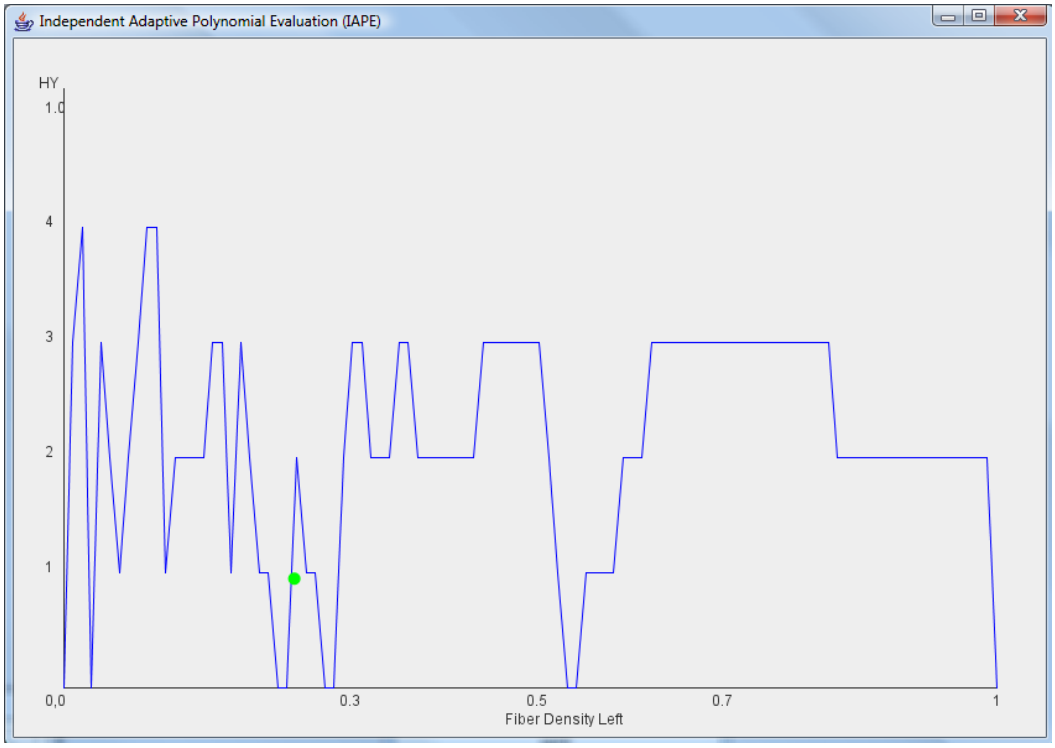

Figure 5.9: Placing of a new patient using the IAPE approach

5.4 Conclusion

Diagnosis based on a rule-based system is able to rate the patients but as it does not provide a variation function, we are not able to track new data or extrapolate for early diagnosis.

The Prognosis approach based on polynomial functions provides a much more accurate diagnosis and is able to provide an extrapolation for the new cases, as well as for new levels of disease. The polynomial degree of the function determines the data refinement and the function sensitivity. Our own analysis approach determines an adapted system for the envisioned task.

For the prognosis method, our approach proposes an ANFIS architecture based on a fuzzy inference system with a rule-based definition and several hybrid approaches at the network level. We define the required polynomials for each set of input data and we adapt it to the constraints imposed by the medical knowledge when delivering a prognosis value.

Chapter 6

Evaluation and Results

Contents

A complete procedure of a research study integrates several evaluation stages. These stages determine the study orientation by confirming or invalidating the theoretical hypothesis. Each stage is important for the overall result. Both statistical and technical aspects are tested. The statistical studies validate the theoretical approaches, whereas the technical ones, determine the research results and the method performances. There are also statistical evaluations applied to determine the impartiality of the technical methods or the one used for testing. By analyzing these tests, we are able to follow and determine if the methods applied are affecting the quality and/or quantity of the information. An important aspect for determining the evaluation methods is their impartiality to other features than the PD affected ones. The overall conclusion can be affected by incompatible tests.

As presented in figure 6.1 there are several stages where evaluation has to answer several questions. In our research, the feasibility evaluation *at the pre-processing level* needs to determine if the information at the DTI level is valuable. The DTI information relevance determines a follow-up on its traceability at the image level. The assessment includes analysis and evaluation of the correspondence between the image information and the PD severity. As presented in the schema, the results of these tests affect the next level of evaluation. The general analysis and the localized one from the feasibility, determine the degree relevancy of the PD information. A comparative analysis between the two aspects affects the segmentation.

The anatomical structures required for *the processing level* are the result of the feasibility study and are obtained using the pre-processing elements. The extraction process could affect the data and this is the reason for determining their relevancy by comparing the correlation level after this process with the one obtained during the feasibility study. The level of focalization refers to the question whether extracting the midbrain is enough or we need to determine the SN. This question is answered only after the processing level, when the relevancy of the fibers extracted denote the finesse of the tractography. As the midbrain is offering much more fibers than just the neuromotor ones, an analysis to determine whether the extracted fibers are the required ones validates the midbrain as a reliable source, even if it is vast. This analysis validates the approach used for the tractography, but the statistical

analysis of the extracted fibers determines whether the initial information is lost during extraction.

This aspect is linked to *the analysis stage* as well. The correlation of the fibers with the PD severity, expressed by the numerical measures and the concordance determined during the feasibility testing, should be at the same level or even higher. This evaluation determines if the measures affect the information revealing their reliability. Their correlation with the disease severity is exploited at the analysis stage. The questions from the analysis stage represent the global values for our study. The answers to these questions provide the conclusions to our research and they are given by the evaluation presented in this chapter.

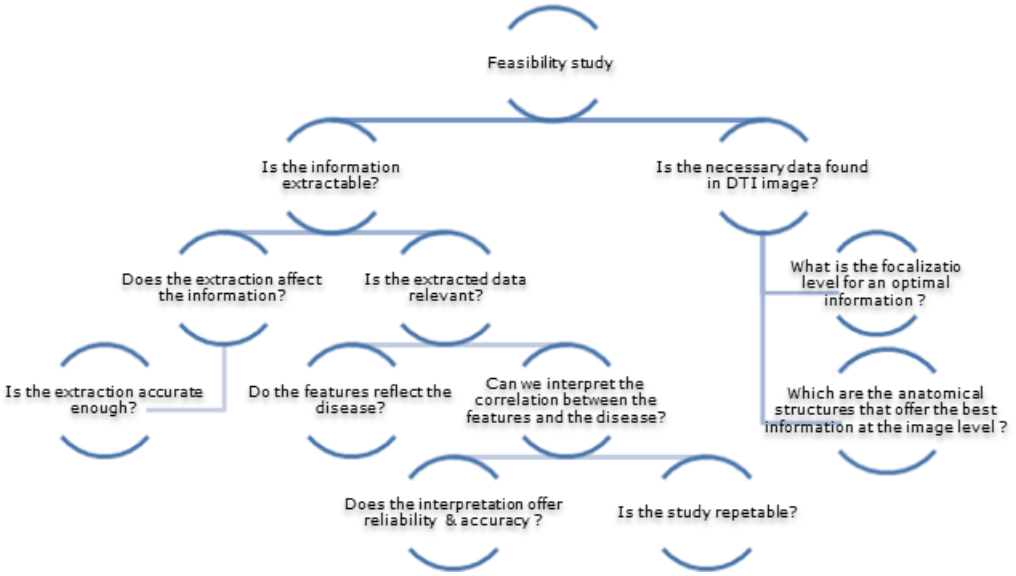

Figure 6.1: The evaluation process during our study

There are evaluation stages for determining the relevance of the contributions on each phase of the project development. These progressive tests determine if the considered approach can be further developed. This is the case for the feasibility study, performing an analysis of the green channel from the FA image on a segmented volume of the midbrain. This study, presented in [Teodorescu 2009a], determines if there are fibers correlated with the PD severity on the AP diffusion direction. The tests are performed on test-batches that determine the immunity of the testing method. This aspect of the evaluation detects the appropriate study that targets just the correlation. The same test is used for each level of information afterwards. *For the medical relevance, we use the T-Test* for detecting the correlation between the obtained values and the cognitive evaluation (ground truth).
The results of this study determine the choice of the Putamen for segmentation, as it is placed in the direction of diffusion, indicated by the fibers staring from the midbrain area. The choice is determined by the conclusion of the test the similar studies indicating that its physiology is affected by the PD pathology.

After the feasibility study defining the path and the context of our prototype, we evaluate the entire study. As each module of the prototype contains contributions and has original ideas, their estimated values define the local performances. For the global view, we consider the intermediate results and the technical aspects affecting the overall study.

The overall estimation for the medical imaging as biomarker should offer not only relevance to the disease, but also performance characteristics and generalization capabilities.

We have evaluated the DTI information relevance for the disease by determining the correlation for each level of information processing. We evaluate the criteria defining a new marker by testing the DTI performances obtained for the entire database. The ground truth, represented by the values of the PD severity on the H&Y scale, is provided the Singapore General Hospital (SGH), together with the image database. For our database, the heterogeneity of the patients provides generalization evaluation capabilities.

Another aspect of the overall evaluation is represented by *the platform introduced as prototype* (Fig. 6.2) from the technical point of view. This evaluation uses other approaches and is comparing our results with the ones obtained with other methods (software/algorithms) using our images. The goal is to determine the algorithm accuracy. The overall performances are affected by these techniques and their ability to accurately and correctly extract and analyze the medical image and its derived information. The automatization of the entire process determines original solutions that could affect the data.

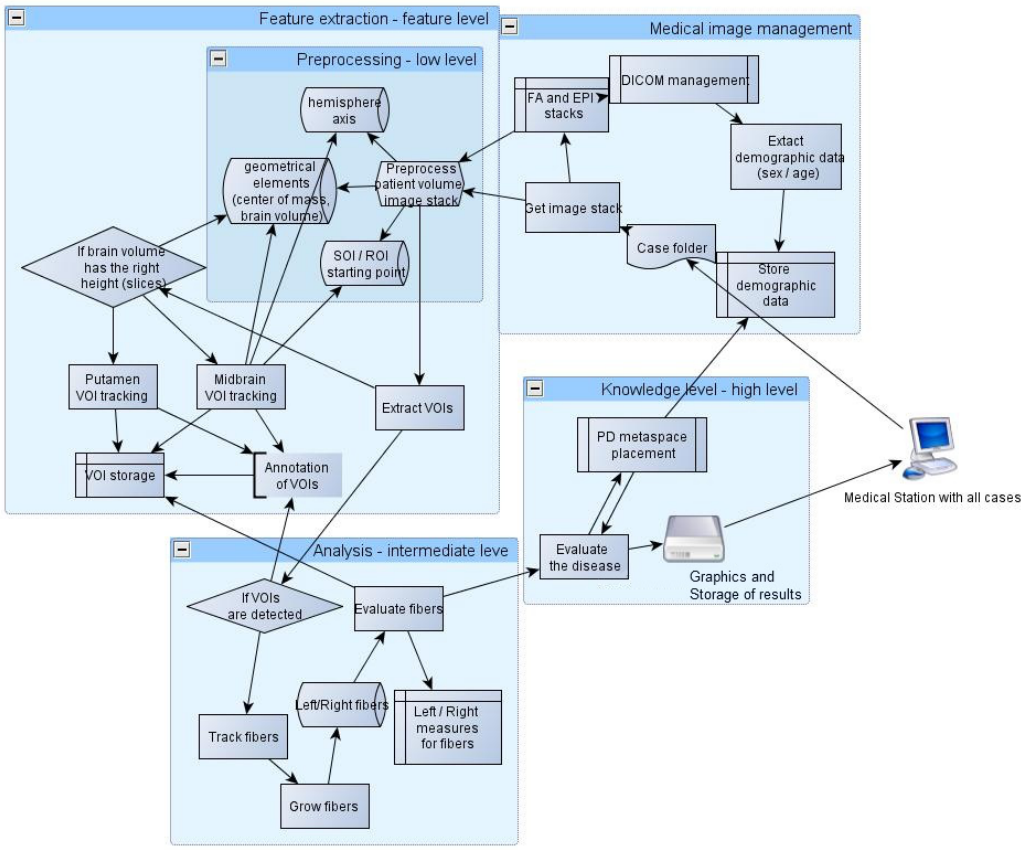

Figure 6.2: The main stages for data management for DTI image using our prototype, PDFibAtl@as

Another validation and evaluation is performed at the processing level, for the segmentation methods, in order to determine their accuracy and to ensure that this process does not affect the quality of the information extracted. The neurologist evaluates the automatic detection method of the midbrain. We validate the volumes obtained by running the results under the supervision of our partner neurologist, to verify the placement of the detected

elements on the initial images. The detected Putamen is evaluated at the image processing level, by comparison with the volume detected by using the manual segmentation of this anatomical area. By performing a logical AND between the two mask images representing the segmentation we determine the difference representing inaccuracy or inadvertence. The resulted image represents the non-overlapping areas. These areas represent the error rate of the automatic segmentation.
Another technical aspect is represented by the fusion. This process is performed using a geometrical registration. The automatic Putamen detected on the FA stack is registered afterwards on the EPI stack. The registration method is fully automatic. This method was visually validated as well, in collaboration with the radiologists.

At the tractography level, the two aspects that need validation are: the correct identification of the neuromotor tract and the relevance of the measures for the detected tract. For the fibers, we can only verify that the detected ones are approximately on the SN area. The correlation of the tracked fibers with the determined PD severity, validated this time not only the fact that the neuromotor fibers are affected by the pathology of the disease, but also that the determined fibers from the image level can be used for determining the condition of the patient. Furthermore, our new metrics that encapsulate the detected fibers are correlated with the severity of the disease as well, indicating the efficiency of these metrics.
The analysis stage is evaluated indicating its accuracy by taking as ground truth the H&Y values of the patients.

Before evaluating our research, we define the metrics used for estimating the performance of each method, the significance of the measures and their relevance. The testing is performed on the entire database, to determine the adaptability and the indifference to the demographic parameters.

The whole database contains 66 patients and 66 control cases that managed successfully to generate the segmented areas. We dispose of 68 patients and 70 control cases, but due to the image stacks unable to provide the entire volume between the midbrain and the Putamen, 2 patients and 4 controls were eliminated from the test. We use this database to evaluate the final results provided by the prototype, representing the overall process for determining the prognosis.

6.1 Evaluating metrics for the overall performance

The performance level of the CAD systems is given by the sensitivity of the detection, together with the specificity and the accuracy. The information extracted from the medical images is evaluated at this level, after the application of all the extraction and analysis methods. When detecting abnormalities in an image, the true and false refer to the decision of the algorithm, compared with the clinician decision.

- TP true positive - the algorithm detects correctly the abnormality
- FP false positive - an abnormality is detected while it is not in the image
- TN true negative - no abnormality exists and the algorithm does not detect one either
- FN false negative - the algorithm does not detect an abnormality when it is there

These terms have different meaning, depending on the evaluated method. Using these terms, we define the metrics that determine the performances: the sensitivity in equation 6.1, the

specificity in equation 6.2 and the accuracy in equation 6.3.

$$Sensitivity = \frac{TP}{TP + FN} \tag{6.1}$$

The sensitivity represents the abnormality rate detected on a set of problematic patients and it is a percentage of success of the algorithm. On the other hand, the specificity represents the normally detected cases, being a percentage measure as well.

$$Specificity = \frac{TN}{TN + FP} \tag{6.2}$$

The sensitivity reflects the positive cases identified correctly and the specificity represents the negative cases identified as such. For a complete analysis of the performances, the accuracy of the system is computed as well. This metric characterizes the overall system. Usually, there is a tradeoff between sensitivity and specificity. The accuracy reflects this tradeoff as it includes both TP and FN.

$$Accuracy = \frac{TP + TN}{TP + FP + TN + FN} \tag{6.3}$$

The graphical representation reflecting the balance between the sensitivity and the specificity is the ROC curve. This statistical parameter defining and estimating the methods proposed is a Receiver Operating Characteristic (ROC) curve representing the two measures: sensitivity versus specificity. This curve applies to our final methods, at the diagnosis and prognosis level of our approach. It estimates the accuracy of the method and ideally has the shape presented in figure 6.3, where the distributions do not overlap. On the diagonal, all the distributions overlap. The Area Under the Curve (AUC) represents an overall measure of the test performance and allows comparison between different methods. This area is interpreted as a distance between the disease and control test results. The AUC is a subunit measure and its maximal value is 1. This represents the ideal value for a test.

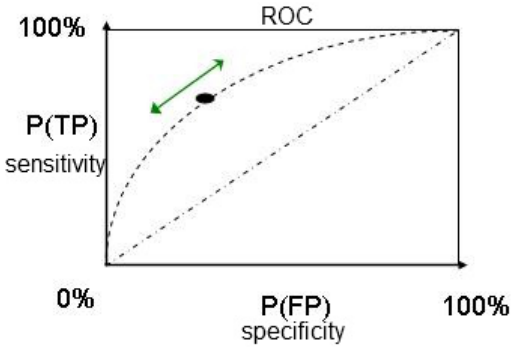

Figure 6.3: Receiver Operating Characteristic (ROC) curve

Using the defined statistical metrics, we test the performances of the prototype for each processing level, the overall performance representing our study's achievement.

6.2 Performances for different stages of the system

We present the results obtained at different evolutionary stages of our approach. The processing level performances are determined at the segmentation level and after performing the tractography. To evaluate the fibers, we consider the fibers association to the strationigral

tract. Together with the cases that did not provide any valid fibers after the tractography, these cases represent the errors for the first stage. Results on different methods validate the approach. For the analysis level, determining the performances for the diagnosis and the prognosis define the global performances of the system. All the evaluations are performed using the entire database with our own methods.

The way that the database is used affects the results obtained. As presented in [Sonka 2009] various computerized methods, the use of different database affects the results. We have ensured the indifference towards the demographic parameters as presented earlier. Nevertheless the quality of the images, better in some cases and more accurate for other patients, influences the results. The subtle cases provide a lower performance level. The database characteristics influence the training and the objective measures.

For the second feature analysis stage, we evaluate the variance of the disease severity: classifying a patient with PD among the controls or classifying a control case among the PD patients. The variance of the disease determines another error rate among the PD patients - considering a patient more or less affected by the disease than it really is the case. The input and output data are important when evaluating the independent modules of our prototype. Their nature is different, following the transitional stages defined for the DTI image information migration advancing from the image to the knowledge level.

For the image processing level of the prototype, we have as input data the images and we test the automatic detection against the manual one. The tractography uses images as input as well, but it determines the values for the new introduced parameters: FD, FD_{3D}, FD_{rel}, FV. At the feature level, we have as input data, the extracted values for the neural fibers on the left and the right side, expressed using the new metrics and the detected volumes on both sides. The diagnosis and prognosis module provide, as output, the disease severity on the H&Y scale.

6.2.1 Segmentation evaluation

The importance of the segmentation is revealed by the Putamen detection methods. The different methods changed the diagnosis sensitivity with 19% . The correct detection of this volume of interest, determines an accurate selection of the fibers and this aspect is translated at the diagnosis level.

In order to estimate the performance of the Putamen detection, we use the manually detected areas as the ground truth, against the automatically detected ones. *The manually detected areas are detected on 42 subjects: 22 patients and 20 control cases.*

When computing the sensitivity and specificity for the image processing level, we obtain values of *0.63%*, respectively *0.87%*. The same evaluation is momentarily impossible for the diagnosis, as we need confirmation for the FP and FN cases.

In our evaluation, we consider several parameters like the *technical efficacy, the diagnostic accuracy and the error rates.*

The difference between the number of fibers detected with the manually segmented Putamen and with the automatic one, for the same patients, determines the error rate for the automatic detection. This error rate is measured by the *relative error* value presented in equation 6.4.

$$Err_{rel} = \frac{x - X}{X} * 100[\%] \tag{6.4}$$

where x represents the measured value and X is the average value of all the measurements - in our case, the difference between the manually detected Putamen area and the automatic one.

Test type	Left(Err_{rel} [%])	Right(Err_{rel}[%])
Unaligned volumes	34.66	35.75
Volumes aligned	37.26	39.6

Table 6.1: Relative error rate for Putamen

Regarding the methods used for the segmentation of the Putamen, we are testing an inter-slice alignment of the detected masked slice images. This alignment is based on the center of mass of the detected region. As table 6.1 presents, the aligned volumes do not perform better than the method that is choosing the seed as the center of mass of the detected region in 2D. As for the error rate, it is computed using the area of the manually detected Putamen and the one of the automatically detected one, on the tractography process. For the method using exclusively the triangular shape for the Putamen segmentation we detect an error rate of *34.66%* for the left side and *35.75%* for the right side of the brain. Evaluating the alignment algorithm based on the center of mass offers a the relative error rate of *37.16%* on the left side and *39.6%* on the right side.

The reason for the influence of the Putamen on the tractography results is that the fibers crossing trough the detected Putamen are usually placed on the posterior part of this anatomical area most of the time left outside by poor detection methods. A good detection places the Putamen mask accurately on this area, detecting all the neuromotor fibers.

The results show a smaller error rate for the left Putamen area, which has more clear boundaries than the right Putamen area. This correct detection is desired from our perspective as it is consistent with the medical approach which has determined that PD patients are usually more affected on the left side of the brain by this disease.

As the correct placement of the Putamen determines the validation for the strationigral fibers, its placement, together with the correct detection of the volume, determines the number of fibers and directly affects the analysis results.

6.2.2 Tractography effectiveness

For fiber evaluation, the number of fibers identified for each patient, represents the measure of a correct or an incorrect segmentation. The tracking algorithm is sensitive to the Putamen detection and to the EPI image quality. Values for the fibers higher than 20 represent a misplacement of the Putamen area or an incorrect detection, as we have concluded. The reason for this conclusion is represented by the fact that when the Putamen is incorrectly detected, the tractography algorithm validates more than just the strationigral tract. Based on these elements, we define the parameters for the sensitivity, specificity and accuracy evaluation.

- TP - PD patients that have a correct segmentation compared to the manual approach that have less than 20 fibers
- FP - PD patients with a correct segmentation and more than 20 fibers
- TN - Patients that do not have correct identification of the volumes of interest
- FN - Patients with volumes detected that provide no fibers after tracking

With these categories of patients, we obtain *89%* specificity, *80%* sensitivity and *82%* accuracy *on the PD patients* for the left side. Detection for the Putamen for this test represents the combined triangular and quadrilateral approach algorithm. The same approach *on the*

Test	Specificity [%]	Sensitivity[%]	Accuracy[%]
Patients	89	86	82
Control	37	82	75
Overall	63	81	78.5

Table 6.2: Tractography performances

control subjects provides values of *37%* specificity, *82%* sensitivity and *75%* accuracy. Determining the *overall performance of the algorithms on the data*, we obtain *63%* specificity, *81%* sensitivity and *78.5%* accuracy (table 6.2).

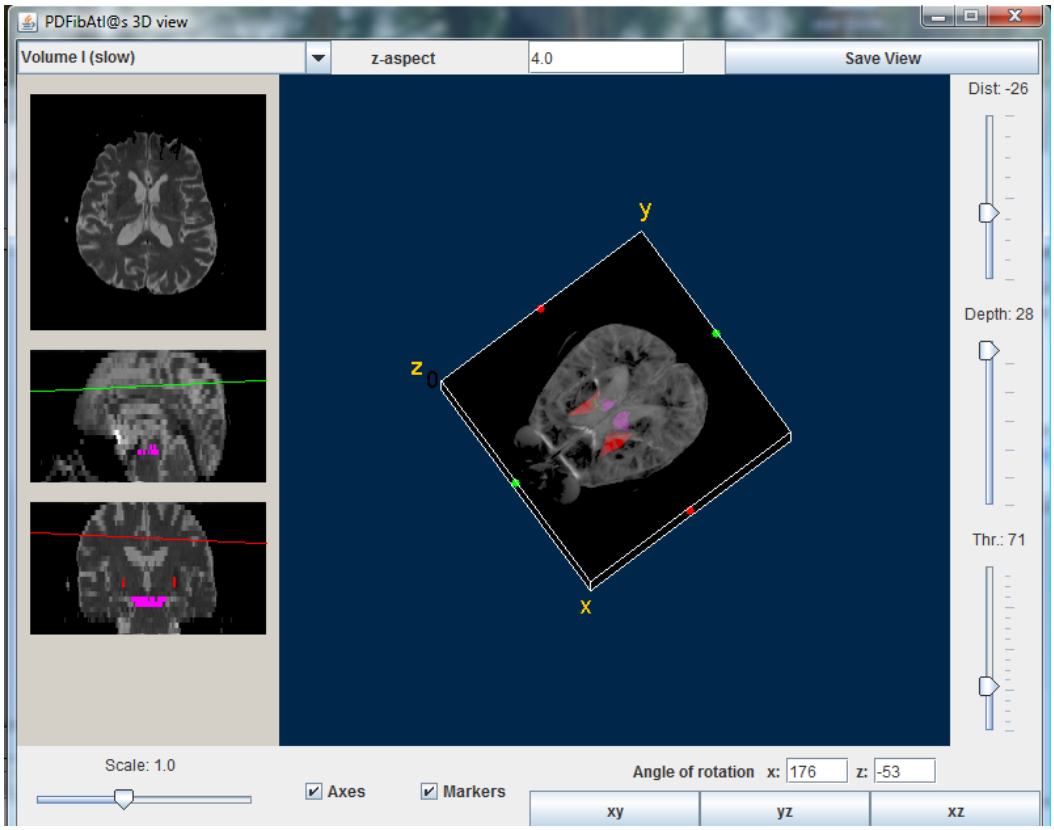

Figure 6.4: Fibers determined by tractography using the automatic segmentation methods for VOIs

The neurologist also performs the validation of the fibers, so that we can be sure of detecting the right bundle of fibers for further study. The neuromotor fibers start from the SN area in midbrain and are validated only if they reach the Putamen. The thresholds for tractography are 0.1 for the FA value and 0.6 for the fiber angulations. The number of fibers represents the output of this module. Together with the values of the segmented volumes of interest, the fibers provide the measures used as input by the diagnosis and prognosis module.

6.2.3 Diagnosis performance

Using the neuromotor extracted fibers from the processing level, we interpret the extracted data by using the fiber density defined in equation 4.10 and the recalculated values in

equation 5.1.

The training set is composed by the 42 patients (22 PD diagnosed patients and 20 control cases) that have the Putamen manually detected. In this case the Putamen segmentation does not affect the results from the diagnosis.

The normalized extracted data represent the input for this module. We perform pretesting on 26 patients, to determine an applicable approach. The diagnosis is achieved by using the rule based system on the intervals defined in table 5.2 for the extracted normalized features. We test the system on the intervals for the left fiber density. After training the rule-based system on the test batch, we retrieve a *61.53%* success rate [Pataca 2010] with 16 cases correctly identified and 10 cases not detected, where 6 from these 10 are not valid and 4 are incorrectly placed on the scale. The cases that are incorrectly placed represent cases where the tractography was not able to provide fibers for the left side.

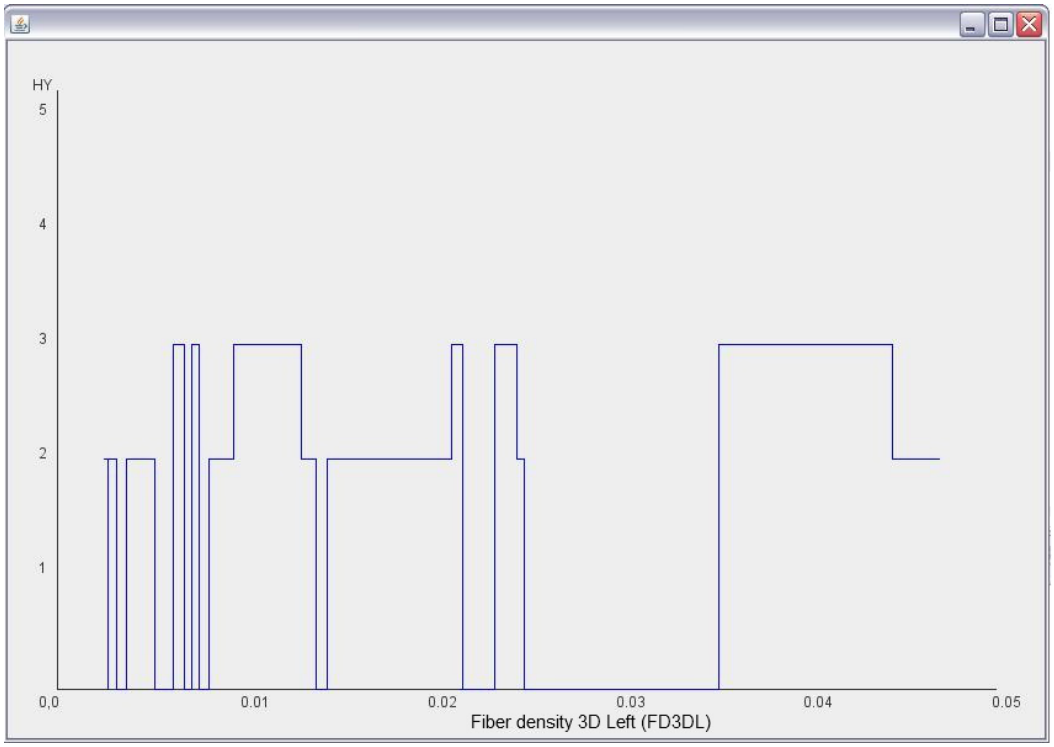

Figure 6.5: Classification based on the FD_{3DL} [Pataca 2010]

As shown in figure 6.5, the diagnosis is able to determine, based on the rules, only what it has learned. This represents cases graded on the H&Y scale from stage 2 to stage 4, as we do not have patients with level 5 due to their immobility. A patient at stage 1 of PD is not detectable yet as this stage represents the mild cases and it is considered early diagnosis.

From the biomarkers standpoint, the diagnosis approach determines the relevance for the disease of the medical image represented by the neuromotor fibers. Using the rule-based approach, we provide a correlation with the disease for the DTI image information, based on the fibers with 61% accuracy. At this level, the downside is that only by introducing new rules we can estimate the early cases. Although this method is expandable and it can integrate the clinical aspects as well, there is currently no solution for determining the early cases in this manner. There is additional knowledge involved for this purpose and it is not available at this point. Without it, early PD stages are not approachable in this manner.

As these cases are not detectable, the ground truth is not currently available either.

Taking another approach by using the prognosis functions, we are able to expand our research and offer a possibility to reach the early cases by extrapolation.

6.2.4 Prognosis evaluation

For the prognosis approach, our study is based on the ANFIS architecture, but it studies several possibilities for the interpolation approach. Considering the input data characteristics, this architecture offered a reliable base. For the interpolation function development, we train the methods using the data set obtained from the manual detected Putamen application for fiber detection (41 subjects). We choose this set as it represents the "ideal" data, unbiased by the Putamen detection. Our interpolation methods are compared to determine their strong and weak points for further development.

Using the second and the forth degree polynomial determined in chapter 5, we first test *the prognosis module on the batch represented by 26 patients*. The results on the *second degree polynomial function* represent *19%* for the error rate on the training set and *34%* success rate for the *forth degree polynomial function*. The functions are defined using the fiber density normalized values on the left side of the brain [Pataca 2010].

We evaluate the *Fuzzy Adaptive Evaluation prognosis function* on a batch from the training set (37 PD patients and 52 control cases that provided valid features after the fiber extraction). We include randomly 5 PD patients from the initial training set with 42 cases that have been processed using the entire automatic approach. With a rate of accuracy of *32.43%* on the patients and *46.15%* on the control data, the overall system provides a *40.44%* correct identification rate.

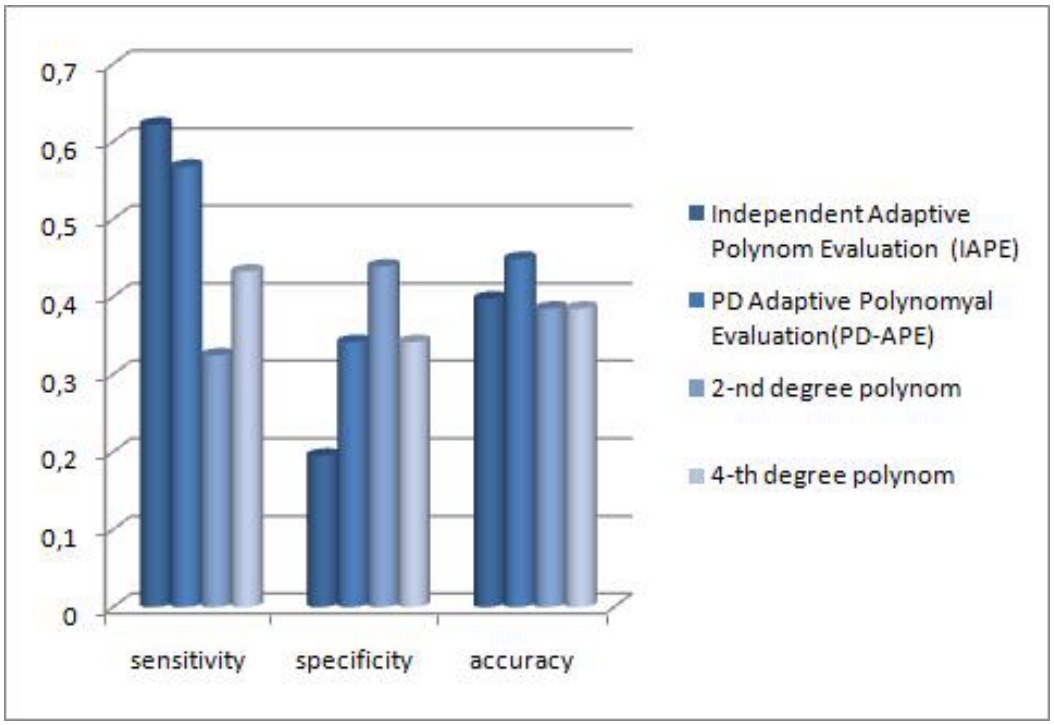

Figure 6.6: The Sensitivity, Specificity and Accuracy of the prognosis methods

An evaluation of the diagnosis and prognosis module is performed using the all automatic

methods applied on the database (68 patients and 66 controls). These results are presented in figure 6.6. For computing the values for these parameters using the equations 6.1, 6.2, respectively 6.3, the values for the coefficients represent the following:

TP cases with PD correctly identified

FP control cases identified as PD

TN control cases correctly identified

FN unidentified PD cases

The patients are characterized by the value of the sensitivity with the best result determined by using the Independent Adaptive Polynomial Evaluation (IAPE) method with a value of *62.16%*. On the control cases, the specificity represents the defining value and the best performance is obtained by using the second degree polynomial approach with *43.9%*. The accuracy represents the overall performance of the algorithms and from its perspective the method that performs the best is the PD Adaptive Polynomial Evaluation (PD-APE) providing a value of *44.87%*.

The overall performance of the prognosis module is provided by the ROC curve. We compute this metric using the SPSS 17.0 (Statistical Package for the Social Sciences). We estimate separately the patients to determine the relevance for the disease in determining the severity degree. The controls are tested for determining the sensitivity factor of the methods. *Evaluating the IAPE method using this metric, the area under the curve (AUC) is 0.705, whereas for the PD-APE the value is 0.959* (see figure 6.7). This indicates a much better performance on the patients' data for the second method.

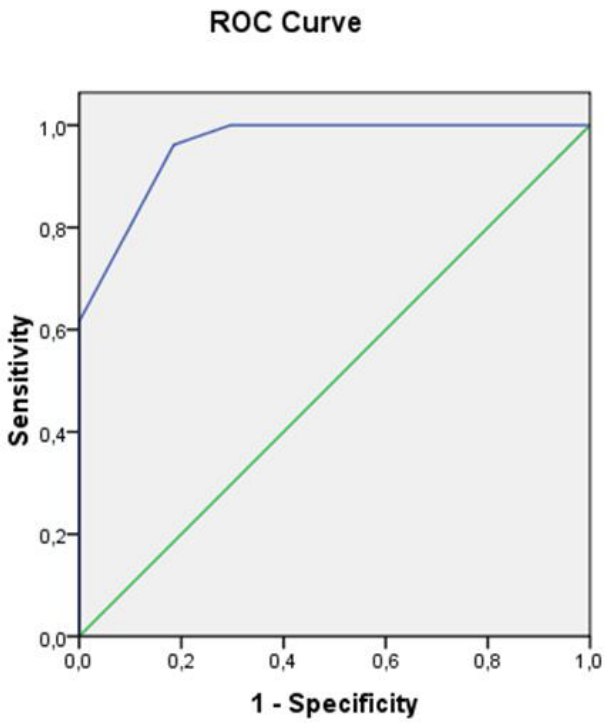

Figure 6.7: ROC curve for PD-APE prognosis method on the patient data. The AUC value for this case is 0.959 on the 68 PD diagnosed patients from the database.

We evaluate the prognosis performances on the control and patient data to estimate the overall capacity of the DTI image information in our approach. We compare the ROC

curves for different methods, and for this purpose, we use the MedCalc[1] software. This software provides two approaches for the ROC curve estimation: De Long and Hanley & McNiel. Using the complete database with all the subjects, the results for IAPE provided the same AUC value for the two ROC estimations. We further use the De Long approach when evaluating the ROC, as the error rate provided on the same test is slightly lower compared with the McNiel approach (0.1%).

For the PD-APE method of prognosis, we obtain a value of 0.569 for AUC for the overall test. The IAPE method for the same the dataset, the AUC value provides a value of 0.745 (see figure 6.8). Comparing the two curves, the difference between the areas is 0.176 - figure 6.9.

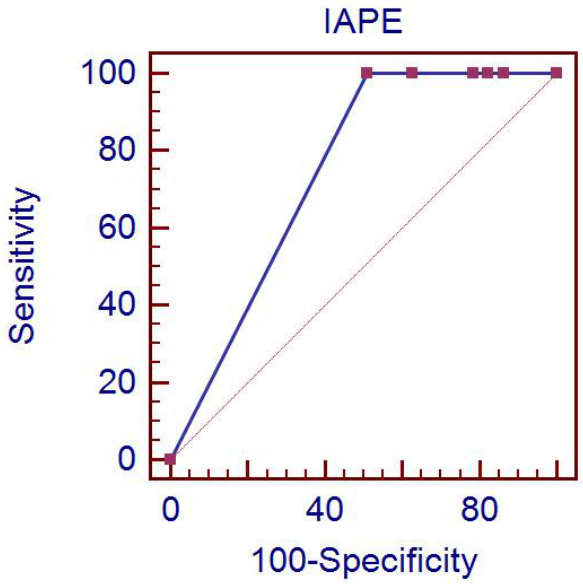

Figure 6.8: The ROC curve representing the IAPE prognosis method applied on the whole database: 68 PD cases and 75 controls. The AUC for this test is 0.745.

Comparing the diagnosis and the prognosis approach, even if the prognosis offers the possibility of determining early cases, its performances are lower. The values obtained nevertheless represent encouraging results from the numerical and biomarker standpoints.

6.2.5 Computational speed and requirements

We use Java for all the systems with imageJ toolbox and bio-medical imaging plug-ins [2]. The image processing corresponding to the pre-processing part is done by enhancing the contrast for the EPI images and removing the noise. For the removal of the skull, we use K-Means method for the segmentation based on the pixel intensity. By removing the skull, we remove the outside noise surrounding the entire brain-the aura effect-induced by the scanner. For the 3D visualization, we are using the Volume Viewer from imageJ [3].

The algorithm is tested on Intel core Quad CPU Q660 (2.4GHz; 4.0G RAM) and *the average time for each patient is 4.68 min with the automatic detection and the fiber growth algorithm.* If with DTI tracker from MedINRIA, the time to perform just the tractography on our images for one patient was 1-5 min, with our prototype, it takes us an average of

[1] MedCalc 11.3.3.0 - www.medcalc.be

[2] Bio-medical image -http://webscreen.ophth.uiowa.edu/bij/ - last accessed on May 2010

[3] Volume Viewer 3D - http://rsbweb.nih.gov/ij/plugins/volume-viewer.html - last accessed on March 2010

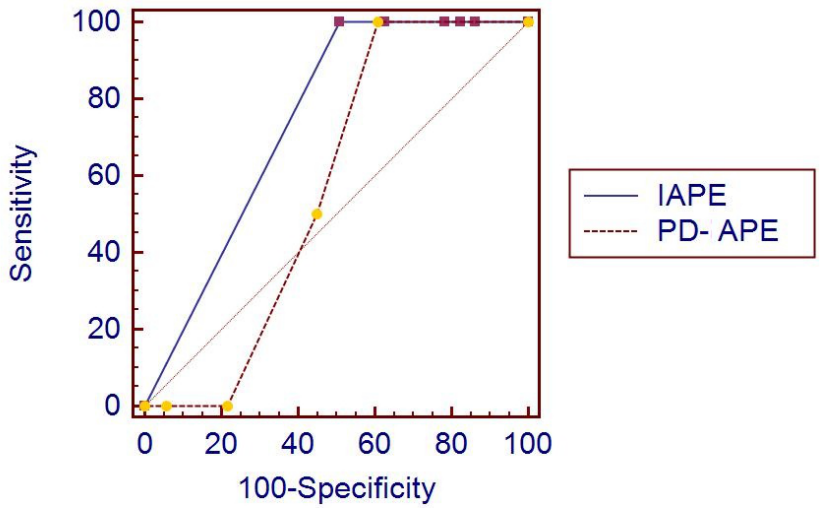

Figure 6.9: The two ROC curves for IAPE and PD-APE methods applied on the database (143 cases: 68 patients and 75 controls). The AUC values for IAPE and PD-APE are 0.745, respectively 0.569. Evaluating the ROC difference between the two tested methods the AUC indicates a difference of 0.176.

2 min. The reason of this computation efficiency is related to the limitation of the area for the fibers when performing a global tractography, whereas the method proposed by the DTI tracking module (MedINRIA) takes a local approach without an ending point for the fibers, selecting at the end the fibers passing through a specific volume of interest. The 2 mins represent for our system all the time needed from the pre-processing to the end of processing level. A similar time (1.2 min) is achieved using a probabilistic global method with the Diffusion Tracking module (TrackVis) for image selection and the tractography, without segmentation and computation of the fiber metrics.

Our system provides a user interface for displaying the results and the obtained numerical values for segmentation and tractography. Figure 6.10 represents the features extracted for each patient after the processing level, the volume extraction and the tractography. It displays the 3D view of the EPI stack, with the segmented volumes of interest and the detected neuromotor fibers highlighted.

6.3 Conclusion

Medical Imaging providing all the information to be used for diagnosis and prognosis purpose represents the technical support for the biomarker study. The correlation with the severity of the disease determined with the cognitive testing represents the relevance to the disease. The performance of the marker is represented by the level of accuracy for de diagnosis and prognosis. The third criterion for validating the biomarker is represented by its generalization capability. The heterogeneity of the database, as well as the large number of subjects provide the validity for this aspect. From our perspective, all the three points defining the biomarker have been attaint. In these conditions we can conclude that medical imaging can effectively be used as a biomarker for PD.

From the point of view of the evaluation and testing criteria, the contributions revealed in this chapter represent the testing technique. This technique mixes the cases for reveal-

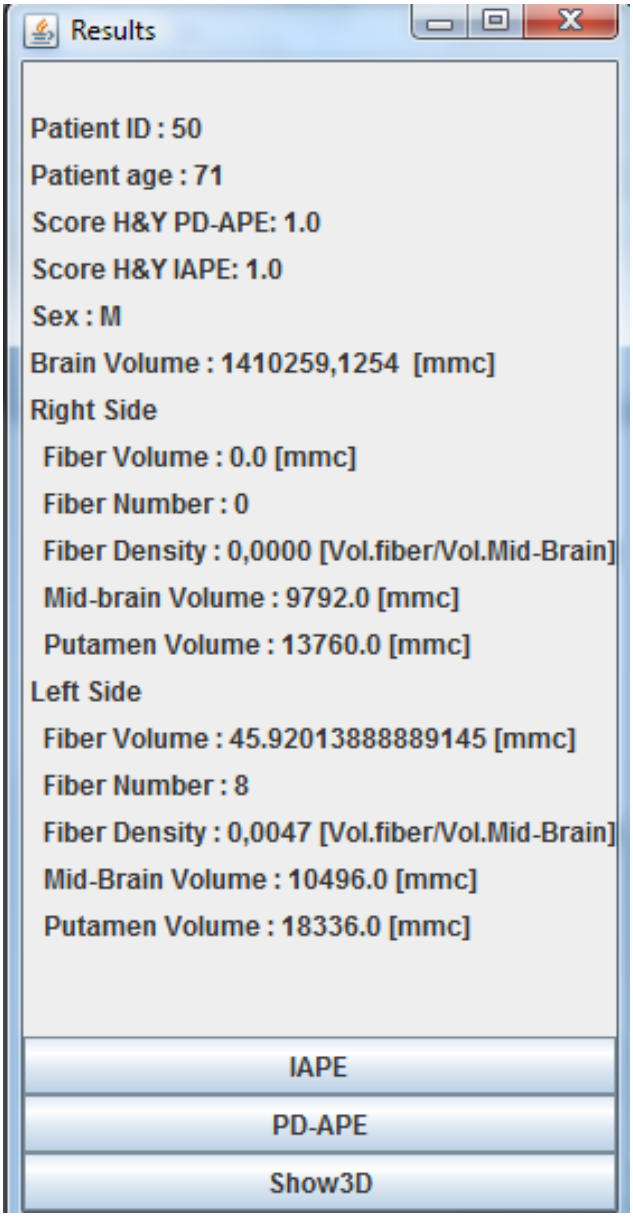

Figure 6.10: The Results Window with numerical evaluation for an example patient. The 3D view of the fibers and VOIs for the same patient is presented in figure 6.4

ing the effects of the cognitive parameters and the tests that are not affected by these parameters. The feasibility analysis has already been presented in [Teodorescu 2009b], [Teodorescu 2009c] and [Teodorescu 2009a]. The original approach on the segmentation of the Putamen was presented in [Sabau 2010]. The fibers and the PDFibAtl@s prototype is presented in [Teodorescu 2010] and as a demo version at [Teodorescu 2009b]. The diagnosis and prognosis, representing the final module of our prototype, using the second and forth degree polynomial algorithms, were presented in [Pataca 2010].

Evaluating the obtained volumes of interest, as well as the techniques implemented,

proved to be appropriated for the type of image that we are dealing with, as well as for the resolution of these images. The speed of computation reveals a system that performs in a few minutes the detection of the regions of interest, as well as the computation of the fibers.

We have found a way to evaluate our algorithms separately and the whole approach as well, using the PDFibAtl@s prototype. We need to tune the diagnosis and prognosis functions for a better detection rate. These functions have been created using the manual segmented Putamen data with additional five cases among the cases processed using the automatic Putamen segmentation.

All the elements in the system affect each other. The Putamen accuracy determines a higher accuracy on the fibers and the fiber accuracy is essential to diagnosis and prognosis module. We note that the results and the algorithms presented in this study have been successfully selected (at the methodology level) and presented in significant radiologic and scientific communications ([Teodorescu 2010] [Teodorescu 2009a] [Teodorescu 2009b]).

Chapter 7

Conclusions and Future perspectives

Contents

The research study presented in this manuscript is performed to determine the possibility to use the DTI image as biomarker. It represents the entire demarche starting from the feasibility study in the context of the existing PD biomarkers and achieving to define and implement, test and validate a prototype integrating all the methods defined by our study.

Our research includes several levels where new scientific methods are developed. Proposing a way for estimating the severity of the PD based on the information provided exclusively by the image, represents altogether a new demarche. The possibility *to use the medical image as biomarker* exploits a new dimension: the visual information that has not been used by itself in PD diagnosis. Determining a measurable value starting from this information represents an alternative to the current cognitive test. The prognosis represents another scientific act that based on measurable functionality and specific features determine an exhaustive scale for the diseases severity. It is moving the diagnosis moment towards the non-specific symptomatic area *determining the medical imaging to be considered as an end-point marker*. Our study placed DTI imaging among the *risk-evaluating markers* by attempting to determine the early cases and evaluate the prognosis.
The system presented considers the PD pathology manifested at the image level in physiology changes and interprets these changes at the clinical level. This perspective places the DTI among the *clinical diagnosis biomarker* as it determines the severity of PD acting at the clinical level.

These scientific aims are reached by *studying the specificities* of the medical images and *evaluating the possibility* to extract and use the technical information related to the disease pathology. The research starts by analyzing the medical premises and their correspondence on the image modality and the specific elements. The technical elements composing the medical image specificities are analyzed as well and their applicability is determined by the PD pathophysiology content. This content represented as information at the image level is investigated by the feasibility study. Correlating this information with the clinical level reveals the relevance to the disease. *This relevance is one of the main criteria for validating a biomarker and the DTI has proven to be meaningful* from the feasibility study until the feature level. From this level on, the computer vision elements interpret the features and the relevance value is transformed in measurable one on the disease specific scale.

Once the relevance is determined, we needed to determine the performance of the DTI as marker. For this purpose, we developed methods and algorithms capable to manage

the information from the DTI level up to the knowledge level, by following the pathology landmarks. Each step of the way, we are performing testing to determine if the information is affected by the methods used or by external factors. The result of the research at the technical level is represented by methods constructing the PDFibAtl@s prototype. The initial results of each method are updated by new methods and the evaluation and validation presented in the previous chapter are promising. Considering this aspect, *we can confirm that DTI medical image possesses the performance characteristics of a PD marker that recommend further study and development for a better exploitation of its capabilities in this sense.*

The third criteria for validating a marker, according to [Marck 2008], is its degree of generalization. This aspect is treated by the heterogeneity of our database where just the damaged images could not be used. The aspect of demographic variability, as well as the intra and inter-patient variability is taken into consideration by our study and solutions are found. In this case we can certify the degree of generalization of the DTI independent of the demographic aspect or the patient variability.

The DTI image confirms the three general criteria for defining a biomarker, based not only on the theoretical aspects and hypotheses, but backed up by the technical development and implementation and by the study on a vast database.

There are three aspects that can be evaluated in our work: the main purpose of our research for establishing the DTI image as a biomarker, the technical elements developed and implemented for that purpose and the clinical applicability of this marker. As the first aspect is the defining element for the technical elements, its validity has been determined by the results obtained.

PDFibAtl@s, the prototype system that encapsulates all the new proposed methods and algorithms presented in this thesis, represents the applicability of the study. It designed to be an aid, an alternative to the cognitive testing to reveal a more complex image of the PD, offering quantitative unbiased information from the medical image level. In this manner, by using the computerized analysis of the images, according to recent studies [Sonka 2009], the performance of the radiologist increases. We eliminate completely the observer from the image study, by modeling and including at the same time its experience. Therefore, we aim at being more accurate at the feature detection and quantification phase.

Analyzing the results obtained by each new method, we have to take into account the fact that the image quality together with patient variability influences the algorithms. The inter-patient variability solved at the pre-processing level by the geometrical parameters, together with the intra-patient variability solved by developing separate algorithms for each hemisphere of the brain are new elements introduced for facilitating the management of the image information. The pre-processing algorithms eliminate the noise and offer, together with a clean start for the processing level, valuable elements further used.

At the processing level, the DTI information analyzed is extracted by segmentation and tractography. The image information is fused to beneficiate of two specific features from the DTI protocol base: the FA and the EPI. The segmentation offers an error rate of 37-40%, which affects the tractography performance. When developing our new segmentation method, the upgrade on this method determined better results on the tractography as well, resulting on an increase with 19%. This aspect reveals the importance of the Putamen in the tractography as well as the robustness of the segmentation method with the direct implication at the feature extraction level. The importance of the segmentation is given also by the fact that unlike the manual segmentation, the automatic approach is much faster and is not influenced by the specialist skills and his capacity to distinguish between close levels of entropy on the image voxels. The computational speed is superior also on the tractography, due to the use of less memory as we are taking into account only the

fibers starting from the midbrain and we are validating only those reaching the Putamen volume. The performances of the tractography with a level of 78.5% accuracy provide a feature database that can be further used for the diagnosis and prognosis purpose. The metrics introduced for the fibers evaluation provide viable data for the prognosis functions so that a value of 45% accuracy can be obtained.

PDFibAtl@s is a new system, able to automatically detect the volumes of interest for PD diagnosis using the DTI images and a geometrical approach. The algorithms included in this platform are original and are based not only on the brain geometry, but also including medical knowledge by taking into account the position of different anatomical structures at the brain level, hence *the atlas dimension*. At the anatomical level, introducing parameters for fiber evaluation and eliminating the demographic factors represents another important contribution of this thesis. *The automatic dimension* of the prototype is achieved by these parameters used in the new algorithms that perform detection of the elements that until now were obtained by user interaction: detection of the slice of interest, detection of volumes of interest, automatic detection of the registration parameters. The registration itself represents a manner to fuse information from two different type of DTI. Concerning *the fusion* contribution of our work, it brings together the FA clarity at the Putamen level with the tensors matrix for the fiber tracking algorithms.

The technical element performing the transfer of information from the feature level to the clinical one is the method able to evaluate and predict PD. This method is contemplating the possibility to obtain numerical relevant measures on the early cases as well, not only on those starting from the second stage of the disease. The method includes evaluation and interpretation using as source the DTI image features and the medical knowledge. The output is placed on the H&Y scale for estimation and comparison with the cognitive test.

From the clinical standpoint, our study is offering a new method for the neurologists to detect and predict the PD. The disease evolution can be studied from the image level and for now it is a mean to verify/confirm the diagnosis determined by cognitive testing.

7.1 Scientific Contribution

The main scientific contribution is the proposition of a new PD biomarker represented by the DTI. The theoretical premises for this purpose have as source both the medical and the technical domains: the PD pathology and physiology reveal the elements that can be found in the image, the technical aspect studies the presence at the image informational level of these elements and the way to use them. The theoretical premises are studied and validated by the feasibility study, original trough the testing method that had to be sensitive only to PD and unbiased by other elements. This study offered the possibility for the technical aspect to be studied.

The scientific aspect refers to the originality and the impact of the method, as well as its necessity on the area where this method is employed. Both technical and medical areas have to gain from new methods in the medical image processing domain. Combining medical knowledge with new technical approaches, we are able to offer new information that can be exploited for a new overview on the PD. At this point, we are analyzing the originality of the methods, the challenges overcome and the difference with other methods.

Our scientific contribution starts at the **pre-processing level** where we develop methods to overcome the noise specific for head DTI images, with even higher interference in the low resolution images. According to our preliminary study, the skull influences the overall results at the anisotropy level. The method removing the skull performs the noise removal as well, so its utility is doubled.

For the *geometry based parameters*, used further at the volume segmentation level, additional study and more complex methods are developed. The automatization of the segmentation approach, as well as the registration is implemented by using these parameters. The fact that the parameters are independent on the patient demographics offers inter-patient independence and overcomes this barrier making possible the automation of the methods at the processing level. The inter-hemisphere axis used for the volume segmentation and for the registration method, is one of the elements used for overcoming the intra-patient variability. The same variability has to be overcome at the volume level prior to the segmentation.

The *slice detection* method procures the automatic placement for the volume segmentation algorithm and takes into account the volumetric and anatomical aspects of the brain. This method considers the position of the patient in the image - patients having smaller or bigger skulls or slices starting higher or lower on the patients skull (e.g. at the ear level or under the level of the nose). Using this algorithm, we overcome the differences between patients and we provide a robust placement for the volume segmentation.

In this manner, *the sex difference transposed as volume difference is overcome, together with the race difference resulting also in volume difference.* The fact that we take into account these variables from the demographic of the population constitutes a contribution by itself. This variability is transposed into parameters at the geometric level providing the elements an automatic approach on the segmentation and the registration methods.

The specificity of each patient is given also by the shape and the placement of the volumes of interest inside each image (e.g. some patients have one hemisphere more developed than the other and the anatomical regions are thus differently developed or placed higher on hemisphere than on the other). This *variability is surmounted by the methods that establish the starting points for the active volume detection.* We surmount the specificity problems by using for the seed placement the anatomical map of the brain and the relative placement of the volumes of interest inside the brain combined with the geometrical parameters. Depending on the volume of interest, the algorithm that detects the relative placement on the axial slice is different. The midbrain volume is placed on the inter-hemisphere axis and the Putamen is placed on the superior axial slices of the brain, next to the anatomical area named Globus Pallidus. This relative placement is based on the anatomy of the brain, like an atlas. The atlas mapping of the brain offers just the relative positioning; the actual positioning is given by the intensities of the pixels. **The segmentation process** is based on automatic detection of the region based on the voxel intensity. This approach determines the volume of interest independent on the size of the anatomical region and its angulations or its positioning inside the brain. Our method is automatic but also adaptive to each patient. The **volumes of interest are specific** for the disease - the substantia nigra and the Putamen - and the manner in which they are detected, by combining the image specific processing methods, together with the geometrical elements and by integrating the anatomy elements. The method is applicable to any patient as it does not take into account the provenance of the case, for shape variability, or the volume of the brain, changing according to the sex of the subject. For these reasons, the method is a complex one, integrating concepts from the medical knowledge for technical purpose.

For the **midbrain** area, we are using the clustered EPI image that is able to determine the midbrain, independent on the intra-patient variability.

At the **Putamen** level, the algorithms are different on the left and the right side of the brain, as we take into account the differences between the two hemispheres. Also, the shape is taken into account at different levels of the volume by applying the triangular or quadrilateral approach. This versatility makes the difference between our approach and the classical atlas based approach. On the manual segmentation directly on the FA image,

the anisotropy with the piercing fibers on the image determines "holes" on the volumes due to the difference between the voxels. Our approach using the clustered image with the geometrical segmentation does not have this problem and eventual fibers passing through the Putamen are validated, which is not the case for the eventual fibers passing through "holes" on the manual determined volume.

The registration method combines the manual method and the geometrical approach, but it is automatic, as it detects the geometrical elements at the pre-processing level. The robustness of the geometrical approach, combined with the fact that this method eliminates the inter-image variability as well, represents upgrades to the manual approach, which does not beneficiate of the accuracy and objectivity of an automatic approach. This method actually fuses the information extracted by segmentation form the FA image to the EPI volume.

The most important aspect of the originality of the approach is the combination between the automatic volume detection integrated on the global tractography. The metrics used for estimating the fibers are specific to this approach and are meant not only to evaluate the fibers, but also to overcome demographic variation.

The tractography methodology that uses the volumes of interest is faster than the original one by the fact that it uses only a small volume of the brain for the fiber growth: the midbrain, it researches 2-4 slices and validates only the fibers reaching the Putamen. The originality is sensed not only by the computational time, but also by the ability to automatically separate the fibers we need from all those residing on the midbrain. **Using the fibers** to evaluate the PD evolution is highly reliable. Our method adds the 3D aspect in the evaluation, by including the fibers.

From the **analysis and interpretation** perspective, using just the fuzzy rules from an ANFIS architecture for diagnosis proved to be a good approach, but this approach is limited by what the system knows, by what it has learned. This is the reason why a variation function on the features is more suitable for diagnosis and extrapolation. The contribution at this level is given by the function performance and its rate of transfer of knowledge from the feature level to the semantic level. The prognosis evaluation using the ANFIS architecture represents a first approach with the additional Lagrange polynomial functions. This approach defines not only the functions but also a hybrid adaptation using our new features for the IAPE and for PD- PD-APE methods. Our methods combine the knowledge form the fuzzy systems with the mathematical evaluation of the features from the neural networks offering exactitude.

The anatomy of the brain incorporates the medical knowledge to the approach, supports the technical elements and is able to link the processing algorithms by offering decisional rules for the detection steps of our system. *The PD pathology determines physiological changes that are exploited and taken into account with our approach from the image standpoint. In this manner we introduce pathophysiology on the diagnosis process and we estimate it using medical knowledge in order to transfer the information to the clinical level.*

7.2 Clinical Impact and Prognosis potential

Being able to confirm the cognitive test performed to place the patient on a severity scale is helpful for the medical doctor and offers the possibility to augment the degree of trust on the diagnosis. This reliability is achieved by the fact that our test is entirely based on the image.

Another important aspect is represented by the fact that the diagnosis is directly liked to the severity of the disease, as it can be detected and placed only after it passes the second

level on the H&Y scale. The technical measurable system presented in our approach offers the possibility to apply it on any patient at any level of severity of the disease.

The lightness of these algorithms is contained in the versatility, as these volume algorithms can be applied on other types of medical images. We can extend this approach to other similar diseases like Alzheimer by determining in the same manner the specific bundles of interest. We can envision an automatic intuitive atlas of the brain by using the detection of all the anatomical structures. The advantage in this case would be that mapping is not involved and therefore, the demographic aspect is not a problem anymore.

The diagnosis and the prognosis are highly dependable as the early diagnosis is unreachable without having the prognosis step defined. This step attained by evaluating the patients from our database and placing them on an evolutive function. Extending this function and extrapolating towards the low values of the scale we can reach the early stages of the disease severity. The features values for this PD severity provide the information necessary for placing new patients at this level and providing early diagnosis. In this manner we use the prognoses for establishing new diagnosis support. The medical doctors can study the detected early cases provided by the prognosis functions and define tests at the cognitive level as well.

With the first results from the feature extraction module, we are able to estimate the severity of the disease, using standard polynomial functions. Modifying these standard functions by adding medical knowledge as well as cases for the stages that were not present in our database will certainly improve this part of PDFibAtl@s.

7.3 Scientific Perspectives

The scientific contributions offer new perspectives and can be further improved as well. The thesis represents a study at the image level with new methods that provide measurable values of the PD severity. As these types of images have not been used as source for biomarkers, our approach not uses the information content as biomarker itself. The research opens new perspectives for biomarkers as a precedent for other methodologies and represents a comparison element for future approaches. As our biomarker is based on the image information and we are fusing it in our approach, new DTI images can provide additional complementary information and upgrade the marker.

From the technical perspective we propose a robust system - PDFibAtl@s - that encapsulates all the necessary image treatment starting from the scanned images to the motor fibers and their density. Automatic detection of the volumes of interest contours an atlas-based method entirely independent on the subject. Even if this approach is specific for the disease, the proposed detection methods can be used for other diseases, once the specific VOIs related to the disease have been identified (with the support of neuro-radiologists). For each stage of the system, there are interesting perspectives for our new algorithms.

The **pre-processing methods** used for eliminating the noise and the skull, independent on the shape of the head and its volume, can be applied on any type of head medical image. The fact that our approach provides good results on low-resolution images like EPIs, means that on high resolution images the result can be improved. The geometrical feature detection is a useful tool on any type of image, independent on the anatomical region. The inter-hemisphere axis detected has multiple applications as well, offering not just a limitation for the segmentation algorithm, but also directionality on the positioning of the patient in the image, useful in registration methods, warping or fusion. This particular element has its utility in other diagnosis methods that need a comparison between the two hemispheres (e.g. brain stroke or tumors).

At the **segmentation** level, our method can be applied for any anatomical volume of the brain, as long as its relative position inside the brain volume and its position at the axial level are known. The fact that the active tracking algorithms are either based uniquely on the voxel entropy, or on the geometrical limitations, provides a wide range of applicability. In case of an anatomical region well defined, the method developed for the midbrain segmentation can be useful, together with the algorithm for determination of the seeds (e.g. the caudate nucleus positioned on the inter-hemisphere axis and having well defined contour). The algorithm developed for the Putamen can be applied for structures that are not positioned on the hemispherical axis (e.g. the fornix formations).

For positioning the structures we can even envision an *automatic specific atlas* that combines our segmentation methods and uses geometrical adapting algorithms for the anatomical elements that provide this information, together with the malleability of the free-form intensity based algorithm developed for the midbrain area. In the case of such an atlas, the anatomical regions that do not consist of a specific form and/or clear limitation can be detected using the surrounding structures as limitations. This type of atlas differs from the classical one, by the fact that it uses only the relative positioning contained in a classical approach, but it is entirely molded on the specific structures of each patient. In this way, a much more correct evaluation of the structures can be achieved.

A follow-up study using our method of segmentation on the volume of specific anatomical regions of the brain can be used to determine the geriatric effects on a normal brain on the control cases, by comparison with those affected by the disease. Similarities among control patients at the volume level define a "normal" aging brain. Volumetric elements that are similar among PD cases but differ from the controls, represent specific metrics for the disease and its severity and can be used for a PD model definition.

The registration method, fully automatic, based on the geometric elements can be further developed for determining skewness elements. Starting from our method, other type of DTIs can be fused at the information level, even if they have different size and orientation. This purpose can be reached as we already have the volumetric elements and relative positioning of the patient in the image, therefore the ration between two different images as size and skewness should be straightforward. Not only fusion can be achieved in this manner, but also other similar processes like warping and alignment. The automatic method for determining the corresponding structures for the registration algorithm can be applied for other registration approaches that use parameters, as these elements are not affected by changes at the structural level of the brain (e.g. tumors and/or brain stroke). An iconic registration, using the geometrical parameters determined with our method and computing the affine elements as presented like we did could be upgraded and automatized as well.

Another very important aspect of our approach is **the tractography** algorithm based on the anatomical elements: the deterministic approach for the fibers - the WM importance and the way the motor tract is placed inside the human brain used for the global methodology. The method itself can be improved and the angulations limitation eliminated as only fibers having certain directionality will reach the second volume of interest. The information at the voxel level providing the directionality of the fibers can be further used to verify if the same fiber passes more than once trough the same slice, eliminating in this way a source of error. This approach is only feasible when having a limited amount of fibers, just like our case, otherwise the computational effort would be much too heavy on the memory capabilities.

Another application of this approach using a limited amount of fibers can be detected in annotating the fibers and by performing comparison between patients to measure the difference on the severity of the disease between the left and right side. Performing the same

study at different time lines on the same patient can provide information on the way that those fibers are affected, the most affected ones and/or the anisotropy levels that are critical for the most affected fibers.

The limits imposed for the fiber tracts are not only for achieving a certain sensitivity in choosing the bundle of interest, but also to validate the obtained bundle from the anatomical point of view. This validation based on the placement of the fibers in the volumes of interest is performed by the neurologist. The volumetric elements can determine other bundles of interest, depending on the volumes that these fibers pass trough.

Refining the fiber detection method and making it specific to the gray matter can augment the degree of trust for the diagnosis and add reliability to the system. It can also offer a higher correlation factor between the diagnosis success rate and the detected fibers. These fibers offer the possibility to study not just the effects of this particular disease, but also the dopamine flow changes and the degeneration of the fibers depending on the severity of the disease. Applying the global tractography approach on the same patient and providing a follow-up in time, the fibers value affected by the pathology define the disease progression. This progression is not linear and using this method we can determine its variation in time. Our metrics at the fiber level can be further used for this purpose, indicating the pathology level. These metrics would not be affected by an atrophy that is unavoidable in geriatrics.

The inter-hemisphere independence of the metrics can be used to determine the distinction at the 1.5 and 2.5 H&Y severity levels. This independence can be exploited by the fact that the disease affects more the left side, as well as the degree in which the left side is more affected than the right one. This information included in the diagnosis and prognosis method makes the difference between the old H&Y scale and the new one. In this case we can refine the results from the prognosis method and to update the diagnosis set of rules.

Using a newer tractography method can provide more accurate results and augment the prognosis rate. A probabilistic approach can be used as well because we need just a bundle of fibers and thus the computation time would not be too long, like in the Diffusion Tracking module from TrackVis, but in this case, the noise must be eliminated.

The diagnosis and prognosis are linked by the variation function of the fibers measures on the H&Y scale. This approach provides the system with a reliable and flexible way to include an evaluation based on medical knowledge, but also the possibility to change the set of rules by adding new ones that can provide a better clustering. A combination of expert systems and neural networks can provide also better finesse on the diagnosis step.

The prognosis provides values for new cases, even for the early cases of the disease. Our own method for prognosis based on Lagrange polynomial functions can be upgraded by using functions that have a higher sensitivity to the metrics that we are using. As the detection of the polynomial degree that better determines the severity of the disease has proved to be a good step on the right direction. Introducing the new cases correctly detected among the initial points can augment the rate of prognosis. A mathematical analysis of the variation function can provide a better evaluation at this point. Different metrics provided for the prognosis step can result in different values for this function, but our approach can be used even in these circumstances. Using the anisotropy level from the Substantia Nigra, or a combined value between this value and the fiber density, can be used with the same prognosis method. This prognosis method can be applied in other systems or for other diseases as well because it is entirely independent.

DTI image can be used as a biomarker in PD detection and prediction and we are offering an entirely automatic prototype that using these images provides a numerical value of the disease severity on any patient for the H&Y scale.

Appendices

Appendix A

User Guide for PDFibAtl@s

Contents

A.1 Introduction and applicability of PDFibAtl@s

Despite the advances in medical imaging and analysis for Parkinson's Disease diagnosis, the cognitive testing methods are the ones used, almost exclusively. Our prototype proposes an alternative method for these tests, using the same scale as the one used in cognitive ones. In cognitive testing the patient's estate is estimated based on the evaluation placed on dedicated scales like UPDRS (Unified Parkinson's Disease Rating Scale) and H&Y (Hoehn and Yahr) scale. On the same scale we illustrate the severity of the disease based exclusively on information from the Diffusion Tensor Imaging (DTI) images. The advantage of introducing these data resides not only on its nature, but also on providing a measurable value for the disease and the possibility to use it for prognosis.

In our approach we extract and fuse image information from different Diffusion Imaging types (DTI): Echo-Planar Imaging (EPI) and Fractional Anisotropy (FA). We are using a rather large database, having 143 subjects: 68 PD patients and 75 control cases in developing our prototype. *These subjects underwent DTI imaging: TR/TE 4300/90; 12 directions; 4 averages; 4/0 mm sections; 1.2 x 1.2 mm in-plane resolution.* The images are produced using the DICOM standard and our system used this format for handling the axial slices for pre-processing.

A.1.1 Image Processing Features

The processing is based on the fact that the dopamine, one of the main neurotransmitters, is lost when PD is installed, determining the trembling effect on the patients. Recent studies have shown that by the time the disease is detected, 89-90% of the dopamine is no longer produced. The quantity of this neurotransmitter affects the motor fibers and determines, among other symptoms, the specific tremor for the patients when its producing decreases. We extract the neuromotor fibers and use them to determine the patient's condition, evaluating it on the H&Y scale. For the processing stage, using the EPI and the FA image

stacks, we extract two volumes of interest: the midbrain containing the Substantia Nigra, the source of dopamine and the Putamen, brain anatomical region affected by the disease where the neuromotor fibers pass through. The extracted volume of the two anatomical structures can be studied as results after the image processing stage.

A.1.2 Analysis Features

For estimating the extracted neuromotor fibers we are using a global deterministic tractography. After the fiber tracking the extracted values on both sides of the brain are displayed for the user and estimated by using our metrics based on density and volumetric elements:

$$FD = \frac{F_{Nr}}{Vol_{Brain}} \tag{A.1}$$

$$FD_{rel} = \frac{F_{Nr}}{Vol_{VOI}} \tag{A.2}$$

where FD represents the fiber density measured using the obtained fiber number, F_{Nr}, and the brain volume; FD_{rel} Is the fiber density evaluated relative to one of the volumes of interest: the midbrain or the Putamen. As for the volumetric measurement, it is based on the fiber number F_{Nr} and the voxel measures (V_{height} , V_{width} and V_{depth}):

$$FV = F_{Nr} * V_{height} * V_{width} * V_{depty} \tag{A.3}$$

A.1.3 Diagnosis and prognosis evaluation

These measures are displayed and used on the diagnosis and prognosis module, providing the H&Y (Hoehn & Yahr scale) estimated value. This value represents the severity of the disease, making also the difference between the control and PD affected subjects. Providing a value of the PD severity (1-5), even for the mild cases (1 or 1.5 on H&Y scale), we are able to rendering a prognosis measure.

A.2 Using PDFibAtl@s

For using our prototype there are specific requirements regarding the capabilities of the machine where it is installed and the image protocol provided. Specific elements illustrating the parameters for the protocol are required as well.

A.2.1 Requirements

Computing requirements : There are several requirements to be fulfilled for the system so that our prototype can work properly. Also the format of the input information is important for an optimal set of results. The computer used for running the software should be capable to support 3D image reconstruction and high memory capabilities. *The prototype needs 4G of RAM and works well on 4.8GHz (Dual core 2.4 GHz).* We recommend using Windows XP/Vista/7 for running the software.

Files used The image files in DICOM format as acquired with the Siemens Avanto 1.5T are chosen as input for the system. Additionally the *dicomInfo* text file is set to extract the slice number and the imaging type for 3D rendering and further processing. It contains the following information from the DICOM header:
5 -the information for characteristics for the patient identification

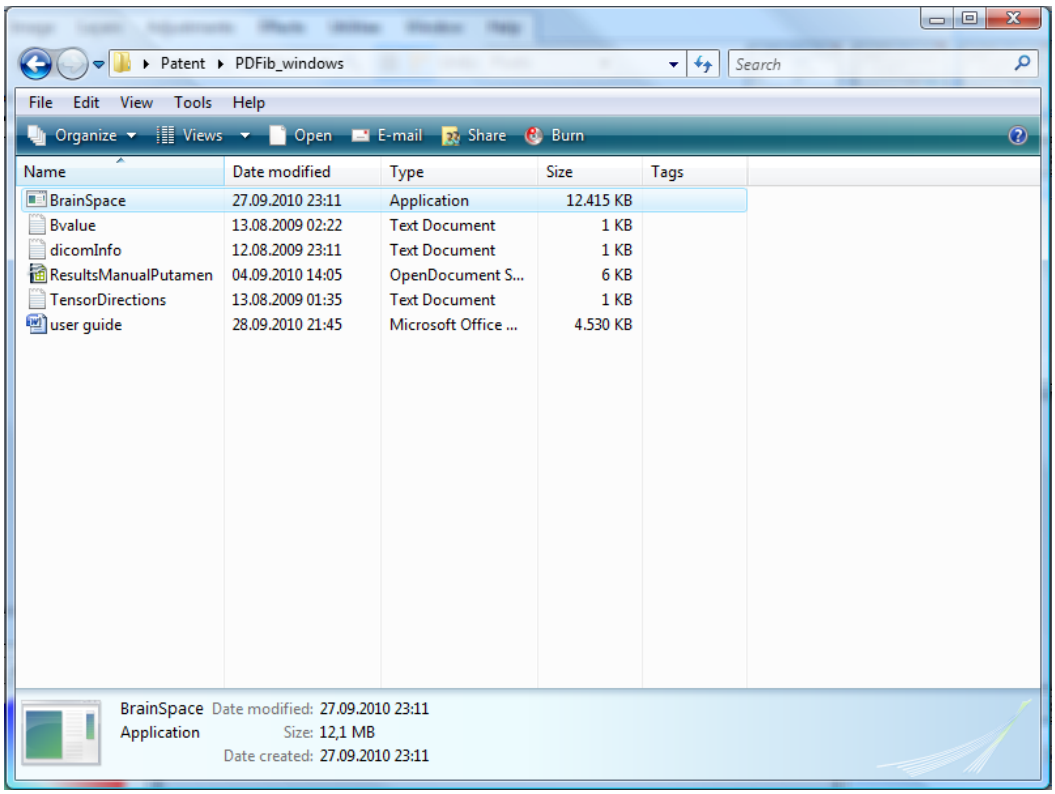

Figure A.1: Windows layout

0010,0020 -patient ID

0010,0040 -patient's sex

0010,1010 -patient's age

0018,0050 -slice thickness

0028,0030 -pixel spacing

7 - the information for image identification and 3D reconstruction

0008,103E -series description

0020,0013 -image number

0018,0050 -slice tickness

0028,0010 -rows

0028,0011 -columns

0028,0030 -pixel spacing

0010,0020 -patient id

1 - information for patient

0010,0020 -patient id

1 -information for EPI diffusion direction

0018,0024 -sequence name

BValue.txt - file containing the B value parameter used for the acquisition protocol, set in our case at 800. TensorDirections.txt file contains the diffusion directions - the number of directions (13 in our case) and each line represents a diffusion direction, starting with the B0, which is (0,0,0).

The *ResultsManualPutamen.csv* file represents the ideal set of values for the evaluation module, diagnosis and prognosis and remains unchanged. Changing this file will result in modifications for the prognosis functions and will affect the H&Y estimated value.

We provide all these files with the settings used for the parameters in our database.

A.2.2 Software Installation

For the developers we can provide the *.jar* file that can be integrated in any Java program and further used. For the uses we provide a basic package with the *.exe* file and the additional files used for our database. These files have to be changed, depending on the protocol for the image acquisition.

A.2.2.1 Main installation steps

- Downloading the application
- Extracting the archive
- Starting the application

Please make sure that the settings from *THE ENTIRE requested files* match with your image acquisition protocol. After downloading the application the files presented in figure A.1 represent the provided data. For running the application in Windows the user needs to run **"BrainSpace.exe"**. There might be a security warning like the one displayed by figure A.2 which depends on the Windows security settings. By choosing the *Run* button as presented in the image, the user is able to start our application.

A.2.2.2 Commands

For the user that provides the medical images (DTI) with the files containing the protocol (see figure A.3), **"BrainSpace.exe"** is sufficient. This application starts by requesting the location of the protocol files (fig. A.4), if they are different from ours, and the location of the DICOM patient files . Note that changes can be made directly into our text files for the protocol parameters.

For selecting the patient DICOM flies the used needs to indicate the location of the folder containing all the images with the **"Patient folder"** button from figure A.3. The used is requested to indicate the location of the folder as presented in figure A.5.

After choosing all the requested files, the systems starts processing like in figure A.6.

This processing stage is indicated by the main application window by displaying the message *"Processing"* and once a patient is identified and computation is started from that patient, its ID is displayed as well. The finalization for each patient is signalized by the system by writing *"done"* on the main application widow and the display of the **"Results"** window.

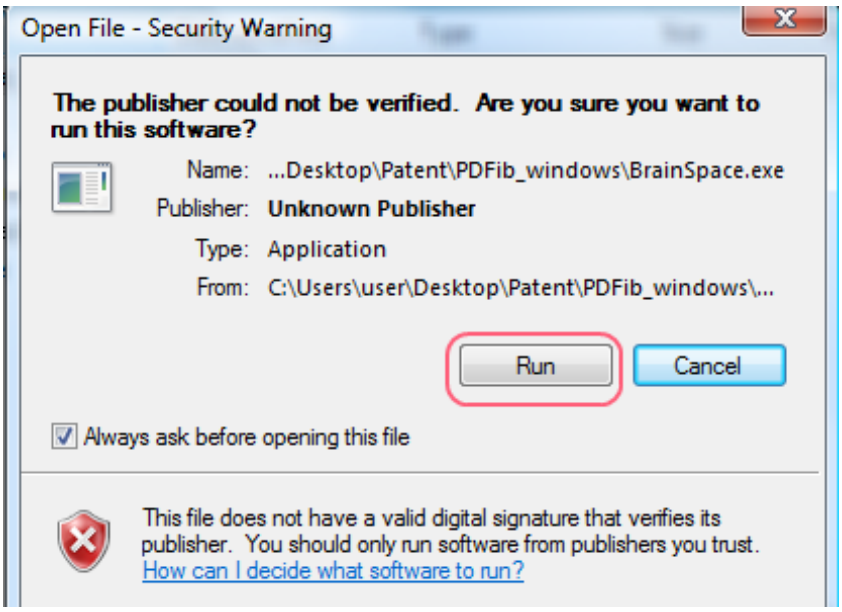

Figure A.2: Run the application

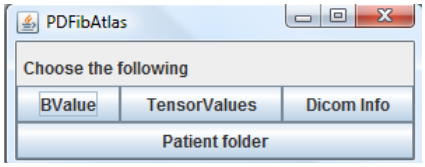

Figure A.3: Starting window for the application

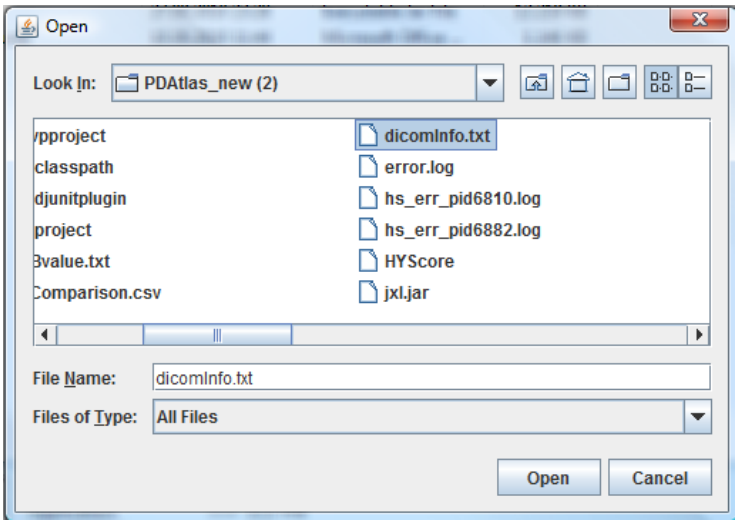

Figure A.4: Choosing the DICOM files

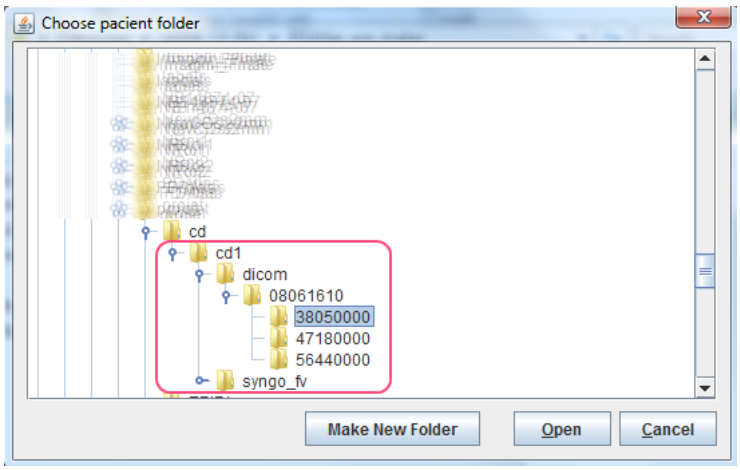

Figure A.5: Choosing the DICOM files

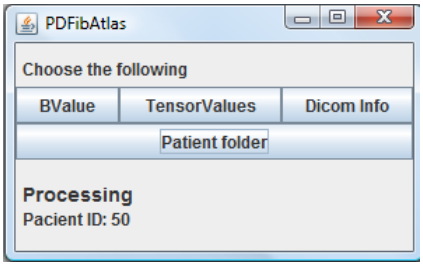

Figure A.6: Processing the patient

A.2.2.3 Results.Interpretation

The patient data is displayed first: Patient Id, age and sex for statistical analysis and further study purposes. The brain volume is computed in mm^3 and similarly the volume for the segmented midbrain and the Putamen in mm^3, but on each side of the brain to determine differences in the structures affected, for each hemisphere.

The number of fibers crossing the two regions at the same time is provided for each side as well and displayed in the window by the **"Fiber Number"**. Using the voxel size (equation A.3) we estimate the fiber volume as well in mm^3 and display it under **"Fiber Volume"**.

For the fiber density we provide the relative value to the midbrain volume computed using our equations in A.2 displayed by the **"Fiber density"** line for each hemisphere.

After the computation is finished, the results window displayed (see fig. A.7) and all the values for the fibers, together with patient identification and the estimated H&Y value are provided. Once these files provided, the 3D rendering is performed and the user has the possibility to observe the motor tract by selecting the **"Show 3D"** button.

The user has the possibility to display a graphical function that illustrates the placement of the patient on the "ideal" data set. This data set is the one containing the Putamen manually segmented. This graphics is provided for two distinctive methods: IAPE (Independent Adaptive Polynomial Evaluation) and PD-APE (Parkinson's disease - Adaptive Polynomial Evaluation). Accessing the corresponding buttons from the results window displays the graphics (e.g. figure A.8).

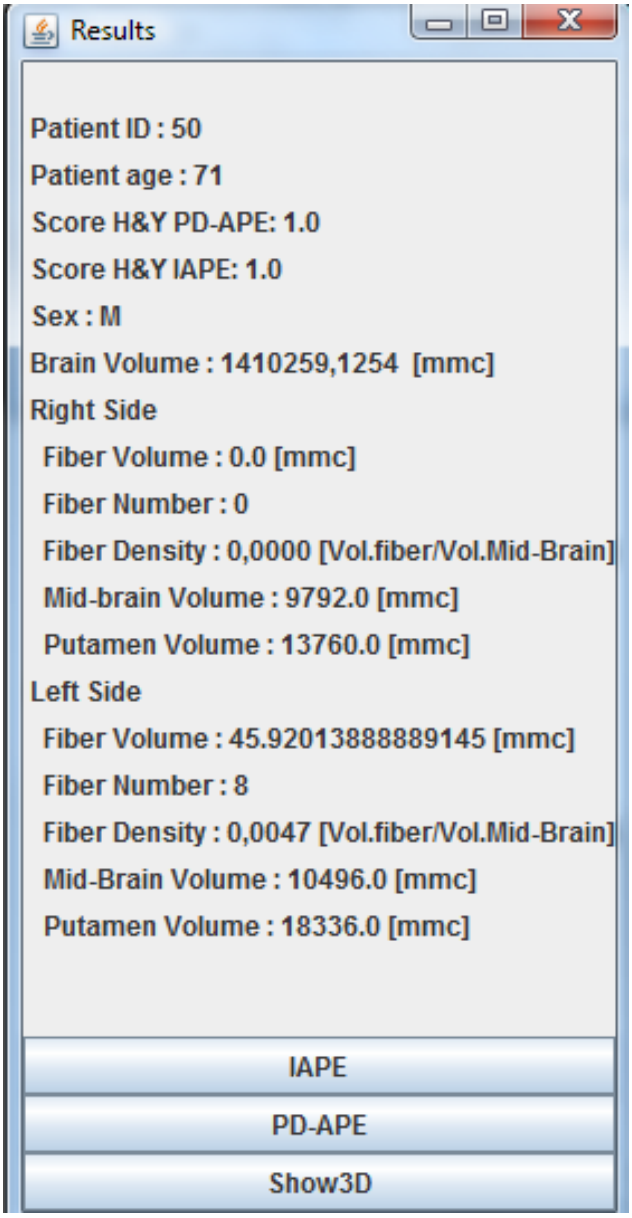

Figure A.7: Results for patient 50

A.2.3 Single patient processing vs. multiple subjects processing

The software is able to process one or more patients, depending on the images from the source folder. If there is only one patient in the indicated folder, the system stops after processing this patient, otherwise it starts automatically processing the next patent (see figure A.9). For processing a set of patients automatically, all the images must be placed in the same folder. For processing the patients one by one, they have to be separately stored in folders.

When all the patients from the folder have been processed, the system displays the message **"Finished"** and its execution is terminated (see figure A.10), but it still provides

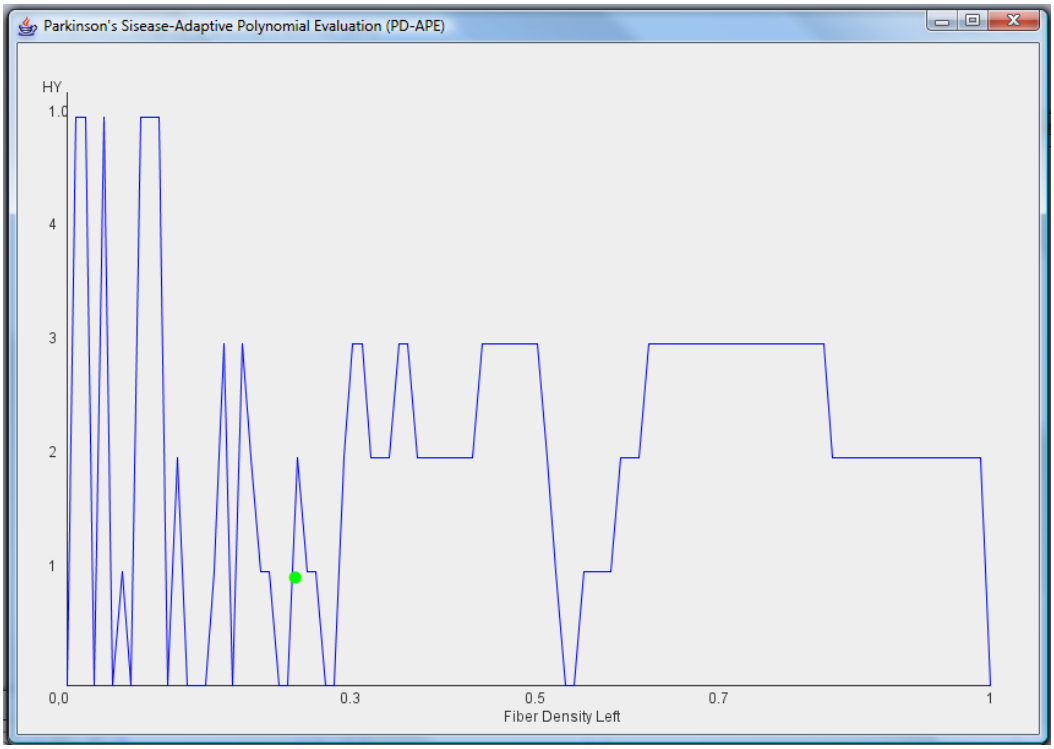

Figure A.8: PD-APE for patient 50

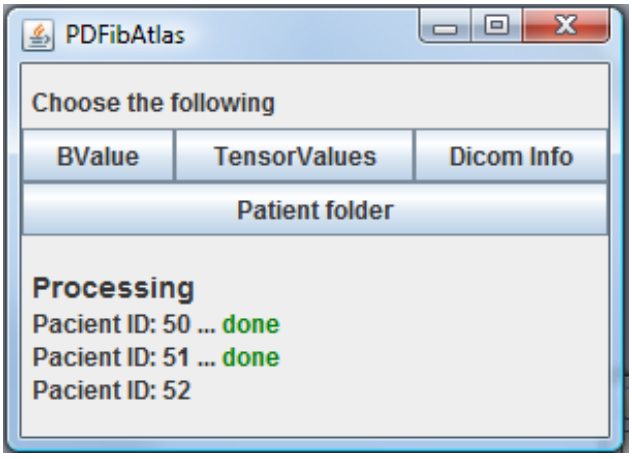

Figure A.9: Processing Multiple patients

the results and graphics, until the user chooses to close the specific windows or the main application window.

The value for the H&Y is presented using two methods: IAPE and PD-APE as they provide different accuracy. The PD-APE provides 95% accuracy but only on patients, whereas IAPE provides for all the cases 74% accuracy.

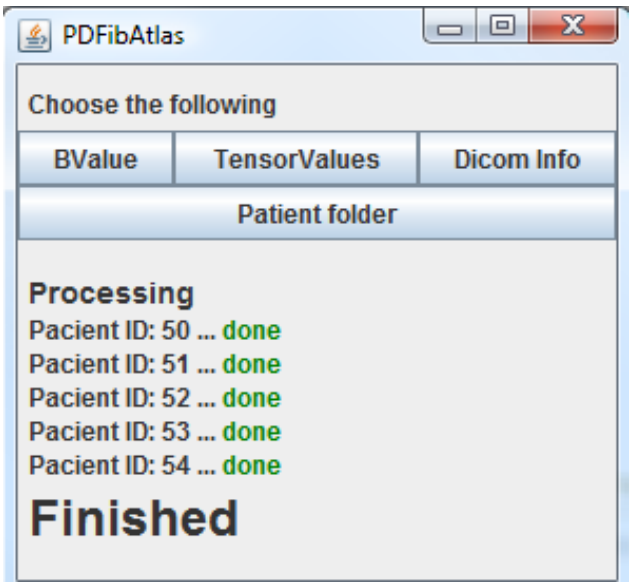

Figure A.10: Finishing all the patients from the folder

A.3 Errors and contact

The system has an error log (**"error.txt"**) where all the malfunctions detected by the system are registered.

For malfunctions and further questions please contact us:

IPAL (UMI 2955)
1 Fusionopolis Way
#21-01 Connexis (South Tower)
Singapore 138632
DID: (65) 6408 2542
Tel: (65) 6408 2000
Fax: (65) 6776 1378

Email: *Daniel Racoceanu: daniel.racoceanu@ens2m.fr*
Roxana Teodorescu: ro.teodorescu@gmail.com

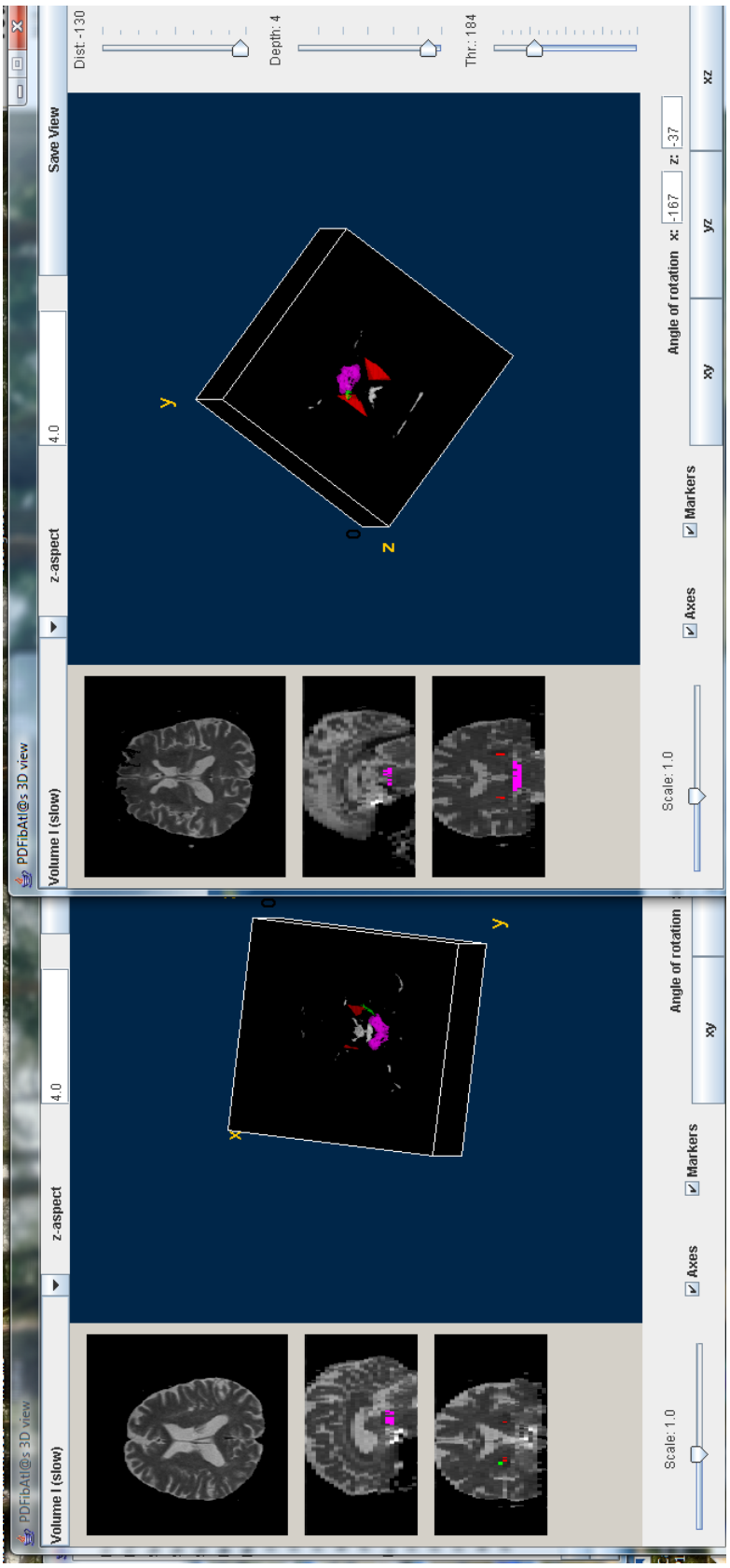

Figure A.11: Simultaneously display of two patients

Appendix B

Dissemination

B.1 Journals

Teodorescu, R.; Racoceanu, D.; Leow, W.-K. & Cretu, V. *Prospective study for semantic Inter-Media Fusion in Content-Based Medical Image Retrieval* Medical Imaging Technology, 2008, 26, 48-58

Anda Sabau, **Roxana Oana Teodorescu** and Vadimir Ioan Cretu. *A New Cerebral Anatomical-Based Automated Active Segmentation Method* - to appear, Scientific Bulletin of the Politehnica University of Timisoara, Transactions on Automatic Control and Computer Science,IEEE Catalog Number: CFP10575-CDR, ISBN 978-4244-7431-8, 2010.

B.2 Book Chapters

Roxana Oana Teodorescu, Vladimir Ioan Cretu and Daniel Racoceanu *Medical Image Processing and Analysis for Parkinson's Disease Diagnosis and Prognosis*, book title "Biomedical Engineering, Trends in Electronics, Communications and Software", Ed. Anthony N. Laskovski, http://www.intechopen.com/articles/show/title/parkinson-s-disease-diagnosis-and-\prognosis-using-diffusion-tensor-medical-imaging-features-fusion, ISBN 978-953-307-475-7, published by INTECH, 2011

Lacoste, C.; Chevallet, J.-P.; Lim, J.-H.; Hoang, D. L. T.; Wei, X.; Racoceanu, D.; **Teodorescu, R.** & Vuillenemot, N. *Inter-media concept-based medical image indexing and retrieval with umls at IPAL* Lecture Notes in Computer Science, Evaluation of Multilingual and Multi-modal Information Retrieval, 2007, 4730, 694-701.

Racoceanu, D.; Lacoste, C.; **Teodorescu, R.** & Vuillemenot, *N. A semantic fusion approach between medical images and reports using umls Lecture Notes in Computer Science*, (Eds.): Asian Information Retrieval Symposium, 2006, 4182, 460-475.

B.3 Conferences & Workshops

Anda Sabau, **Roxana Oana Teodorescu** and Vadimir Ioan Cretu. *Automatic Putamen Detection on DTI Images. Application to Parkinson's Disease.* ICCC-CONTI, vol. 1, pages 1-6, may 2010.

Teodorescu, R.; Racoceanu, D.; Smit, N.; Cretu, V. I.; Tan, E. K. & Chan, L.-L. *Parkinson's disease prediction using diffusion based atlas - poster session* SPIE - Computer

Aided Diagnosis [7624-78] PS2, 13-18 Febr., San Diego CA, USA 2010.

Teodorescu, R.; Racoceanu, D.; Chan, L.; Lovblad, K. & Muller, H. *Parkinson's disease detection using 3D Brain MRI FA map histograms correlated with tract directions - oral presentation Neuroradiology (Brain: Movement and Degenerative Disorders SSC13 - 09)* RSNA,95th Radiological Society of North America Scientific Conference and Annual Meeting, November 29 to 4 December, McCormick Place, Chicago IL, USA, 2009.

Teodorescu, R. O. & Racoceanu, D. *Prognosis of Parkinson's Disease - poster session*, A*STAR Scientific Conference, 28-29 Oct., Biopolis, Singapore 2009.

Teodorescu, R. O.; Racoceanu, D. & Chan, L.-L. *H&Y compliant for PD detection using EPI and FA analysis - poster session*, NIH Workshop Inter-Institute Workshop on Optical Diagnostic and Biophotonic Methods from Bench to Bedside, 1-2 Oct, Washington DC, USA 2009.

Teodorescu, R.; Cernazanu-Glavan, C.; Cretu, V. & Racoceanu, D. *The use of the medical ontology for a semnatic-based fusion system in Biomedical Informatics - Application to Alzheimer disease* ICCP Proceedings, 2008, 1, 265-268.

Teodorescu, R.; Cretu, V. & Racoceanu, D. *The use of medical ontology in a semantic-based fusion system* CONTI, 2008, 1, 48-52.

R. Teodorescu and D. Racoceanu. Semantic Inter-Media Fusion Design for a Content-Based Medical Image Retrieval System. Japanese Society of Medical Imaging Technology - JAMIT-ONCO-MEDIA workshop, vol. Tsukuba, Japan, pages 43-47, 21 - 22 july 2007.

B.4 Technical reports

Roxana Teodorescu. *H&Y Compilant for PD Diagnosis and Prognosis using EPI and FA images.* Phd report no. 2, Politehnica University of Timisoara, February 2010.

Roxana Oana Teodorescu. *Feature extraction and Ontology use for Brain medical images - PhD Report No 1.* Rapport technique 1, UPT and UFC, January 2009.

B.5 Research stages

February-April 2009 Research stage in Singapore at IPAL(Image & Pervasive Access Lab)- the Singaporean-French Image & Pervasive Access Lab under the supervision of Prof. Daniel RACOCEANU

April -October 2009 Research stage in Singapore at Image & Pervasive Access Lab under the supervision of Prof. Daniel RACOCEANU from French National Research Center.

18-20 February 2009 Participation at the French-Singaporean symposium at NUS and IPAL Singapore.

July -October 2008 - Image Processing Stage in Geneva at Université de Geneve with the MedGIFT laboratory - Collaborator Dr. Henning Müller

March-June 2007 - ONCO-MEDIA project at IPAL (Image Perception Acess and Language) Laboratory, joint research laboratory in Singapore - CNRS (French National Research Center), A* Singapore - Institute for Infocomm Research, NUS (National University of Singapore) and UJF (Joseph Fourrier University) France - Supervisor Dr. Daniel RACOCEANU(UFC), collaborator Dr. Wee Kheng LEOW (NUS)

March - September 2006 - IPAL (Image Perception Acess and Language) Laboratory, joint research laboratory in Singapore - CNRS (French National Research Center), A* Singapore - Institute for Infocomm Research, NUS (National University of Singapore) and UJF (Joseph Fourrier University) France - 21 Heng Mui Keng Terrace, Singapore - Supervisor Dr. Daniel RACOCEANU

B.6 Scholarship

June 2007-December 2009 Young Doctors Scholarship TD (Tineri Doctoranzi) 46/2008 from the Romanian Research and Learning Ministry.

Appendix C

DICOM Header Example file

This Appendix contains an example of several tags used in our system from the DICOM header files. These files are more complex and contain more tags, but we extract just the ones presented here.

Title: 21599424
Width: 201.25 mm (448)
Height: 230.00 mm (512)
Resolution: 2.226 pixels per mm
ID: -2
Coordinate origin: 0,0
Bits per pixel: 16 (unsigned)
Display range: 0 - 754
No Threshold

code	Information
0002,0003	Media Storage SOP Inst UID: 1.3.12.2.1107.5.99.2.2716.30000008042402440731200014325
0008,1030	Study Description: headŜGH Brain
0008,103E	Series Description: t2_tse_DTI_overlay_highRes
...	...
0010,0010	Patient's Name: 001
0010,0020	Patient ID: 001
0010,0030	Patient's Birth Date: 19411122
0010,0040	Patient's Sex: M
0010,1010	Patient's Age: 064Y
...	...
0018,0023	MR Acquisition Type: 2D
0018,0024	Sequence Name: *tse2d1_13
0018,0025	Angio Flag: N
0018,0050	Slice Thickness: 4
0018,0080	Repetition Time: 5700
0018,0081	Echo Time: 89
0018,0083	Number of Averages: 3
0018,0084	Imaging Frequency: 63.673778
0018,0085	Imaged Nucleus: 1H
0018,0086	Echo Numbers(s): 0
0018,0087	Magnetic Field Strength: 1.4939999580383
0018,0088	Spacing Between Slices: 4
...	...
0020,0013	Image Number: 10
0020,0032	Image Position (Patient): -121.20970194079 -122.75359890362 -9.4565671015186
0020,0037	Image Orientation (Patient): 0.99817062741895 -0.0175064983057 0.05786986327205 0.02265170415277 0.99573051228909 -0.0894854580112

Table C.1: Example of DICOM header tags

Appendix D

Hoehn & Yahr classification

Stage	Symptoms
HY-I	1. Signs and symptoms on one side only
	2. Symptoms mild
	3. Symptoms inconvenient but not disabling
	4. Usually presents with tremor of one limb
	5. Friends have noticed changes in posture, locomotion and facial expression
HY-II	1. Symptoms are bilateral
	2. Minimal disability
	3. Posture and gait affected
HY-III	1. Significant slowing of body movements
	2. Early impairment of equilibrium on walking or standing
	3. Generalized dysfunction that is moderately severe
HY-IV	1. Severe symptoms
	2. Can still walk to a limited extent
	3. Rigidity and bradykinesia
	4. No longer able to live alone
	5. Tremor may be less than earlier stages
HY-V	1. Cachectic stage
	2. Invalidism complete
	3. Cannot stand or walk
	4. Requires constant nursing care

Table D.1: Hoehn and Yahr Staging of Parkinson's Disease [Goetz 2004]

Bibliography

[1752 2008] NEMA Suite 1752. *DICOM Standard.* electronic, Medical Imaging and Technology Alliance, december 2008. 12, 13

[Ashburner 2000] John Ashburner and Karl J. Friston. *Voxel-Based Morphometry - The methods.* Neuroimage, vol. 11, pages 805–821, 2000. The Wellcome Department of Cognitive Neurology, Institute of Neurology. 26, 58

[Awate 2008] Suyash P. Awate, Hui Zhang, Tony J. Simon and James C. Gee. *Multivariate Segmentation of Brain Tissues by Fusion of MRI and DTI data.* IEEE Xplore, vol. 8, pages 213–216, 2008. 60

[Bagci 2007] Ulas Bagci and Li Bai. *Multiresolution Elastic Medical Image Registration in Standard Intensity Scale.* XX Brasilian Symposium on Computer Graphics Image Processing - IEEE Computer Society, vol. 24, pages 1–8, 2007. 57

[Bankman 2009] Isaac Bankman, editeur. Handbook of medical image processing and analysis. Academic Press Series in Biomedical Engineering. Academic Press in an imprint of Elsevier, 2 édition, 2009. 48, 73

[Basser 2000] Peter J. Basser, Sinisa Pajevic, Carlo Pierpaoli, Jeffrey Duda and Akram Aldroubi. *In vivo fiber Tractography using DT-MRI data.* Magnetic Resonance in Medicine, vol. 44, pages 625–632, 2000. 63, 64

[Berg 2008] Daniel Berg. *Biomarkers for the Early Detection of Parkinson's and Alzheimer's Disease.* Neurodegenerative Diseases, vol. 5, pages 133–136, 2008. 5, 12

[Beyer 2007] Mona K. Beyer, Carmen C. Janvin and Jan P. Larsen. *A magnetic resonance imaging study of patients with Parkinson's disease with mild cognitive impairement and dementia using voxel-based morphometry.* J. Neurol. Nuerosurg. Psychiatry, vol. 78, pages 254–259, 2007. 58

[Bonissone 1997] Piero P. Bonissone. *Adaptive Neural Fuzzy Inference Systems (ANFIS): Analysis and Applications.* GE CRD Schenectady, NY USA, 1 1997. 74

[Burger 2008] Wilhem Burger and Mark J. Burge. Digital image processing - an algorithmic introduction using java, volume 1 of *1.* Springer, first édition, July 2008. 44

[Cachier 2003a] P. Cachier and et al. *Iconic feature based nonrigid registration : the PASHA algorithm.* Computer Vision and Image understanding, vol. 89, pages 272–298, 2003. 56

[Cachier 2003b] Pascal Cachier and et al. *Iconic feature based non-rigid registration: the PASHA algorithm.* Computer Vision and Image understanding, vol. 89, pages 272–298, 2003. 56, 59

[Center For Biomarkers in Imaging 2007] (CBI) Center For Biomarkers in Imaging. *Catalog of Biomarkers by disease.* Rapport technique, Massachusetts General Hospital, 2007. 7

[Ceritoglu 2009] Can Ceritoglu, Kenichi Oishi, Xin Li and et al. *Multi-contrast large deformation diffeomorphic metric mapping for diffusion tensor imaging.* NeuroImage, vol. 47, pages 618–627, 2009. 58, 59

[Chan 2007] L-L Chan, H. Rumperl and K. Yap. *Case Control study of Diffusion tensor imaging in Parkinson's disease.* J. Neurol. Neurosurg. Psychiatry, vol. 78, pages 1383–1386, 2007. 31

[Chetelat 2005] G. Chetelat, B. Landeau, F. Eustache and et al. *Using voxel-based morphometry to map the structural changes with rapid conversion in MCI: A logitudinal MRI study.* NeuroImage, vol. 27, pages 934–946, 2005. 58

[Clatz 2009] Oliver Clatz. *Fundamentals of Medical Image Registration.* ppt, june 2009. 56, 57, 59

[Curran 2005] K.M. Curran and D.M. Alexander. *Comparison of Similarity Measures for Driving Diffusion Tensor Registration.* Proc. Intl. Soc. Mag. Reson. Med., vol. 13, page 226, 2005. 15, 58

[Descoteaux 2007] Maxime Descoteaux, Rachid Deriche and Alfred Anwander. *Deterministic and Probabilistic Q-Ball Tractography: from Diffusion to Sharp Fiber Distorsions.* Rapport de recherche 6273, INRIA Sophia Antipolis, August 2007. Projet Odyssee. 62

[Dictionary 2010] Medical Dictionary. *The Free Dictionary By Farlex.* On-line, april 2010. http://encyclopedia.thefreedictionary.com/. 22

[Dinov 2002] Ivo D. Dinov, Michael S. Mega and Paul M. Thompson. *Quantitative Comparison and Analysis of Brain Image Registration Using Frequency- Adaptive Wavelet Shrinkage.* IEEE Transactions on Information Technology in Biomedicine, vol. 6, pages 73–85, 2002. 57

[Disease 2009] Parkinson's Disease. *Parkinson's disease statistics.* Rapport technique, eMed TV, July 2009. http://parkinsons-disease.emedtv.com/parkinson2

[Dorsey 2006] ER Dorsey, RG Hollway and BM Ravina. *Biomarker's in Parkinson's Disease.* Expert Rev. Neuroteh., vol. 6, pages 823–31, 2006. 2

[Duzel 2009] Emrah Duzel, Nico Bunzeck, Marc Guitart-Masip and Bianca Wittmann. *Functional imaging of the human dopaminergic midbrain.* Trends in Neuroscience, vol. 32, pages 321–328, 2009. 13

[Facon 2005] David Facon, Augustin Ozanne and Pierre Fillard. *MR Diffusion Tensor Imaging and Fiber Tracking in Spinal Cord Compression.* ANJR, vol. 26, pages 1587–1594, 2005. 17

[Feldmann 2008] Adam Feldmann, Zsolt Illes and et al. *Morphometric Changes of Gray Matter in Parkinsons Disease with Depression: A Voxel-Based Morphometry Study.* Movement Disorders, vol. 23, pages 42–46, 2008. 58

[Fillard 2002] Pierre Fillard and Guido Gerig. *Analysis Tool for Diffusion Tensor MRI.* MICCAI, vol. 1, no. 1, pages 1–3, sept. 2002. 29

[Fillard 2007] Pierre Fillard, Jean-Christophe Souplet and Nicolas Toussaint. *Meidcal Image Navigation and Research tool by INRIA (MedINIRA).* Rapport technique, INRIA Sophia Antipolis, 2007. 37

[Fillard 2009] Pierre Fillard, Cyril Poupon and Jean-Francois Mangin. *A novel global tractography algorithm based on an adaptive spin glass model.* MICCAI, vol. 1, pages 1–8, 2009. 62

[Friston 2000] Karl J. Friston. *Experimental Design and Statistical Parameter mapping.* Dept. of Cognitive Neurology, vol. 1, no. 1, page 25, September 2000. SPM Presentation. 28, 29, 30

[Gabrys 2005] Bogdan Gabrys, Kauko Leiviska and Jens Strackeljan. Do smart adaptive system exist?, volume 173 of *Studies in fuzziness and soft computing.* Springer, 2005. ISBN: 978-3-540-24077-8. 75

[Gaser 2008] Christian Gaser. *VBM5 (for SPM5).* Rapport technique, Structural Brain Mapping Group, december 2008. Software presentation and download site. 28

[Gholinpour 2007] Ali Gholinpour, Nasser Khetanarvaz and et al. *Brain Functional Localization: a Survey of Image Registration Techniques.* IEEE Transactions on Medical Imaging, vol. 26, page 20, 2007. 56, 59, 61

[Gilles 2008] Benjamin Gilles and Dinesh K. Pai. *Fast Mukuloskeletal Rgistration Based on Shape Matching.* LNCS- Medical Image and Computer-Assisted Intervention MICCAI, vol. 5242/2008, pages 822–829, 2008. 57

[Goetz 2004] Christopher G. Goetz, Werner Poewe, Olivier Rascol, Cristina Sampaio and Glen T. Stebbins. *Movement disorder society task force report on the Hoehn and Yahr staging scale: Status and Recommendations.* Movement Disorders, vol. 19, no. 9, pages 1020–1028, June 2004. 130

[Graeber 2009] Manuel B. Graeber. *Biomarkers for Parkinson's Disease.* Experimental Neurology, vol. 216, pages 249–253, 2009. 6, 11

[Guillaume 2008] Guillaume. *SPM Documentation.* pdf technical report, October 2008. Trust Center for Neuroimaging. http://www.fil.ion.ucl.ac.uk/spm/doc/ - last accessed on May 2010. 28, 58

[Jain 1988] Anil K. Jain and Richard C. Dubles. Algorithms for clustering data. Prentice Hall Advanced Reference Series. Prentice Hall, 1988. 52

[Jain 1997] A. Jain and D. Zongker. *Feature selection: Evaluation, application and small sample performance.* IEEE Transactions on Pattern Analysis and Machine Intelligence, vol. 19, no. 2, pages 153–158, 1997. 73

[Jensen 2010] Walter Jensen. *About Biomarker Commons.* Biomarker Commons Newsbot, vol. 1, page 1, June 2010. 7

[Jones 2008] Craig Jones. *Matlab Scripts.* web presentation, University of Western Ontario, July 2008. http://www.imaging.robarts.ca/ cjones/software/ - last accessed on May 2010. 27

[Jyh-Shing Roger 1995] Jang Jyh-Shing Roger and Sun Chuen-Tsai. *Nuero-Fuzzy Modeling and Control.* The Proceesings of IEEE, vol. 83, pages 387–406, 1995. 74

[Karagulle Kenedi 2007] AT Karagulle Kenedi, S. Lehericy and M. Luciana. *Altered Diffusion in the Frontal Lobe in Parkinson's Disease.* AJNR Am J Neuradiol Brain - Original Research, vol. 29, pages 501–05, 2007. 64

[Kiebel 1999] S.J. Kiebel, J.B. Poline, K.J. Friston, A.P. Holmes and K.J. Worksley. *Robust Smoothness Estimation in Statistical Parametric Maps Using Standardized Residuals from the General Linear Model.* NeuroImage, vol. 10, pages 756–766, 1999. 26

[Klein 2007] Stefan Klein, Marius Staring and Joselin P.W. Pluim. *Evaluation of optimization methods for non-Rigid medical image registration using mutual information and B-Splines.* IEEE Transactions on Image Processing, vol. 16, pages 34–40, 2007. 57

[Klein 2009] A. Klein, J. Andersson, B.A. Ardekani, J. Ashburner, B. Avants, M.-C. Chiang, G.E. Christensen, D.L. Collins, J. Gee, P. Hellier, J.H. Song, M. Jenkinson, C. Lepage, D. Rueckert, P. Thomson, T. Vercauteren, R.P. Woods, J.J. Mann and R. Parsey. *Evaluation of 14 nonlinear deformation algorithms applied to human brain MRI registration.* NeuroImage, vol. 46, no. 3, pages 786–802, 2009. 58

[Kor 2004] Sudipta Kor and Umashanker Tiwary. *Feature Level Fusion of Multimodal Medical Images in Lifting Wavelet Transform Domain.* Proceedings of the 26th Annual International Congerence of the IEEE EMBS, vol. 26, pages 1479–1482, 2004. 60

[Le Bihan 2001] Denis Le Bihan, Jean-Francois Mangin, Cyril Pupon and Chris A. Clark. *Diffusion Tensor Imaging : concepts and application.* Journal of Magnetic Resonance Imaging, vol. 13, pages 534–546, 2001. 63, 64

[Lehericyr 2004] S. Lehericyr, M. Ducros, P.F. Van de Moorele and et al. *Diffusion tensor fiber tracking shows distinct corticostriatal circuis in humans.* ANN Neurol, vol. 55, pages 522–529, 2004. 14

[Maintz 2000] Antoine J.B. Maintz and Max A. Viergever. *A survey of medical image registration.* Medical Image Analysis, vol. 1 and 2, pages 1–32, 2000. 56, 59, 61

[Marck 2008] Keneth Marck, Danna Jennings, Gilles Tamagnan and John Scibyl. *Biomarkers for Parkinson's Disease: Tools to Assess PArkinson's Disease Onset and Progression.* American Neurological Association, vol. 2, pages 111–121, 2008. 1, 5, 6, 10, 11, 104

[Marek 2009] K. Marek, D. Jennings, G. Tamagnan and J. Seibyl. *Biomarkers for Parkinson's disease: tools to assess Parkinson's disease onset and progression.* Ann Neurol., vol. 65, pages 232–21, 2009. 13

[Mitchell 2004] A.W Mitchell, S.J.G. Lewis, T. Foltynie and R.A. Barker. *Biomarkers and Parkinson's Disease.* Brain, vol. 127, no. 8, pages 1693–1705, 2004. Downloaed from brain.oxfordjournals.org. 3, 5, 7, 8, 9

[Mizuno 2010] Y. Mizuno. *Neuroimaging, Parkinson's Disease.* Experimental Neurology, vol. 216, pages 249–253, 2010. 13

[Modersitzki 2004] Jan Modersitzki. Numerical methods for image registration, volume Oxford Science Publications of *Numerical Mathematics and Scientific Computation.* Oxford University Press, hardcover édition, 2004. 57, 58

[Nandhagopal 2007] R. Nandhagopal, Martin J. McKeown and A. John Stoessl. *Invited Article: Functional imaging in Parkinson disease.* Neurology, vol. 70, pages 1478–1488, 2007. 14

[O'Donnell 2009] Lauren J. O'Donnell, Carl-Frederik Westin and Alexandra J. Golby. *Tract-based morphometry for white matter group analysis.* NeuroImage, vol. 45, pages 832–844, 2009. 58

[Park 2004] Sang-Hyun Park and Hyung Jin Sung. *Assessment of Image Registration Interpolation methods for Pressure- Sensitive Paint Measurements.* 11th International Symposium on Flow Visualization, vol. 1, pages 1–7, 2004. 57

[Parkinson's Disease 2010] online research Parkinson's Disease. *PD Guide - Imaging.* Rapport technique, powered by Michael J. Fox foundation, Feb 2010. http://www.pdonlineresearch.org/pdguide/imaging. 14

[Pataca 2010] Cristina Izabela Pataca. Detection and prognosis of parkinson's disease. Master's thesis, "Politehnica" University of Timisoara, Romania, June 2010. 78, 80, 95, 96, 100

[Pew-Thian 2009] Yap Pew-Thian, Wu Guorong, Zhu Hongtu and et al. *TIMER: Tensor Image Morphing for Elastic Registration.* NeuroImage, vol. 27, pages 549–563, 2009. 57

[Piccini 2004] Paola Piccini and Ann Cheesman. *Functional Imaging of movment disorders.* ACNR, vol. 4, pages 10–13, 2004. 13

[Pluim 2000] Josein P.W. Pluim, Antoine J.B. Maintz and Max A. Viergever. *Interpolation Arefacts in Mutual Information - Based Image Registration.* Computer Vision and Image understanding, vol. 77, pages 211–232, 2000. 57

[Radiological Society of Norh America 2009] (RSNA) Radiological Society of Norh America. *Experts See Integration of Imaging Biomarkers by 2025.* on-line, May 2009. 17

[Rorden 2008] Rorden. *DTI analysis.* Rapport technique, Georgia Institute of Technology, Neuropsychology Lab, Atlanta, October 2008. last accessed on May 2010. 15, 16

[Roussinov 2001] Dimitri G. Roussinov and Hsinchun Chen. *Information navigation on the web by clustering and summarizing query resuls.* Information Processing & Management, vol. 37, no. 6, pages 789–816, November 2001. 75

[Sabau 2010] A. Sabau, R.O. Teodorescu and V.I. Cretu. *Automatic putamen Detection on DTI Images. Application to Prakinson's Disease.* Proceedings of the IEEE International Joint Conference on Computational Cybernetics and Technical Informatics, ICCC-CONTI, vol. 1, pages 95–100, May (27-29) 2010. IEEE Catalog Number: CFP10575-CDR, ISBN: 978-4244-7431-8. 54, 66, 100

[Scherfler 2006] Cristoph Scherfler, Michael F. Schocke, Klaus Seppi, Regina Esterhammer, Christian Brenneis, Werner Jaschke, Gregor K. Wenning and Werner Poewe. *Voxel-wise analysis of diffusion weighted imaging reveals disruption of the olfactory tract in Parkinsons disease.* Brain, vol. 129, pages 538–542, 2006. 13

[Seibyl 2005] J. Seibyl, D. Jennings, R. Tabamo and K. Marek. *The role of neuroimaging in the ealderly diagnosis and evaluation of Parkinson's disease.* Minerva medica, vol. 96, no. 5, pages 353–364, 2005. ISSN 0026-4806. 12

[Sidka 2008] Michael Sidka. *A fast non-rigid Image Registration with constraints on the Jacobian using large scale constrained optimization.* IEEE Transactions on Medical Imaging, vol. 27, pages 356–362, 2008. 57

[Singh 2009] Richa Singh, Mayank Vatsa and Afzel Noore. *Multimodal Medical Image Fusion using Redundant Discrete Wavelet Transform.* IEEE Computer Society - Seventh International Conference on Advantages in Pattern Recognition, vol. 9, pages 232–235, 2009. 60

[Smith 2003] John J. Smith, A. Gregory Soresen and James H. Thrall. *Biomarkers in Imaging: Realizing Radiology's Future.* Radiology, vol. 227, pages 633–638, 2003. 17

[Sonka 2009] Milan Sonka and J. Michael Fitzpatrick, editeurs. Handbook of medical imaging, volume 2 Medical Image Processing and Analysis of *Diagnostic Imaging - Handbooks*. SPIE Press, P.O. box 10 Bellingham, Washington 98227-0010 USA, 3 édition, 2009. ISBN 0-8194-3621-6. 27, 48, 49, 73, 92, 104

[Starr 2009] Cindy Starr and George Mandybur. *Grant to improve targeting in Parkinson's Surgery*. University of Cincinnati neuroscience institute, January 2009. Mayfield Clinic. 53

[Talos 2003] Ion Florin Talos. *Slicer 3 Tutorial The SPL PNL Brain Atlas*. presentatin, Brigham and Womens Hospital, march 2003. Surgical Planning Laboratory. 47, 59

[Teodorescu 2009a] R. O. Teodorescu, D. Racoceanu and L.-L. Chan. *H&Y compliant for PD detection using EPI and FA analysis*. Presentation Number: NIH09-NIH01-88, 1-2 October 2009. Natcher Auditorium, National Institutes of Health in Bethesda, MD USA. 88, 100, 101

[Teodorescu 2009b] Roxana Teodorescu, Daniel Racoceanu and L.L. et al. Chan. *Parkinson's disease detection using 3D Brain MRI FA map histograms correlated with tract directions*. RSNA, vol. 8015681, page 1, 2009. Chacago, IL USA. 33, 34, 100, 101

[Teodorescu 2009c] Roxana Oana Teodorescu and Daniel Racoceanu. *Prognosis of Parkinson's Disease*. In A-Star Scientific Conference, 28-29 Oct. 2009. Biopolis, Singapore. 100

[Teodorescu 2010] Roxana Teodorescu, Daniel Racoceanu, Nicolas Smit, Vladimir Ioan Cretu, Eng King Tan and Ling-Ling Chan. *Parkinson's disease prediction using diffusion based atlas*. In SPIE 2010, 13-18 Feb. 2010. SPIE Medical Imaging, Computer Aided Diagnosis, San Diego, California, USA. 69, 70, 100, 101

[Tharin 2007] Suzanne Tharin and Alexandra Golby. *Functional Brain Mapping and Its Applications to Neurosurgery*. Operative Neurosurgery, vol. 60, pages 185–202, 2007. 57

[Theverovskiy 2006] Leonid Theverovskiy, Owen Carmichael and et al. *Feature-based vs. Intensity-based brain image registration: voxel level and structure level performance evaluation*. Carnegie Mellon, vol. 6-118, pages 1–30, 2006. 56, 57

[Thomopoulos 1994] Stelios C. A. Thomopoulos. *Sensor Selectivity and Intelligent Data Fusion*. Proceedings of the 1994 International Conference on Multisensor fusion and Integration for Intelligent Systems (MFI94), vol. 2, no. 5, pages 529–537, oct 1994. decision and control systems lab - sensors data fusion. 30, 56

[Today 2009] Medical News Today. *Brain bank Appeal aims to double number of brain donors*. www.medicalnewstoday.com, March 2009. Parkinsons awareness week 2009, 20-26 April. 1, 2

[University 2008] South Carolina University. *The DICOM standard*. Rapport technique, University of South Carolina, december 2008. Technical Report. http://www.sph.sc.edu/comd/rorden/dicom.html - last accessed on May 2010. 12

[Vaillancourt 2009] D. Vaillancourt and et al. *Imaging Technology May trace Development of Parkinson's disease*. University of Illinois at Chicago, Rush University, vol. 1, page 3, 2009. 14, 57

[van Heckle 2007] Wim van Heckle and et al. *Non-Rigid Co-Registration of Diffusion Tensor Images Using a Viscouosis Fluid Model and Mutual Information*. IEEE Transactions on Medical Imaging, vol. 26, pages 1–8, 2007. 57

[Vercaunteren 2008a] T. Vercaunteren, X. Penec and et al. *Diffeomorphic Demons: Efficient Non-parametric Image Registration*. NeuroImage, vol. 45, pages 61–72, 2008. 57

[Vercaunteren 2008b] Tom Vercaunteren, Xavier Pennec, Aymeric Perchant and Nicholas Ayache. *Symmetric Log-Domain Diffeomorphic Registration: A Demons - Based Approach*. Lecture Notes in Computer Science - Medical Image Computing and Computer-Assisted Intervention -MICCAI, vol. 5241, pages 754–761, 2008. 46, 57, 58

[Wang 2007] Ruopeng Wang, T. Benner, A.G. Sorensen and V.J. Wedeen. *DiffusionToolkit: A software package for diffusion imaging data processing and tractography.* ISMRM abstract, vol. 15, page 3720, 2007. Martinos Center for Biomedical Imaging, Massachusetts General Hospital. 48

[Westermann 2008] B. Westermann, E. Wattendorf, U. Schwerdtfeger and A. Husner. *Functional imaging of cerebral olfactory system in patients with Parkinson's disease.* J Neurol. Neurosurg. Psychiatry, vol. 79, pages 19–24, 2008. 13

[Wirijadi 2001] Oliver Wirijadi. *Survey of 3D Image Segmentation Methods.* Fraunhoffer technical report, vol. 1, page 1, 2001. 57, 61

[Yaasa 2004] Michael A. Yaasa. *Voxel - Based Morphometry.* Electronic presentation (ppt), The Johns Hopkins School of Medicine, Division of Psychiatric Neuroimaging, december 2004. 29, 30, 58

[Yendiki 2010] Anastasia Yendiki. *Future duirections: TRActs Constrained by UnderLying Anatomy (TRACULA).* ppt presentation, February 2010. HMS/MGH/MIT Athinoula A. Martions Center for biomedical imaging. 62

[Yeo 2009] Thomas B.T. Yeo, Mert R. Sabuncu and Tom et al. Vercaunterenet. *Spherical Demons: fast Differomorphic Landmark-free Surface Registration.* Draft for IEEE Transactions on MEdical Imaging, vol. 36, pages 1–8, 2009. 57

[Yushkenvich 2008] Paul Yushkenvich, Hui Zhang and James Gee. *Tract-Specific Analysis for DTI of Brain White Matter.* presentation- IPAM Summer School, july 2008. PICSL. 29

[Zitova 2003] Barbara Zitova and Jan Flusser. *Image Registration: A Survey.* Image and Vision Computing, vol. 21, pages 977–1000, 2003. 57, 61